SOVIET ATOMIC ENERGY

АТОМНАЯ ЭНЕРГИЯ
(ATOMNAYA ÉNERGIYA)

TRANSLATED FROM RUSSIAN

CONSULTANTS BUREAU, NEW YORK

SOVIET ATOMIC ENERGY

Soviet Atomic Energy is a cover-to-cover translation of Atomnaya Energiya, a publication of the Academy of Sciences of the USSR.

An agreement with the Copyright Agency of the USSR (VAAP) makes available both advance copies of the Russian journal and original glossy photographs and artwork. This serves to decrease the necessary time lag between publication of the original and publication of the translation and helps to improve the quality of the latter. The translation began with the first issue of the Russian journal.

SOVIET ATOMIC ENERGY

A translation of *Atomnaya Énergiya*

March, 1980

Volume 47, Number 3   September, 1979

CONTENTS

Engl./Russ.

CONTENTS

CONTENTS

The Russian press date (podpisano k pechati) of this issue was 8/23/1979.
Publication therefore did not occur prior to this date, but must be assumed
to have taken place reasonably soon thereafter.

THIRTIETH ANNIVERSARY OF THE GERMAN DEMOCRATIC REPUBLIC

DEVELOPMENT OF THE NUCLEAR POWER INDUSTRY
IN THE GERMAN DEMOCRATIC REPUBLIC*

W. Mitzinger†

In the 30 years of the German Democratic Republic (GDR) the power industry of the country has to an every increasing extent become an important factor in the growth of the national economy. In accordance with the further development of the socialist society the energy policy of the country is aimed at ensuring the well-being of the nation, in the service of the working class and all working people. The General Secretary of the Central Committee of the Socialist Unity Party of Germany (CC SUPG) and Chairman of the State Council of the GDR, E. Honnecker, stated at the Ninth Congress of the Party that the creation of a powerful modern energy and raw materials base is a fundamental condition for the development of the productive forces for the gradual transition to communism and its material and technical foundations. The energy policy of the country, determined at the Eighth Congress of the SUPG and reaffirmed at the Ninth Congress is based on three main premises:

security of fuel and energy supplies through maximum use of domestic energy and raw-material resources;

rationalization of the processes of conversion, transportation, and application of energy for a further decrease in the specific fuel and energy consumption;

implementation of a comprehensive program of socialist economic integration for the extensive utilization of the scientific and technological advances, the creation of specialized production of highly efficient plant, particularly in electrical machine construction, and stable, long-term supplies of raw materials and fuel for the country.

In accordance with these premises, low-calorie brown coal will, as before, remain the main source of primary energy in the country, at least up to the year 2000. In the future as well a large proportion of the energy demand will be covered by domestic brown coal. The directives of the Ninth Congress of the SUPG set the goal of "ensuring the production of domestic solid fuel with the minimum possible costs by increasing the power and efficiency of existing strip mines and concentrating plants in combination with the discovery of new open pits." However, because of the limited possibilities of increasing extraction and the increasing deterioration of the geological and hydrological conditions, further expansion of brown coal production, especially after 1990, will be restrained by natural causes. In the light of present concepts, atomic energy presents the only possible alternative for meeting the requirements of the GDR for energy, especially after 1990. Thus, the early development of an industrial base for nuclear power in the country is envisaged. With due regard for the scientific and technical potential and the structure of industry, this problem can be solved only in close cooperation with the Soviet Union and other COMECON member-nations. As long ago as 2 years after the start-up of the Obninsk Atomic Power Plant (APP) an intergovernmental agreement was signed on the joint construction of the Rheinsburg APP with a VVÉR (water-moderated−water-cooled power reactor) with an electrical power of 70 MW. During the design, construction, and operation of this APP scientists, designers, builders, erectors, and operators of our country had the opportunity to become acquainted with the new technology in close cooperation with Soviet specialists. While the technical design and the principal equipment of the APP were supplied by the Soviet Union, the detail design and auxiliary equipment, including the stream generator, were elaborated and built in the GDR. The construction and the assembly of the equipment of the APP were carried out by GDR specialists.

The successful start-up of the Rheinsburg APP on May 8, 1966, on the anniversary of liberation from fascism, demonstrated that in the GDR the prerequisites had been created for mastering atomic energy in fraternal cooperation with the Soviet Union. Thus, the road was laid for mastering a new source of energy, atomic energy. Already in 1965 a new agreement was concluded with the Soviet Union on joint work on the con-

---

struction of the next APP. The site chosen for it was the Lubmin wasteland on the shore of the Baltic Sea, roughly 20 km to the northeast of Greifswald. The choice of site was due mainly to the presence of cooling water as well as the inadequate supply of electrical energy in the northern regions of the country. The reactors chosen for this APP were of the pressurized water type of reliable Soviet design, similar to those installed at the Novovoronezh APP. The electrical power of each energy unit is 440 MW. Such reactors have come into most widespread use primarily because of their economy, high degree of safety, and use of pressurized water as the working medium, which has been well investigated in ordinary engineering. The first unit of the Greifswald APP, which has been named the Bruno Loischner APP, went into operation at the end of 1973. The commercial introduction of atomic energy thus began in the GDR. At present, the APP operates four energy units with VVÉR-440 reactors with a total power of 1760 MW. The APP accounts for more than 9% of the power of all the electricity generating plants of the GDR. The next energy units are to be constructed both on the site of the Bruno Loischner APP and on the Elba, about 25 km from Stendal. Over the next decade the contribution of the APP to the installed capacity of electric power stations in the GDR will rise to 15-20%. At the same time, plans call for a transition to pressurized-water reactors with a higher unit power.

The APP built in the country have displayed high operating characteristics. In the first place this pertains to operating readiness and safety. The Rheinsberg APP has been operating consistently for more than 13 years. In recent years it has been reequipped into a research center and a center for training personnel for the nuclear power industry. With a training unit coming into service here in 1975, conditions approximating those in practice as closely as possible were created for training and raising the qualifications of operating personnel for APP of the GDR and other COMECON member-nations. In the critical months of the 1978-1979 winter the operational readiness of the units of the Bruno Loischner APP was 95-100%. Operation in January and February, 1979, which were particularly severe in the northern regions of the country, demonstrated that the APP is relatively independent of the weather conditions. Operating at full capacity, it ensured electrical energy for the country even when, because of exceptionally heavy snowfalls, the plant was temporarily cut off from the outside world. Under the conditions existing in the GDR a capacity of 440 MW for a power unit is economically justified. As for the capital investment and energy costs, a unit with a VVÉR-440 reactor is comparable with a modern 500-MW unit operating on brown coal.

The construction and operation of APP in the GDR are under strict government control. Operating experience has confirmed that the characteristics are favorable for the environment. The radiation in the direct vicinity of the APP is less than 1% of the natural radiation. The long-range energy policy of the GDR is aimed at the continuous development of nuclear power with the use of mastered, reliable, and tested APP and invididual APP systems. In order to increase operating safety provision has been made for continuous and annual inspection of the state of the APP, especially the nuclear part, this being done in the form of comprehensive examinations of the equipment on the basis of instructions strictly laid down by law. The high requirements concerning the professional training of operating personnel, regular enhancement of the qualifications in combination with qualification examinations, and continuous and concrete monitoring of the state of the training of operating personnel by on-the-spot analysis of maladjustments and regular training sessions for handling emergencies are also important measures for ensuring the required high safety of APP.

Supplies of nuclear fuel for APP in our country as well as the return of spent fuel are ensured by long-term agreements and treaties with the Soviet Union. Thus, there is no need to reprocess spent fuel on the territory of the GDR in order to extract highly active fission products and recover the uranium and plutonium not used in the reactor. This results in very visible streams of nuclear materials, which makes it possible for the IAEA, on the basis of the treaty of nonproliferation of nuclear weapons, to carry out effective inspection of the pureful peaceful use of nuclear technology in the GDR. Special railway cars and containers have been constructed for the safe transportation of fresh and spent fuel. Low-level and medium-level radioactive waste formed as the result of the operation of the APP and the application of radioisotopes in many areas of the national economy are appropriately processed and then stored on the territory of the GDR.

All of these successes would not have been possible without the close, fraternal cooperation with the Soviet Union and other socialist countries on the basis of bilateral government agreements within the framework of COMECON, especially in the domain of science and engineering. Already in the early stage of development of nuclear energy, in October 1960, COMECON established a Standing Committee on the use of atomic energy for peaceful purposes. It has ensured long and fruitful cooperation among the COMECON membernations in mastering a new source of energy. The principal task of the Committee consists in coordinating the scientific research and long-term developments in the field of nuclear energy. To this end, working bodies were set up to deal with particular problems, especially the development of pressurized-water reactors, preparation for the introduction of fast breeder reactors, elimination of radioactive wastes, reprocessing of spent

fuel, as well as problems of radiation protection and protection of the environment. An international research team was created in Budapest to develop reactor physics and study related problems. The COMECON Standing Committee on Electrical Energy also set up a special working group of specialists engaged in the design, construction, and operation of APP with water-moderated—water-cooled reactors.

Specialists of the GDR are participating actively in the activities of these international working bodies. In this connection mention should be made first of all of the creative teams of the Central Institute of Nuclear Research at Rossendorf, the Academy of Sciences, the Bruno Loischner APP, and the industrial group for the construction of electric power plants.

The main efforts of the GDR in the further joint development of water-moderated—water-cooled power reactors and preparation for the introduction of fast breeder reactors are aimed at creating neutron-physics and heat-engineering programs for designing reactors, improving their water conditions and regulating and control systems, developing methods of deactivating an individual piece of equipment and the entire primary circuit of a water-moderated—water-cooled power reactor, methods of monitoring the state of the equipment and metal during inspection and operation of APP, as well as developing methods and special equipment for packaging, transporting, and storing radioactive wastes. This work, as well as the creation of special methods for monitoring the sodium circuits of fast reactors, are conducive to a further increase in the safety, operational readiness, and economy of APP. The GDR also participates in improvement of the designing, construction, assembly technology, and start-up and loading operations in the construction of APP.

On the 30th anniversary of the GDR it is with satisfaction that we note the successes of our workers, engineers, and scientists during the 23 years since the conclusion of the first intergovernmental agreement with the Soviet Union on the establishment of a nuclear-energy base in the country. They have earned our gratitude, as also have our Soviet friends, whose great professional knowledge and participation created the scientific, technical, and economic prerequisites for the introduction of atomic energy into the power industry of the GDR.

NUCLEAR RESEARCH OF THE ACADEMY OF SCIENCES OF THE GERMAN DEMOCRATIC REPUBLIC IN THE LIGHT OF THE DECISIONS OF THE NINTH CONGRESS OF THE GERMAN SOCIALIST UNITY PARTY*

K. Fuks†

The first report concerning the birth of the Academy of Sciences of the German Democratic Republic was inscribed with the motto "theoria cum praxi," framing a miniature portrait of Leibnitz on the cover of the journal Kernenergie. Such, too, was the sense of the second report, dated July 1, 1946, and called "enlistment of science in the construction of a democratic Germany."

In the first years of nuclear research in the GDR controversies arose over whether "current issues" were a matter for the research and design organizations of the heavy power engineering industry whereas the activities of the Central Institute of Nuclear Research should be devoted exclusively to future development of reactors.

The controversies have long since ceased. Now everyone has taken to heart the words of the General Secretary of the Central Committee of the German Socialist Unity Party (CC GSUP) and Chairman of the Council of State of the GDR, E. Honnecker, that "socialism is sole appeal to science." The profound sense of this statement can be comprehended when one examines how in fact the ideal of unity of the economic and social policy of the Party is accomplished. Particularly large changes have occurred in the style of management and

psychological climate of enterprises since the resolution adopted by the Ninth Congress of the SUPG stating that acceleration of scientific and technological progress is the basis for the intensification of production.

The Academy of Sciences bears a dual responsibility: for the development of science as a source of new knowledge and for the effective use of its results. It is called upon not simply to link theory with practice but to ensure the most efficient performance of the social purposes of fundamental research. In 1975, when the program for physics research was being drawn up, we tried to answer this question. The answer can be formulated as follows: work on the development of the fundamental problems of physics and individual areas of physics makes it possible to discover and understand many new physical phenomena with great potentialities for practical use. The discoveries must be directed at solving the basic problems of society, primarily those of the national economy.

This approach refutes the mechanistic view that only "appropriate" fundamental research should be engaged in. Also refuted was the demand that each line of research have an unquestionable economic purpose. How did we arrive at this answer and what is the crux of it?

It was useful for us to have the development of nuclear energy in a leading position among the principal areas of research. And this is no accident since the experience gained from the development of nuclear power should be used to solve other major problems. The development of the nuclear power industry in the GDR, therefore, has two tasks in the main. One of them is the result of agreements within the framework of COMECON. The second stems from the need for such a scientific basis for the technological processes in the nuclear reactor which will ensure safe and efficient operation of atomic power plants (APP). Accordingly, for this reason and also for the diagnostics, monitoring, and control of the processes reactor physics has been transformed from an exact science into one of the technological areas of research. This has occurred to the extent that the neutron-physical characteristics determine the engineering factors of APP. Thus, neutron characteristics are now studied not as a physical but rather as a technological phenomenon. Finally, the reactor installation, including the primary circuit, attracts attention as an object of research, as evidenced by the intensive exchange of specialists as well as instruments and technical information between the central nuclear research institutes and APP of the country.

The knowledge that the information participates in the technological process is important for the extension of the experience. The growing size and complexity of industrial plants of another type lead to the same problem. It cannot be resolved without a precise technique for data acquisition and computer processing of the data.

At an exhibition devoted to the 275th anniversary of the Academy of Sciences of the GDR, the state of the research program at that time was illustrated schematically. This aspect of information science has been confirmed in part. Reactor physics, as a technological discipline, realizes the link between fundamental research and the technology of APP. However, the link between fundamental research and information science continued to be an "uninvestigated area." The gap between fundamental research and the use of the results of research was understood and the first steps were taken to eliminate it. Thus, we were not unprepared when we encountered this problem in microelectronics.

Microelectronics is of interest to us as a material carrier of complex informational processes and as a difficult branch of manufacture. It was first used to automate scientific experiments in the domain of nuclear research. In nuclear power engineering the application of microelectronics has taken the route of construction of hierarchical monitoring and control systems which are in accord with the technique of automating the developing socialist society. In turn, nuclear research was conducive to the development of microelectronics. Thus, the many years of experience of the Academy of Sciences with ion implantation was used in the production of some microelectronic devices. The ion-beam technique still has many undiscovered technological capabilities which will also lend themselves to application. The Central Institute of Isotope and Radiation Research and the Central Institute of Nuclear Research have developed nuclear methods of analysis which are used in microelectronics to solve problems of pure materials. In many cases only such methods are sensitive enough to permit a transition from materials "as pure as possible" to materials "as pure as required." Clearly, there are sufficient examples to show the effect of technology on research in the realm of physics. Technology is that mirror with which a variety of possible areas of development are focused on the most important directions, yielding the greatest effect from the intensification of production today and at the same time significantly improving the production technology of tomorrow.

The nuclear research of the Academy of Sciences encompasses problems such as those below.

1. Continued research on the fundamental laws of space, time, and matter. The physics of the nucleus and elementary particles makes a contribution to this work. The goal is to determine the limits of present-day knowledge. The point is to penetrate further into the microcosm and to create the instruments necessary to do this. In this connection one should not neglect the practical application of knowledge, methods, and instruments which in many ways promote general process. Elementary-particle physics has been stimulated with the appearance of a possibility of experimental verification of the quark hypothesis. New current research has been concentrated in the Institute of High-Energy Physics at Zeuthen and is being conducted in close cooperation with the Joint Institute of Nuclear Research (JINR). The work is planned so as to utilize the unique capabilities of the experimental facilities as Dubna and Serpukhov. Moreover, we can count on the use of the experimental capabilities of CERN. Theoretically validated problems should be subjected to critical analysis at JINR and obtain experimental confirmation with the aid of high-quality modern technology. Major results from such work were obtained at the end of 1978: an international team of specialists at Zeuthen built an apparatus for processing and interpreting photographs of particle tracks.

In nuclear physics note should be taken of a developed generalized method of describing the mechanism of reactions on the basis of an exact many-particle theory. The high level of nuclear-engineering instrumentation facilitated a center for the development of instruments for scientific research in the Central Institute of Nuclear Research.

Interesting results on the dependence of nuclear decay on the chemical bonds were obtained in the Central Insitute of Isotope and Radiation Research. Laws which were discovered will probably lend themselves to use in the development of nuclear-medicine preparations.

These are only some of the results. Reviews published in Kernenergie in July 1975 to mark the 275th anniversary of the Academy of Sciences of the GDR can be recommended to the interested reader.

2. The next problem is that of studying complex physical structures of a natural origin. Of greater interest in this respect is work done at the boundary with other sciences, which was the case particularly in isotope and radiation research. Thus, research on isotopic effects in geochemical processes makes it possible to obtain interesting data about the history of elements and the origin of deposits, data which could be used in geological prospecting. The similarity theory can be used to model the combined processes and to determine their parameters. Researches carried out in the Central Institute of Isotope and Radiation Research with nitrogen-15 have attained a high level and have produced results applicable in biology, agriculture, and medicine. Radiation-chemical research has been enriched with fundamental work on the effect of irradiation on elementary processes which could find application in radiation-chemical chlorination of polyvinyl chloride and development of cable insulations.

3. An important place in the investigations of the Academy of Sciences of the GDR is occupied by the study of artificial physical structures, i.e., the fundamental laws of technology. Research for nuclear power engineering and microelectronics are the most prominent, but not the sole example of work in this area. Along with personnel from the Bruno Loischner APP further research is planned with other APP. Thus, within the framework of the international team in Budapest, established for preparations for the introduction of the VVÉR-1000 water-moderated—water-cooled power reactor, specialists of the Academy of Sciences of the GDR are engaged in work on problems pertaining to diagnostics from noise analysis. Other problems for this team are being worked on in collaboration with specialists from the Rheinsburg APP. In conjunction with workers of the Scientific-Research Institute for Atomic Reactors (NIIAR) research is being conducted on fast reactors. In the realm of thermonuclear research two substantial projects were conducted in 1978. One of them was the construction by the Institute of Electronic Physics of an instrument for analysis of the interaction of plasma with a wall. Such an instrument was installed in the T-10 tokamak at the I. V. Kurchatov Institute of Atomic Energy. A considerable contribution to the solution of technological problems was made by research with isotopic tracers. The use of the results of the work for analysis of processes in chemistry, metallurgy, and coal dressing increased the efficiency of these processes.

These are only some examples of work which has been done in recent years in 15 areas of research in the domain of physics. Basically, this work was aimed at ensuring energy, material, and information, as well as the development of instrumentation and health protection.

The solution of numerous problems of nuclear research is impossible without international cooperation. Joint work with specialists of the Soviet Union means much to us. The successes mentioned above and the problems formulated are at the same time an expression of gratitude for invaluable assistance.

Faithful to the behest of Ernst Thaelmann, we know on whose side we stand in the class struggle. "Human failure" is the usual conclusion when western atomic power plants experience a breakdown. And the question is not asked as to why a human, endowed with talent and ability, proved to be such a weak link in the production system controlled by automatic devices that it is best to replace that human by a microprocessor. The purpose of our automation of APP is to provide the human with information and instruments for monitoring and control while relieving him of heavy physical and monotonous mental work. We proceed from the premise that atomic energy and microelectronics are indispensable aids in the construction of a socialist society. Atomic energy will never be used for the annihilation of mankind; this is the highest demand of our time.

696

ARTICLES

EFFECT OF NONUNIFORMITY OF FUEL DEPLETION
WITH HEIGHT ON THE PHYSICAL CHARACTERISTICS
OF A REACTOR

A. M. Afanas'ev and B. Z. Torlin   UDC 621.039.51

The development of the reactor for an atomic power station usually passes through several stages. The early stages are characterized by numerous variant calculations and economic estimates, in which an important role is played by the attainable depletion of the fuel (burn-up) S as a function of its initial enrichment, the parameters of the lattice, the construction of the fuel elements, the method used to cool them, the frequency of recharging with fuel, and so on. Comparatively simple relationships for estimating the burn-up are proposed below; they are of acceptable accuracy and they allow for the distorsion of the neutron field with height under steady conditions as a result of burn-up and boiling of the coolant. To refine these estimates and also to calculate the neutron field itself, the isotopic content of the discharged fuel, and a whole string of other parameters, we describe a simple and effective method of numerical computation.

Describing the neutron field by the diffusion approximation, we write the starting equations in the form:

$$\hat{H}\psi(z) + f(S, \varphi, z)\hat{A}\psi(z) = 0;$$
$$\psi(0) = \psi(H) = 0,$$

(1)

where, in the one-group approximation,

$$\hat{H} = (d/dz)\, D^*_{th}(d/dz);$$
$$\hat{A} = 1; \quad f = [k(S, \varphi, z) - 1]/M^2(S, \varphi, z); \quad \psi = N(z),$$

and, in the two-group approximation,

$$\hat{H} = \begin{pmatrix} \frac{d}{dz}D^*_{d}\frac{d}{dz} - \frac{1}{\tau(z)}; & \frac{1}{\tau(z)} \\ \frac{1}{L_0^2}; & \frac{d}{dz}D^*_{th}\frac{d}{dz} - \frac{1}{L^2(S, \varphi, z)} \end{pmatrix}; \quad \hat{A} = \begin{pmatrix} 0; & 1 \\ 0; & 0 \end{pmatrix};$$

$$f = \frac{k(S, \varphi, z) - 1}{\tau(z)}; \quad \psi = \begin{pmatrix} n(z) \\ N(z) \end{pmatrix}.$$

The notation here is as follows: $D^*_{th(d)} = D_{th(d)}(z, \varphi)/D_{th(d)}(z_0, 0)$; D_{th} and D_d, diffusion coefficients for thermal and delayed neutrons; z_0, arbitrary point of the core; k, multiplication factor for thermal neutrons; S(N), fuel depletion (burn-up); $\varphi(N)$, vapor content; M^2, L, τ, square of the migration length, the diffusion length, and the neutron age, evaluated at $D_{th}(z_0, 0)$ and $D_d(z_0, 0)$; N(z) and n(z), flux density distributions of thermal and delayed neutrons; and H is the core height. The dependence of k on the depletion S can be calculated as described in [1]. The dependence of k on the vapor content φ we expressed in the following manner:

$$k(S, \varphi, z) = k(S, \gamma_0, z) + \Delta k_{\kappa}(H, S)\, g(z)\, \varphi(z)/\varphi(H);$$

$$\varphi(z) = \int_{h_{ec}}^{z} \Sigma_f(S, z')\, N(z')\, dz',$$

$$g(z) = \begin{cases} 0; & 0 \leqslant z \leqslant h_{ec}; \\ 1; & h_{ec} \leqslant z \leqslant H, \end{cases}$$

(2)

where γ_0 is the mean coolant density in the economizer zone; $\Delta k_{\kappa}(H, S)$, change in the multiplication factor due to vapor formation at the point z = H at depletion S; h_{ec}, height of the economizer section, determined from the equation:

$$\int_0^{h_{ec}} \Sigma_f N\, dz = q \int_0^{H} \Sigma_f N\, dz.$$

697

Here q is the proportion of energy liberated on the economizer section; Σ_f is the macroscopic fission cross section. The dependence of $1/L^2(S, \varphi, z)$ and $D_{th(d)}(z, \varphi)$ on vapor content is expressed in a similar manner.

The dependence of S on $N(z)$ is determined by the manner in which the fuel is recharged. We shall consider a continuous recharging regime. In this regime channels which have been run for the operating period T are replaced by new ones; this process being carried out continuously and uniformly over the cross section of the core. Thus, in cross section z, channels of all ages, from the new to the completely spent, are uniformly distributed. Accordingly, we shall assume in the first approximation that the following expressions hold for each z:

$$k(z, \gamma_0) = \frac{1}{S_{max}(z)} \int_0^{S_{max}(z)} k(S, \gamma_0, z)\, dS;$$

$$\frac{1}{L^2(z, \gamma_0)} = \frac{1}{S_{max}(z)} \int_0^{S_{max}(z)} \frac{1}{L^2(S, \gamma_0, z)}\, dS, \tag{3}$$

where $S_{max}(z)$ is the maximum depletion in cross section z. The suffix will be omitted in future. As we are considering the steady state of the reactor, it follows that

$$S_{max}(z) = \sigma_5 T N(z), \tag{4}$$

where σ_5 is the microscopic absorption cross section of ^{235}U.

In this manner, the determination of the depletion, the energy distribution, and the other characteristics of a reactor, reduces to solving Eqs. (1)-(4), the characteristic feature of which is their nonlinearity.

The approximate method of solution is based on perturbation theory [2, 3], well known in linear analysis. The approximate solution is constructed in the following manner. A new sought function $\Phi(z)$ is introduced:

$$\Phi(z) = S(z)/\bar{S}H; \quad \int_0^H \Phi(z)\, dz = 1, \tag{5}$$

where $\bar{S}$ is an unknown number, equal, by virtue of definition (5), to the mean depletion of the discharged fuel.

After insertion of expressions (2)-(4) into Eq. (1), we obtain:

$$\hat{H}_1\chi + l_1\hat{A}\chi = -\varepsilon[f_1(\bar{S}\Phi, \varphi, z) - l_1]\hat{A}\chi; \quad \chi = \begin{pmatrix} \tilde{n}(z) \\ \Phi(z) \end{pmatrix}$$

with homogeneous boundary conditions and normalization (5). Here $\hat{H}_1$ and f_1 coincide with $\hat{H}$ and f if $D_{th(d)}^*$, M^2, $\Delta k_k(H)$, and Σ_f are constants and $g(z) = 1$*; ε is an artificially introduced dimensionless parameter in terms of which the solution $\chi(z)$ and $\bar{S}$ is investigated; l_1 is the first eigenvalue of the unperturbed problem

$$\hat{H}_1\varphi_1(z) + l_1\hat{A}\varphi_1(z) = 0 \tag{7}$$

with the same boundary conditions as Eq. (6). The solution of (7) is found in the form of a power series in ε:

$$\chi = a(\varepsilon)\varphi_1 + \sum_{k=1}^{\infty} \varepsilon^k \chi_k = a_0\varphi_1 + \sum_{k=1}^{\infty} \varepsilon^k [\chi_k + a_k\varphi_1];$$

$$\bar{S} = \bar{S}_0 + \sum_{k=1}^{\infty} \varepsilon^k \bar{S}_k. \tag{8}$$

Since Eq. (6) is nonlinear, the normalization of χ is not arbitrary. With the aid of the coefficient a_k, the condition expressed by (5) is satisfied in each approximation. After approximation of f_1 by a power series in S, we insert expression (8) into (6) and demand that the coefficients in front of like powers of ε be equal. Allowing for normalization (5), we obtain a closed system of linear equations which can be solved in turn for χ_k, a_k, and $\bar{S}_k$. This method of solution will be called the ε-method. By analyzing the ε-method for the case of slow convergence of the approximations, we were able to develop methods of improving it. Thus, in the course of solving the problem for an enriched-uranium reactor, a λ-method was developed which, even for deep burn-up, gives for $\bar{S}$ an estimate with an error not exceeding 2-3% when the first correction $\bar{S}_1$ to $\bar{S}_0$ is taken into account. The scheme whereby the solution is constructed according to this modified method is as follows. Expressions (2)-(4) are first inserted into Eq. (1) and the latter then written, using (5), in the following form:

$$\hat{H}_1\chi^{(\lambda)} + \lambda l_1\hat{A}\chi^{(\lambda)} = -\varepsilon\lambda[f_1'(\bar{S}\Phi, \varphi, z) - l_1]\hat{A}\chi^{(\lambda)}, \tag{9}$$

where λ is an artificially introduced parameter; for $\lambda = 1$, $\chi^{(\lambda)} = \chi(z)$.

---

*In future, to simplify the final expressions, the approximate solution is constructed subject to these assumptions.

TABLE 1. Depletion Calculated by Approximate and Exact Methods

$\Delta k'_{ex}(\Delta k_0)$	4,07 (0,06)		9,13 (0,12)			14,2 (0,18)			
$\Delta k'_{к}$	0	6,0	0	6,0	9,0	0	6,0	9,0	12,0
$\bar S_{b,\,exact}$	6,460	11,07	15,11	20,06	22,35	24,09	29,22	31,64	33,98
$\bar S^{(0)}_b$	6,099	10,60	13,70	18,20	20,45	21,30	25,80	28,05	30,30
$\bar S^{(1)}_b$	6,562	11,44	16,04	21,76	24,39	26,95	33,52	36,58	39,48
$\bar S^{(1)}_{b,\,m}$	6,513	11,20	15,15	20,15	22,56	23,90	28,97	31,43	33,86

Assuming that $\bar S$ is known and that λ is an unknown eigenvalue, we represent the latter as a series in ε and solve (9) by the method described above. Equating in each m-th approximation $\lambda^{(m)} = \lambda_0 + \sum_{k=1}^{m}\varepsilon^k\lambda_k$ to unity, we obtain an expression with which to determine $\bar S^{(m)}$.

For an enriched-uranium reactor, the multiplication factor k averaged over all S is quite well approximated by a polynomial of the first degree [4]:

$$k(z) = \frac{1}{S}\int_0^{S1} k(S')\,dS' = k_0 - \frac{b_1}{2}S. \tag{10}$$

In this case, for the approximate determination of S by the ε-method, we shall have*:

$$\bar S^{(0)} = \bar S_0 = \frac{3}{2b_1}\left[\Delta k_{ex} + \Delta k_{к}(H)\frac{1-2q}{2(1-q)}\right] = \bar S^{(0)}_b\frac{\Delta k_{ref}}{b_1}, \tag{11}$$

$$\bar S^{(1)} = \bar S_0 + \bar S_1 = \bar S^{(0)}[1 + 1.245\cdot10^{-2}\bar S^{(0)}_b - A^2/64\bar S^{(0)}_b] = \bar S^{(0)}_b\frac{\Delta k_{ref}}{b_1}, \tag{12}$$

where the burn-up reactivity margin $\Delta k_{ex} = (k_0 - 1) - \Delta k_{ref}$; $A = \Delta k_к(H)/(1-q)\Delta k_{ref}$; and Δk_{ref} in the one- and two-group approximations is given, respectively, by $\Delta k^{(I)}_{ref} = (\pi/H)^2 M^2$ and $\Delta k^{(II)}_{ref} = \Delta k^{(I)}_{ref}\cdot(1 + \Delta k^{(I)}_{ref}L^2\tau/M^4)$.

By the λ-method, $S^{(0)}_M$ coincides with $\bar S^{(0)}$:

$$\bar S^{(1)}_M = \bar S^{(0)}\left\{1 + [1/(1-\beta)]\left[\left(\beta - \frac{3}{4}\bar S^{(0)}_b\right) + \sqrt{\left(\beta - \frac{3}{4}\bar S^{(0)}_b\right)^2 + (1-\beta)\left(\beta - \frac{3A^2}{128\bar S^{(0)}_b}\right)}\right]\right\} = \bar S^{(1)}_{b,M}\Delta k_{ref}/b_1, \tag{13}$$

where $\beta = 1.868\cdot10^{-2}$.

It can be seen from (11)-(13) that the convergence of the approximations is determined by the values of $\Delta k'_{ex} = \Delta k_{ex}/\Delta k_{ref}$ and $\Delta k'_к = \Delta k_к(H)/\Delta k_{ref}$ (i.e., by the burn-up reactivity margin and by the change of reactivity due to vapor formation divided by Δk_{ref}) and by the quantity q.

Table 1 shows the results of calculations using formulas (11)-(13) and also the exact values of $\bar S_{b,exact} = \bar S_{exact}\Delta k_{ref}/b_1$ obtained numerically for various $\Delta k'_{ex}$ and $\Delta k'_к$ for $\Delta k_{ref} = 0.01184$ and $q = 0$. It can be seen that even for large values of $\Delta k'_{ex}$, formula (13) can be used to calculate S to within 1%.

We note that formula (11) is in good agreement with a more exact expression derived without assuming the function g(z) to be constant only provided $q \le 0.3$ and $\Delta k_{ex}/\Delta k_к > 1$. These conditions are normally satisfied.

The effect on $\bar S$ of end reflectors can readily be estimated using the approximate method. Replacing the reflectors by an effective increase of size up to h_{eff}, we obtain:

$$\bar S^{(0)}_h = \bar S^{(0)}\frac{H + 2h_{eff}}{H}\cos\frac{\pi h_{eff}}{H + 2h_{eff}}; \tag{14}$$

$$\bar S^{(1)}_h = \bar S^{(0)}_h\left[\frac{\bar S^{(1)}_M}{\bar S^{(0)}} - 2\bar S^{(0)}_b\sum_{h=3,\,5,\,7}\left(\cos\frac{\pi h_{eff}}{H + 2h_{eff}} - \cos\frac{k\pi h_{eff}}{H + 2h_{eff}}\right)\frac{1}{k^2(k^2-4)(k^2-1)}\right]. \tag{15}$$

---

*The derivation of expressions (11) and (12) is given in the Appendix.

The results of an estimate of $\bar{S}$ using formulas (13)-(15) for a high-powered water-cooled channel (RBMK) type reactor with $h_{eff} = 30$ cm were compared with the value of $\bar{S}$ obtained by the numerical method with the dependence of k, L^2, Σ_f, and g on S taken into account exactly. The approximate value of $\bar{S} = 1.37$ (which corresponds to a concentration of fission fragments in the discharged fuel of 20 kg/ton U) differed from the exact value by around 2%.

Usually, in reactors, the fuel is recharged periodically and not continuously. Suppose N rechargings take place in time T. In this case, in place of expression (10) we shall have:

$$k(z) = \frac{1}{N} \sum_{n=1}^{N} k\left(S \frac{n}{N}\right) = k_0 - b_1 \frac{N+1}{2N} S.$$

Thus, compared with continuous recharging, N partial replacements of fuel reduces the burn-up by a factor of $N+1/N$.*

For reactors using natural uranium, k(S) is approximated quite well by a polynomial of the second degree:

$$k(S) = k_0 + b_1 S + b_2 S^2. \tag{16}$$

The burn-up reactivity margin in these reactors is not large, with the result that determination of $\bar{S}$ by the ε-method is sufficiently accurate. For continuous recharging of fuel,

$$\bar{S}^{(0)} = -0.54 \frac{b_1}{b_2} + \sqrt{\left(0.54 \frac{b_1}{b_2}\right)^2 - 1.62\left[\Delta k_{ex} + \Delta k_{\kappa}(H) \frac{1-2q}{2(1-q)} \frac{1}{b_2}\right]}; \tag{17}$$

$$\bar{S}^{(1)} = \bar{S}^{(0)}\left\{1 - \frac{b_1}{(1+\alpha)\Delta k_{ref}}\left[2\alpha_2\bar{S}^{(0)}(1 + 1.945\alpha_1 + 0.9295\alpha_1^2) - \left(\frac{\Delta k_{\kappa}(H)}{1-q}\frac{1}{b_1}\right)^2 \frac{1}{64\bar{S}^{(0)}}\right]\right\}, \tag{18}$$

where $\alpha_1 = 1.85\bar{S}^0 b_2/b_1$; $\alpha_2 = 6.226 \cdot 10^{-3}$.

Formula (18) was used to estimate the burn-up of uranium for one of the variants of the CANDU-BLW boiling heavy-water reactor using natural uranium dioxide. We obtained $\bar{S} = 1.18$, which corresponds to a specific burn-up $W_t = 7.54$ (MW·days)/ton U. This value differs from that given by the numerical method (allowing for the dependence of L^2 and Σ_f on S and for a more exact dependence of k on S than given by (16)) by $\approx 2\%$.

<u>Numerical Method of Solution.</u> The approximate method described above, which was based upon perturbation theory, is convenient for quick estimates and tentative calculations. For more exact calculations, however, especially in the case of cores with an inhomogeneous composition, recourse must be made to numerical methods. The computational algorithm described below can be realized without difficulty, uses little machine time, and is very useful when one has to perform many variant calculations of the steady-state neutron height field and the depletion distribution. It is based on a sweep (a matrix sweep in the case of a two-group description of the neutron field) in conjunction with iterations of the source to which all nonlinear terms are referred. The nonlinearity of the problem means that normalization of the sought solution is not arbitrary. Accordingly, the normalization of the source on each step of the iteration process that is characteristic for linear problems is not possible in the present case. For convergence of the iterations great care must be taken to correctly formulate the right-hand sides of the system (i.e., the source). The rate of convergence of the iterations can be varied over a wide range by variously formulating the source. When choosing the initial distribution it is of no less importance not to go outside the region of gravitation towards the sought solution. A detailed analysis of these questions is given in [6]. As a result of investigations of this sort, the region of permissible initial distributions was determined and a scheme of organization of the iteration process was constructed that was close to optimum. Compared with the nonoptimal variant, this achieved a considerable reduction in the number of iterations (by 2-3 orders of magnitude in some cases). In the SKUT I and SKUT II programs for constructing the solution of initial equation (1) in the one-group and two-group approximations respectively, an iteration scheme of the following form is realized:

$$\hat{H}_2 \psi^{(n+1)} + \omega_{v_{opt}} \hat{A}\psi^{(n+1)} = -[f(S^{(n)}, \varphi^{(n)}, z) - \omega_{v_{opt}}]\hat{A}\psi^{(n)} + \hat{B}(\psi^{(n)});$$

$$\psi^{(0)} = \gamma_{opt} \sin \pi z/H \begin{pmatrix} 1 \\ 1 \end{pmatrix}. \tag{19}$$

Here $\hat{H}_2$ coincides with $\hat{H}$ for $L^2 = L_0^2$ and $D_{th(d)} = D_{0th(d)}$; the index 0 corresponds to the state for $S = 0$ and $\varphi = 0$; $\hat{B}$ describes the nonlinear dependence of L^2 on S and φ, and also of $D_{th(d)}$ on φ; $\omega\gamma_{opt} = [k_0(1 - \gamma_{opt}) - 1]/F$; in the one- and two-group approximations, respectively, the function F(z) equals $M_0^2(z)$ and $\tau(z)$; γ_{opt} is a parameter whose value is chosen to give the best convergence of the iterations.

*This sort of conclusion was first obtained in [5] under almost the same assumptions as here.
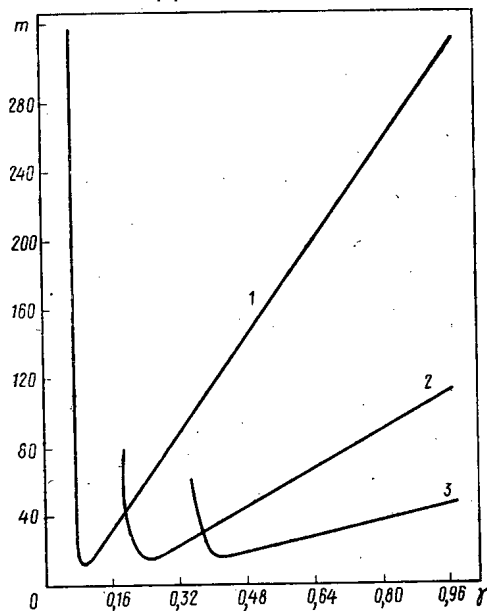
Fig. 1.   Fig. 2

Fig. 1. Dependence of number of iterations m for $\varepsilon_0 = 10^{-4}$ on γ for various initial multiplication factors k_0 for $(M/H)^2 = 0.0012$: 1) $k_0 = 1.06$; $\gamma_{opt} = 0.09$; 2) $k_0 = 1.15$; $\gamma_{opt} = 0.24$; 3) $k_0 = 1.30$; $\gamma_{opt} = 0.44$.
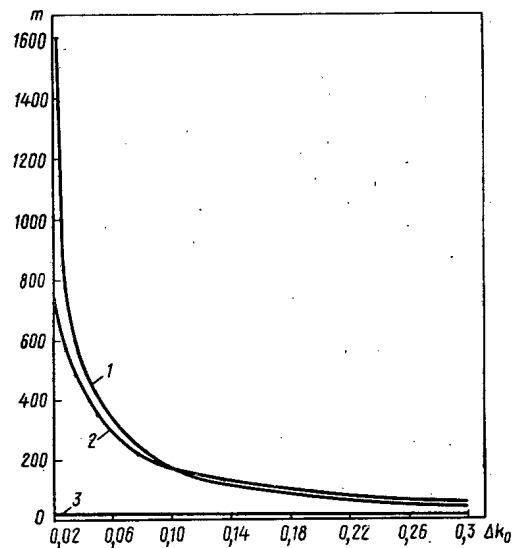
Fig. 2. Dependence of number of iterations m for $\varepsilon_0 = 10^{-4}$ on $\Delta k = k_0 - 1$: 1) $\gamma = 1$; $(M/H)^2 = 0.0012$; 2) $\gamma = 1$; $(M/H)^2 = 0.0003$; 3) $\gamma = \gamma_{opt}$; $(M/H)^2 = 0.0012$ and $(M/H)^2 = 0.0003$.

It is shown in [6] that, for enriched-uranium reactors, for which a linear dependence of k on S is more valid, γ_{opt} should be taken to be $\gamma_{opt} = 2\Delta \bar{k}_{ex}/\bar{k}_0$ when $\Delta \bar{k}_0 \geq 3\Delta \bar{k}_{ref}$ and $\gamma_{opt} = 4\Delta \bar{k}_0/3k_0$ when $1 < \Delta \bar{k}_0/\Delta k_{ref} < 3$, where $\Delta \bar{k}_{ex} = \Delta \bar{k}_0 - \Delta \bar{k}_{ref} + \Delta k_k(H)$ $(1-2q)/2$ $(1-q)$; $\Delta \bar{k}_0 = \bar{k}_0 - 1$; $\Delta \bar{k}_0$, $\bar{k}_0$ and $\Delta \bar{k}_{ref}$ denote averages with $\sin^2 \pi z/H$.

Figures 1 and 2 show the effect of the parameter γ on the number of iterations m* for the case of a homogeneous reactor without boiling of the coolant. Varying γ from 1 to γ_{opt} leads to a substantial reduction in the number of iterations for the entire investigated range of variation of Δk_0 (see Fig. 2).

An error of, e.g., 10% in the determination of γ_{opt} increases m by only 3-5 iterations, as can be seen from Fig. 1. This gives grounds for hoping that an imprecise determination of γ_{opt} will only have an insignificant effect on the iteration process.

For a natural-uranium reactor γ_{opt} is taken to equal $3\Delta \bar{k}_{ex}/\bar{k}_0$.

· The SKUT I and SKUT II programs are written in FORTRAN for the high-speed BÉSM-6 computer. The time to compute the burn-up, the energy distribution, the isotopic composition of the depleted fuel, and other reactor characteristics amounts in all to a few seconds.

APPENDIX

After insertion of Eqs. (2)-(5) and Eq. (10) into (1), we write the latter (in the case of the one-group description of the neutron field) in the following form, convenient for constructing an approximate solution:

$$\Delta \Phi + \Phi = -\varepsilon \left[\Delta k'_{ex} - \frac{\pi}{2} \bar{S}_b \Phi + A' \left(\int_0^z \Phi(z')\, dz' - q \right) \right] \Phi; \quad \Phi(0) = \Phi(\pi) = 0; \tag{20}$$

$$S(z) = \pi \bar{S}_b \Phi(z)/b'_i; \quad \int_0^\pi \Phi(z)\, dz = 1, \tag{21}$$

where $\Delta = \dfrac{d^2}{dz^2}$; $\Delta k'_{ex} = (\Delta k_0 - \Delta k_{ref})/\Delta k_{ref}$; $A' = \dfrac{\Delta k_к(H)}{(1-q)\,\Delta k_{ref}}$; $b'_i = b_i/\Delta k_{ref}$; $\Delta k_{ref} = \left(\dfrac{\pi}{H}\right)^2 M^2$.

*m is the number of iterations required to obtain a solution with a prescribed relative error ε.

701

The solution of (20) is found in the form of a power series in ε:

$$\Phi = a_0\Phi_0 + \sum_{k=1}^{\infty} \varepsilon^k [\Phi_k + a_k\Phi_0]; \tag{22}$$

$$\overline{S}_b = S_{b,0} + \sum_{k=1}^{\infty} \varepsilon^k \overline{S}_{b,k}.$$

We insert (22) into (20), equate coefficients of like powers of ε, and utilize normalization (21), when we obtain:

$$\Phi_0 = \sin z; \quad a_0 = 1/2;$$

$$\Delta\Phi_1 + \Phi_1 = -\left[\Delta k'_{\mathrm{ex}} - \frac{\pi}{2}\overline{S}_{b,0}a_0\Phi_0 + A'\left(a_0 \int_0^z \Phi_0(z')\,dz' - q\right)\right]a_0\Phi_0 = -F_0 a_0\Phi_0; \tag{23}$$

$$a_1 = -\frac{1}{2}\int_0^\pi \Phi_1(z)\,dz;$$

$$\Delta\Phi_2 + \Phi_2 = -F_0(\Phi_1 + a_1\Phi_0) - F_1 a_0\Phi_0; \tag{24}$$

$$a_2 = -\frac{1}{2}\int_0^\pi \Phi_2(z)\,dz,$$

where $\quad F_1 = -\dfrac{\pi}{2}[\overline{S}_{b,0}(\Phi_1 + a_1\Phi_0) + \overline{S}_{b,1}a_0\Phi_0] + A'\displaystyle\int_0^z (\Phi_1 + a_1\Phi_0)\,dz'.$

Inhomogeneous equations (24) and (25) have a unique solution only if their right-hand sides are orthogonal to Φ_0:

$$\int_0^\pi F_0\Phi_0\Phi_0\,dz = 0; \quad \int_0^\pi F_0(\Phi_1 + a_1\Phi_0)\Phi_0\,dz + \int_0^\pi F_1 a_0\Phi_0\Phi_0\,dz = 0. \tag{25}$$

Thus, if the $\Phi_{k-1}(z)$ are known, quadratures can be used to obtain $\overline{S}_b$ in the k-th approximation. The solution Φ_k we seek in the form

$$\Phi_k = \sum_{m \neq 1} C_m^{(k)} \sin mz. \tag{26}$$

Insertion of (26) into (24) and (25) gives the following relationships with which to determine $C_m^{(k)}$ ($m \neq 1$):

$$C_m^{(1)} = \frac{a_0}{m^2-1}\frac{2}{\pi}\int_0^\pi F_0\Phi_0 \sin mz\,dz; \tag{27}$$

$$C_m^{(2)} = \frac{1}{m^2-1}\frac{2}{\pi}\int_0^\pi [F_0(\Phi_1 + a_1\Phi_0) + F_1 a_0\Phi_0]\sin mz\,dz.$$

On evaluating the integrals in expressions (25) and (27) and carrying out some manipulations, we arrive at formulas (10) and (11).

LITERATURE CITED

1. B. L. Ioffe and L. B. Okun', At. Energ., No. 4, 80 (1956).
2. P. M. Morse and H. Feshbach, Methods of Theoretical Physics, McGraw-Hill (1953).
3. A. B. Migdal and V. P. Krainov, Approximation Methods in Quantum Mechanics, W. A. Benjamin (1969).
4. S. M. Feinberg et al., in: Proceedings of the Second Geneva Conference (Reports of Soviet Scientists) [in Russian], Vol. 2, Atomizdat, Moscow (1953), p. 217.
5. E. I. Grishanin, B. T. Ivanov, and V. N. Sharapov, At. Energ., 10, 565 (1961).
6. A. M. Afanas'ev and B. Z. Torlin, "Numerical methods of computing depth of burn-up in a reactor," Preprint ITÉF-19 (1976).

POWER EFFECT OF REACTIVITY IN FAST POWER REACTOR
WITH ALLOWANCE FOR BEHAVIOR OF FUEL UNDER
IRRADIATION

G. M. Pshakin and A. A. Proshkin   UDC 621.039.526

The total power effect of reactivity in a fast power reactor is the sum total of separate effects [1, 2]. The main contribution (90%) comes from the Doppler effect and axial expansion of the fuel slug in fuel elements which depend directly on the fuel temperature under steady-state and transient operating conditions.

Depending on the history of reactor operation and the fuel burn-up attained, the thermal conditions of fuel elements with oxide fuel may vary between wide limits at one and the same power level; this results in power effects of various magnitude. On the basis of numerous experimental data we can distinguish the three most characteristic operating modes of fuel elements and these will be described below. These modes can be established either over the entire volume of the reactor core or in separate parts of it, depending on the power level.

At the present time, a large volume of experimental data on the power effect of reactivity and its variation during operation of the plant has been accumulated on the BN-350. This allows a comprehensive verification of methods for calculating the thermal conditions of fuel elements and the power effect of reactivity with allowance for the history of reactor operation.

Effect of Thermal Loads and Irradiation on Fuel-Transfer Conditions
in Fuel Elements of Fast Reactors

The characteristic features of the behavior of oxide fuel under irradiation and when various thermal loads act on it were considered in detail in [3-11]. It was shown that in the fuel elements of fast power reactors with oxide fuel, under high thermal loads (linear thermal load $q_l \gtrsim 350$ W/cm) there is mass transfer of fuel from the center to the periphery and formation of three structural zones along the radius, i.e., one of columnar grains, one of equiaxed grains, and one of the original structure. As a result, contact between the fuel and the can is established quite quickly.

With reduced thermal loads ($q_l < 350$ W/cm), when there is no process of intensive restructuring, two most characteristic modes of fuel-element operation can be distinguished:

a) a low level of thermal loads, when the thermal stresses arising as the result of the temperature drop over the radius of the fuel slug do not cause the integrity of the fuel core to be disturbed;

b) an intermediate mode of fuel-element operation when the level of the thermal loads is such that the thermal stresses do affect the integrity of the fuel slug; healing of the cracks formed because of mass transfer takes place slowly (in comparison with the operating time of the fuel elements) owing to the comparatively low temperature gradient and temperature of the fuel element.

Let us consider each mode.

Low Thermal Loads on Fuel Element. In this mode the gap between the fuel and the can is determined by the swelling of the fuel and can and their thermal expansion. The thermal load at which there is no cracking of the fuel is found from the condition

$$\varepsilon_i \leqslant \varepsilon_b, \qquad (1)$$

where ε_i is the rate of thermal stain, $\varepsilon_b = f(T, \xi, \beta)$ is the breaking strain of the fuel, which is dependent on the temperature T, the loading rate ξ, and the burn-up β.

The rate of thermal strain on the inner and outer surfaces of a cylinder is easily determined by using the results of [9, 10]:

$$\varepsilon_t = [\alpha_f/(1-\mu_f)]\,\Delta T_f k, \tag{2}$$

where α_f and μ_f are the coefficient of linear expansion and the Poisson coefficient for the material of the fuel, ΔT_f is the temperature drop over the radius of the fuel slug as determined from known solutions of the heat conduction equations for a hollow cylinder with uniformly distributed internal heat sources, $k = [i^2/(b^2-a^2)] - (b^2-a^2)/2[b^2-a^2-2a^2 \,(\ln b/a)]$ is a geometric parameter in which b and a are the outer and inner radii of the fuel slug, and $i = a$ for $r = b$ and $i = b$ for $r = a$ (here r is the running radius).

When we take the relations for ΔT_f into account, Eq. (2) gives the value of the linear thermal load q_l at which the fuel slug retains its integrity;

$$q_l \leqslant 4\pi\lambda_f \varepsilon_b (1-\mu_f)/\alpha_f k', \tag{3}$$

where λ_f is the thermal conductivity of the fuel, depending on the temperature and density of the fuel (see, e.g., [6]);

$$k' = \left\{ \frac{i^2[b^2-a^2-2a^2\,(\ln b/a)]}{(b^2-a^2)^2} - \frac{1}{2} \right\}.$$

For a brittle material in which fracture begins in the elastic region, we can employ the criterion of maximum allowable stress, i.e., $\sigma_i \leq \sigma_b$, and then Eq. (3) becomes

$$q_l \leqslant 4\pi\lambda_f \sigma_b (1-\mu_f)/\alpha_f E k', \tag{4}$$

where $\sigma_b = f(T, \xi, \beta)$ is the ultimate strength of the brittle material and E is Young's modulus. It should be noted that the indeterminacy in the properties of the fuel material under the conditions of irradiation can result in deviations in the values found for q_l. If we use the data for unirradiated uranium oxide in the temperature range from 500 to 1000°C [11], then we can find that for $q_l \leq 70\text{-}100$ W/cm the slug will preserve its integrity.

Up to the level of loads determined by Eq. (3) or (4) the temperature drop between the inner surface of the can and the surface of the fuel is calculated from the model of a conducting gas gap [3].

The thermal conductivity of the medium in the gap is determined with allowance for the composition of the gas mixture (initial helium + gaseous fission products) and its temperature [12]. The composition of the mixture can be found as a function of the thermal conditions and the burn-up of the fuel on the basis of the data of [6, 13]. The can and fuel dimensions necessary for finding the thermal conductivity of the gap can be found from the solution of the equation for the deformed state of the fuel element in accordance with the "gas model" of the fuel−can interaction [14]. Since the thermal conductivity of the gaseous medium in the gap and the fuel and can dimensions depend on the temperature, the temperature drop across the gap is determined by several iterations until the required accuracy is attained.

Intermediate Operating Conditions of Fuel Elements. When the level of thermal loads exceeds the value given by Eq. (3) or (4), the fuel begins to crack and the conducting-gas-gap model becomes physically unreal. A more realistic model should take account of the contact established between fuel and can, at least on a limited area. This model has come to be known as the contact-conductivity model [3]. The known relations [3,15] for this model include various constants which can be found only experimentally and this hinders the use of a computational approach to the determination of the fuel temperature. Experimental data on the contact conductivity for intermediate operating conditions for fuel elements $(100 < q_l < 350$ W/cm) show that it lies within the interval 0.2-0.45 W/(cm$^2\cdot$deg), depending on the initial gap and thermal load [3, 13].

High Thermal Loads on Fuel Elements. With a thermal load $q_l > 350$ W/cm the temperature is found to be high and the temperature gradients over the radius of the fuel slug is found to be large, resulting in the mass transfer of fuel from the center to the periphery and healing of the cracks formed. The restructured fuel comes in contact with the can and thus the conditions of heat transfer in the fuel element. These transformations proceed quite rapidly and the higher q_l is, the more rapidly they occur. As in the case of intermediate conditions, the temperature drop between the fuel and the can for this case is found from the contact-conductivity model. On the basis of numerous experiments it was shown [3, 15] that the coefficient α_c of contact conductivity [W/cm$^2\cdot$ sec] depends on the contact pressure, the state of the contacting surfaces, their temperature, etc. The negligible effect of the gaseous medium in this case is explained by the fact that the main part of the heat is transferred through the contacting surfaces [3].

Analysis of the various experiments [3-5, 15] allows the following empirical relation to be assumed for α_c for thermal loads $q_l > 350$ W/cm:

$$\alpha_c = (\alpha_0 + \alpha_1\bar{p} + \alpha_2\bar{p}^2) + \alpha_3 \exp(\alpha_4 T), \tag{5}$$

where $\alpha_0 = 0.45$, $\alpha_1 = 0.184\cdot10^{-3}$, $\alpha_2 = 0.63\cdot10^{-6}$, $\alpha_3 = 0.035$, $\alpha_4 = 0.9\cdot10^{-3}$, T is the mean temperature in the gap

(in °K), and $\bar{p}$ is the contact pressure at the fuel–can interface (kg/cm²) which is found from the solution of the problem of fuel–can interaction according to the contact model [14]. The temperature distribution over the radius of the fuel slug in this case should be carried out with allowance for changes in its geometry as the result of mass transfer of the fuel. The change in the size of the inner opening and the outer diameter of the slug can be obtained from the condition that the mass of the fuel and the temperatures at which growth of columnar and equiaxed grains occur remain constant. Analytically, this can be written as

$$
\begin{cases}
\dfrac{q_s \, r \, \mathrm{fc\ in}}{2\,(1-\bar{\rho}_0^2)} \left[1 - \bar{\rho}_c^2 - 2\bar{\rho}_0^2 \ln \dfrac{1}{\bar{\rho}_c} \right] = \displaystyle\int_{T_h}^{T_c} \lambda_f(T)\,dT; \\[2ex]
\dfrac{q_s \, r \, \mathrm{fc\ in}}{2\,(1-\bar{\rho}_0^2)} \left[1 - \bar{\rho}_h^2 - 2\bar{\rho}_0^2 \ln \dfrac{1}{\bar{\rho}_e} \right] = \displaystyle\int_{T_h}^{T_e} \lambda_f(T)\,dT; \\[2ex]
\bar{\rho}_0 = \sqrt{ \dfrac{\gamma_1 - \gamma_0}{\gamma_c} - \dfrac{\gamma_c - \gamma_e}{\gamma_c}\,\bar{\rho}_c^2 + \dfrac{\gamma_e - \gamma_1}{\gamma_c}\,\bar{\rho}_e^2 },
\end{cases}
\qquad (6)
$$

where $T_c = 1750°C$ is the temperature of the onset of columnar-grain formation [3, 6, 8], $T_e = 1450°C$ is the temperature of the onset of equiaxed-grain formation [3, 6, 8], γ_1 and γ_0 are the initial and effective fuel densities, respectively, in the cross section of the fuel element, γ_c and γ_e are the densities of the material in the zone of columnar and equiaxed grains, respectively, and $\bar{\rho}_0 = a/r_{fc\ in}$, $\bar{\rho}_e = \bar{r}_e/r_{fc\ in}$, and $\bar{\rho}_c = r_c/r_{fc\ in}$ are, respectively, the radii of the opening and of the zones of equiaxed and columnar grains, transferred to the inner radius of the fuel-element can.

The three characteristic modes considered above for fuel elements of a fast power reactor cannot always be realized during reactor operation. Modes of operation in which power is built up at the outset of reactor operation, after shut-downs for recharging after an emergency signal, transitions from a reduced power to a higher level, and vice versa — all of this can result in various combinations of characteristic operating modes for fuel elements, thermal conditions for the fuel, and therefore to various manifestations of power reactivity effects.

Analysis of Thermal Conditions of Fuel and Power Reactivity Effect of Fast Reactor with Account for Its Operating Conditions

Let us consider the effect of variations in the fuel temperature during operation of a fast reactor on the total power effect and its components:

The sodium component of the power effect is determined as [16]:

$$
\rho_{Na} = \sum_{i=1}^{n} \left(\frac{\partial \rho}{\partial T} \right)_{Na}^{i} \frac{\Delta T_i}{2} + \left(\frac{\partial \rho}{\partial T} \right)_{Na}^{u.e.s\ i} (\Delta T_i + \Delta T_{u.e.s.i}),
\qquad (7)
$$

where n is the number of throttling zones in the reactor; $(\partial\rho/\partial T)_{Na}^{i}$, sodium component of the i-th zone in the isothermal temperature coefficient of reactivity; $(\partial\rho/\partial T)_{Na}^{u.e.s.i}$, sodium component of the end shield above the throttling zone to the isothermal temperature coefficient of reactivity; and ΔT_i and $\Delta T_{u.e.s.i}$, respectively, the heating of sodium in the i-th zone and the upper end shield above that zone.

The changes in coolant heating during operating at fixed reactor power are negligible and have practically no effect on the total power effect of reactivity. According to estimates, the variations in the sodium component owing to the isotope composition of the fuel are about 17% and this results in a slight reduction in the total power effect since the sodium component contributes only 4-6% to it [1, 16]. The sodium heating increases linearly with the power level and this relation is not altered with the fuel burn-up.

The radial part of the geometric component in the power effect is determined only by the heating of the walls of the fuel-assembly walls. This component is not related directly to the fuel temperature and its value in the total power effect does not exceed ~7%.

The axial part of the geometric component in the power effect is determined by

$$
\rho_z = a\alpha_f \Delta \bar{T}_f,
\qquad (8)
$$

where α_f and $\Delta \bar{T}_f$ are the coefficient of linear expansion and the mean temperature drop in the fuel, respectively, and a is a proportionality factor which depends weakly on the fuel burn-up (for BN-350, $a = {}^-0.222$ and $^-0.2136$ for fresh and spent fuel, respectively).

Thus, this component is determined almost completely by the fuel temperature. In calculating the effect of the axial expansion of the fuel it is necessary to take account of the interaction of the fuel with the can. At

705
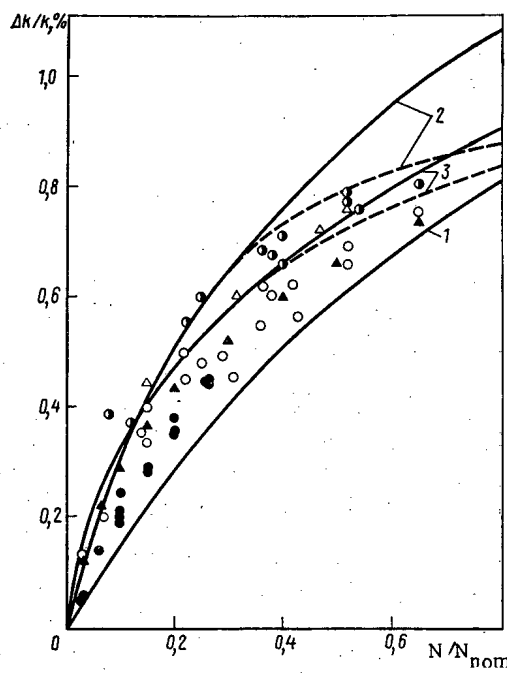
Fig. 1. Power effect of reactivity vs power level in BN-350 for fuel temperature calculated from only conducting-gas-gap model (———) and with allowance for fuel cracking (———): 1) "fresh" fuel; 2, 3) burn-up of 2 and 5% (calculation); ●) power start-up; O, △, ◑, ▲) burn-up of ~2, 3, 4, and 5.5% (experiment).

low thermal loads the increase in the height of the fuel rod can be regarded as free expansion and the effect of reactivity can be calculated from Eq. (8). For the mode of high thermal loads it is necessary to take account of the possibility of the can restraining the expansion of the fuel rod.

The Doppler effect during power build-up in a fast reactor is given by [17]

$$\rho'_D = \int_V \int_{T_0}^{T} \rho'_D(T, r) \, dr \, dT, \qquad (9)$$

where $\rho'_D(T, r)$ is the Doppler coefficient of reactivity for a unit volume dr at a fuel temperature T; V, reactor volume; and T_0 and T, temperatures of the fuel at zero and operating power levels, respectively. Computational studies showed that the change in the Doppler constant as a function of the fuel burn-up is extremely small for the BN-350. Therefore, the change in the Doppler effect as the fuel burns up is due mainly to a change in the thermal conditions of the fuel elements.

Let us consider the variation in the power effects of reactivity in the BN-350 as observed during operation [16, 18, 19] by using the technique of determining the temperature for characteristic operating modes for the fuel elements.

Measurements of the Power Effect during Power Start-Up. At the time of power start-up [16] the reactor core was made up of "fresh" fuel assemblies. The fuel elements had a purely helium medium in the contact gap. During the measurements the reactor was brought up to a power level of 260 MW [16], which resulted in a linear thermal flux at the most stressed point, $q_l \approx 100$ W/cm. With this thermal load the fuel rods retain their integrity and the temperature field can be calculated from the conducting-gas-gap model. The experimental and calculated values of the power effect for the power start-up measurements are given in Fig. 1. The agreement between the experiment and calculations can be considered satisfactory.

Measurement of the Power Effect after Reactor Operation at Low Power Levels. In the initial stage of reactor operation, when the fuel burn-up was ~2%, the power effect of the reactivity was measured at various power levels up to 550 MW [16]. The level of thermal loads in the fuel elements during the measurements reached ~200 W/cm.

As in the previous case, the computational model of the reactor was divided into separate zones in r, z geometry and the calculation was carried out according to the mean heat release in them. The volume of the zones was chosen so that the nonuniformity of the heat release in them would not exceed $\sim 5\%$. As the power level increased, a computational model was chosen for each zone in accordance with the heat load. At $q_l > 100$ W/cm the fuel temperature was calculated from the conducting-gas-gap model; at $q_l > 100$ W/cm, according to the contact-conductivity model and α_c was calculated by means of linear interpolation with respect to q_l between two extreme values: $\alpha_c = 0.2$ W/cm$^2 \cdot$ deg for $q_l = 100$ W/cm and 0.45 W/cm$^2 \cdot$ deg for $q_l = 350$ W/cm.

Measurement of the Power Effect in Intermediate Steady State. While operating at a power level of 650 MW the reactor reached the design burn-up of 5% [18] and began to operate in a settled intermediate steady state. During this period the power effect was measured once again [19]. The level of the thermal loads at a power of 650 MW was 220 W/cm. The calculation for this case was carried out in the same way as for the previous measurements, with account for the burn-up attained (see Fig. 1). Comparison of these results with the experiment reveals quite good agreement. The fact that the calculated values are slightly higher than the experimental values indicates better heat transfer conditions in the fuel elements in reality that assumed in the calculations.

Conclusions. The proposed computational approaches for determining the thermal conditions of the fuel elements with allowance for their operating history have made it possible to bring closer together the calculated and experimental values of the power effect of reactivity and its dependence on the power level in the BN-350.

Analysis of the causes of the divergence of the experimental and calculated values of the power effect of reactivity showed that these divergences, as well as changes in the effect during operation, are due mainly to the thermal conditions of the fuel elements. The principal indeterminacy in the calculation of the thermal conditions of the fuel elements is due to the contact thermal conductivity and its variation with the operating conditions of the fuel elements in the reactor. In order to eliminate this indeterminacy it is necessary to carry out experimental investigations to ascertain the contact thermal conductivity as well as to refine the physico-mechanical properties of the fuel (thermal conductivity, ultimate strength, etc.) as a function of the burn-up and temperature.

LITERATURE CITED

1. V. V. Orlov et al., Kernenergie, **4**, 112 (1969).
2. G. Khammel and D. Okrent, Reactivity Coefficients in Large Fast-Neutron Power Reactors [in Russian], Atomizdat, Moscow (1975).
3. B. Lastman, Radiation Effects in Uranium Oxide [in Russian], Atomizdat, Moscow (1964).
4. I. G. Lebedev et al., Preprint NIIAR P-3 (297), Dimitrovgrad (1977).
5. J. Robertson et al., J. Nucl. Mater., **7**, 225 (1962).
6. M. Lyons et al., Nucl. Eng. Design, **21**, 167 (1972).
7. O. D. Kazachkovskii et al., in: Proc. Symp. of COMECON Member-Nations "State of the Art and Prospects of Work on Creation of Atomic Power Plants with Fast-Neutron Reactors," Izd. ONTI FÉI, Obninsk, Vol. 2 (1969), p. 95.
8. W. Baily et al., Trans. Am. Nucl. Soc., **9**, 42 (1966).
9. B. A. Boley and J. H. Weiner, Theory of Thermal Stresses, Wiley (1960).
10. A. M. Kats, Theory of Elasticity [in Russian], Gosteorizdat, Moscow (1956).
11. R. B. Kotel'nikov et al., High-Temperature Nuclear Fuel [in Russian], Atomizdat, Moscow (1969).
12. H. Ubisch et al., in: Proc. Second United Nations Int. Conf. on the Peaceful Uses of Atomic Energy, Geneva (1958), Vol. 7, p. 697.
13. M. Freshley, Nucl. Eng. Design, **21**, 264 (1972).
14. Yu. I. Likhachev and V. Ya. Pupko, Strength of Fuel Elements of Nuclear Reactors [in Russian], Atomizdat, Moscow (1975).
15. V. S. Yamnikov et al., At. Tekh. Rubezhom, No. 2, 21 (1969).
16. V. V. Orlov et al., At. Energ., **42**, No. 1, 3 (1977).
17. G. M. Pshakin, in: Nuclear Constants [in Russian], Vol. 21, Atomizdat, Moscow (1976), p. 208.
18. D. S. Yurchenko et al., in: Proc. IAEA Symp. on Design, Construction, and Operating Experience of Demonstration LMFBRL, Bologna, April 10-14 (1978), IAEA-SM-225/60.
19. L. A. Alekhin et al., in: Proc. IAEA Symp. of Design, Construction, and Operating Experience of Demonstration LMFBRL, Bologna, April 10-14 (1978), IAEA-SM-225/60.

THEORETICAL AND EXPERIMENTAL INVESTIGATION
OF SODIUM VOID EFFECT OF REACTIVITY

S. P. Belov, P. V. Gerasimov,
Yu. A. Kazanskii, V. I. Matveev,
G. M. Pshakin, and P. L. Tyutyunnikov

In analysis of the safety of fast reactors under design it is absolutely necessary to consider emergency situations due to partial or complete loss of coolant from the reactor core. For power reactors with a high unit power this problem becomes particularly acute since in this case the loss of sodium from the reactor core may result in a large ($\sim 1\%$ $\Delta k/k$) positive reactivity effect.

An emergency situation with escape of coolant is considered both for complete drainage of the reactor and within the framework of a local failure when the coolant escapes from one fuel assembly (FA) or molecule (7 FA). Studies on the dynamics of reactivity variations during local failures are of particular interest since they provide the necessary information for diagnosis of an operating reactor. The methods used to calculate the sodium-void effect of reactivity (SVER) were verified on uranium critical assemblies–models BOR-60 (assembly BFS-21), BN-350 (assembly BFS-22), BN-600 (assembly BFS-24), as well as directly on BN-350.

Method of Calculation of SVER

At the present time the multigroup diffusion approximation is the most widespreadly used technique in design calculations, including calculations to determine the SVER. In view of this, in calculations of SVER experiments performed on critical assemblies, the present authors resorted primarily to computational programs realizing this approximation.

The value of SVER can be found by both the direct method (from the change in the effective multiplication factor) and from perturbation theory. The applicability of perturbation theory in SVER calculations with the introduction of the necessary corrections is quite substantiated [1]. The overall SVER can be calculated by this method as well as by others. The local SVER can be calculated only with perturbation theory.

For SVER calculations use was made of the BNAB-70 catalog of microconstants with various ways of preparing the macroconstants when solving a reactor problem: in the traditional group [2] and subgroup [3] approximations. The calculations are carried out in one-dimensional [2] and two-dimensional [4] geometries. One of the main difficulties in SVER calculations is its sensitivity to the nuclear data used.

Experimental Methods of Studying SVER

Experimentally, SVER is determined as the difference between the reactivity states of the system (reactor or critical assembly) with and without sodium in a chosen volume. The principal difficulty in performing such experiments is associated with ensuring that the other parameters of the system remain constant when the sodium is removed. The sodium is removed from critical assemblies in the following way on BFS stands.

Reassembly of Experimental Ports. The SVER is measured in this way for considerable volumes. The method is laborious since it is necessary to replace the sodium slugs with cans of sodium slugs in a large number of cells. It was determined that the statistical error of reactivity measurement with one experimental port of the BFS stand reassembled, calculated as the rms deviation with repeated reassemblies, is $\pm 8 \cdot 10^{-7}$ $\Delta k/k$ and with reassembly of n ports is $\sqrt{n}$ times larger.

Measurement of the Efficiency of the "Sodium Tube." In this case, measurements are made of the reactivity effect from replacement of a port filled with sodium slugs by a port filled with empty cans. The height of the "sodium column" is equal to the height of the reactor core and the end parts are filled with the same material as are the adjacent experimental ports. This mode of measurement has a number of experimental advantages but is more involved from the point of view of its computational interpretation owing to the necessity of taking account of the anisotropy of neutron diffusion over the empty port.

TABLE 1. SVER in FBFS-21 Critical Assembly, 10^{-4} $\Delta k/k$

Method of calculation*	No. of ports reassembled				
	1	7	19	37	50
Expt.	$-2,8\pm$ $\pm0,1$	$-21\pm$ $\pm1,8$	$-74+$ ±4	$-146+$ ±4	$-194+$ $\pm4,5$
Calc. by perturbation theory (BNAB-64 constants)	$-3,5$	$-28,7$	-84	-166	-228
Calc. by perturbation theory (BNAB-70 constants)	$-3,8$	$-30,8$	$-90,3$	-178	-245
Direct calc. in r, z geometry	—	—	—	—	-211

*The calculated value of β_{eff} was used in determining the reactivity in units of $\Delta k/k$.

Slow Oscillator Method. An experimental rod with the composition of the reactor core is moved over the height by a lifting mechanism so that a chosen volume containing no sodium ("sodium void") can be withdrawn from the center of the reactor core beyond the end shield right during the process of measurement. The change in the neutron density in the critical assembly as the result of this displacement is recorded in the memory of a computer and is processed by solving the transformed kinetic equation [5]. In a 2-h cycle of measurements (20 pairs of displacements) the error in the determination of the change in reactivity with the introduction of a sodium void is $(2-4) \cdot 10^{-7}$ $\Delta k/k$; in this case a correction is made for the drift of the system reactivity with time.

The method for unsealing fuel assemblies in a power reactor consists in the following: the state of the reactor in respect of reactivity is determined with hermetically sealed fuel assemblies (FA) inserted; they are then withdrawn, unsealed, and loaded into the reactor, after which the state of reactivity is determined with the controls in the same position. The main difficulty in such an experiment is that of reproducing the same state in respect of coolant temperature and position of controls after the FA have been reloaded. Careful monitoring of the position and calibration of the controls, measurement of the coolant temperature during the experiment, and prior determination of the isothermal temperature coefficient of reactivity make it possible to quite properly introduce the necessary corrections and to have a total error of $\pm 3 \cdot 10^{-5}$ $\Delta k/k$ for such an experiment, e.g., in a BN-350 reactor.

Results of Experimental and Theoretical Investigations on SVER

BFS-21 Critical Assembly, a Model of the BOR-60 Reactor. In the model of the reactor (as well as in the BOR-60 reactor itself) the SVER depends mainly on the leakage components. In the experiments we employed the method of reassembling fuel rods [6]. The change in the reactivity was determined from the change in the multiplication in the system in the subcritical state as well as before the reactor core was charged up to the critical state. The calculations were carried out according to the perturbation theory and by the direct method (Table 1).

Comparison of calculation with the SVER experiment for the BFS-21 assembly shows that calculation overestimates the leakage components in SVER by 10-20%.

BFS-22 Assembly, a Model of the BN-350 Reactor. This assembly was used to measure the SVER around the central boron rod with an efficiency of ~1% $\Delta k/k$ [7]. The formulation of such an experiment was motivated by the fact that for reactors with a core volume exceeding 1000 liters and with an overall negative SVER there are separate regions with positive SVER since the moderation component near the absorbing rods becomes substantially more positive.

Measurement of SVER on the BFS-22 assembly was carried out by the method of reassembling the technological ports and the reactivity was determined from the period required to build up the power. The calculations were performed by perturbation theory with a correction for unblocking the resonance cross sections of uranium as well as by the direct method. Comparison of the experimental and calculated values of the SVER for the BFS-22 assembly (Table 2) shows that calculation overestimates the absolute value of the moderation components but quite correctly describes the SVER distribution around a highly absorbing rod.

TABLE 2. SVER in BFS-22 Critical Assembly with Absorbing Rod in Center of Core, 10^{-4} $\Delta k/k$

No. of row	Total No. of ports in row	Expt.	Calc. by perturbation theory (BNAB-70 constants)	Calc. by direct method (BNAB-70 constants)
1	10	$+1\pm0,1$	$+1,69$	—
2	16	$+0,47\pm0,1$	$+1,18$	—
3	33	$-0,61\pm0,11$	$+0,18$	—
4	28	$-2,52\pm0,18$	$-0,92$	—
5	34	$-4,12\pm0,21$	$-2,12$	—
6	40	$-6,5\pm0,25$	$-3,48$	—
7	46	$-9,65\pm0,46$	$-5,66$	—
$\sum_{i=1}^{7}$	196	$-21,9\pm1,0$	$-9,13$	$-5,16$

BFS-24, a Model of the BN-600 Reactor. The SVER in the BFS-24 critical assembly with a fully inserted system of absorbing compensators was studied by two methods [8]: by the method of reassembly in the 60° sector and by the sodium tube method. The calculations were carried out in accordance with perturbation theory.

Figure 1 shows the distribution of the efficiency of the sodium tube in the three most characteristic radial directions. The value of the overall SVER in the BFS-24 critical assembly for the 60° sector is $-3.7 \cdot 10^{-4}$ $\Delta k/k$ (calculation) whereas in experiment by the method of reassembly and integration the sodium tube efficiencies are $(-4.6 \pm 0.2) \cdot 10^{-4}$ and $(-9.0 \pm 0.5) \cdot 10^{-4}$ $\Delta k/k$, respectively. The considerable difference in the experimental values is due to the inadequacy of the geometry during the measurements.

Comparing the calculated and experimental distribution of the sodium-tube efficiency (see Fig. 1), we can say that calculation underestimates the absolute value of the SVER but quite correctly describes the character of its volume distribution in the reactor with a system of absorbing rods.

In the model of the BN-600 reactor without boron compensators the SVER was measured for the central region of the core by the reassembly method and the sodium void (height 40 cm) was moved by the slow-oscillator method over the height of the reactor from the central plane beyond the end reflector. The most characteristic height distributions of the SVER are given in Fig. 2.

For the central region we obtained experimental SVER values by using various measuring methods: slow oscillator (central port) $(-6.25 \pm 0.30) \cdot 10^{-6}$ $\Delta k/k$; reassembly of 7 ports in center $(-51.84 \pm 0.52) \cdot 10^{-6}$ $\Delta k/k$; reassembly of 19 ports in center $(-5.76 \pm 0.52) \cdot 10^{-6}$ $\Delta k/k$.
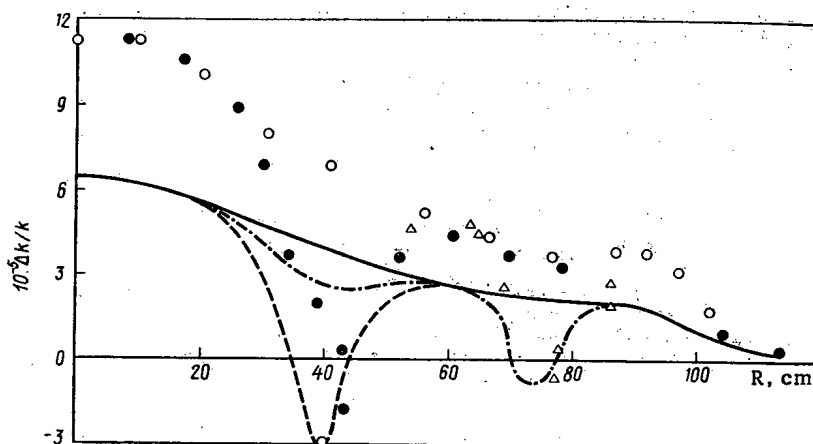
Fig. 1. Radial distribution of efficiency of sodium tube in BFS-24 critical assembly through cell of safety rod [——) calculation; O) experiment]; through boron compensator of first ring [———) calculation; ●) experiment]; through boron compensator of second ring [———) calculation; Δ) experiment].

710
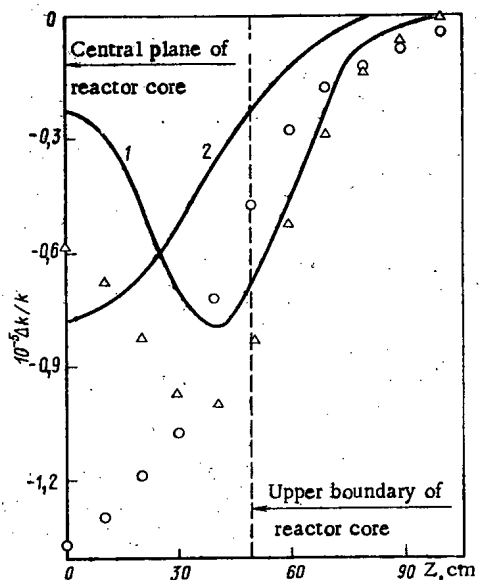
Fig. 2. Axial distribution of efficiency of
sodium void (h = 40 cm) in center of BFS-24
critical assembly [1) calculation; △) experi-
ment] and at interface between reactor core
and side shield [2) calculation; O) experiment].

The agreement between the experimental values obtained by various methods of measurement indicates
the additivity of the effect under an increase in the volume from which the sodium is removed. This makes it
possible to determine SVER for various volumes, taking account of the spatial distribution measured by the
slow-oscillator method.

Calculations by the perturbation theory (Table 3) once again confirmed the conclusions from experiments
on other BFS critical assemblies:

the spatial distribution of the SVER is described quite correctly by calculations according to perturbation
theory;

calculation underestimates the absolute value of the effect, especially in the central region in which the
moderation component predominates.

BN-350 Reactor. Measurements of SVER in the BN-350 were made by the method of unsealing two or
three experimental fuel assemblies at one time [9]. The experimental and calculated SVER values per BN-350
fuel assembly are given in Table 4. Experimental and theoretical investigations of SVER in the BN-350 con-
firmed the results of studies on critical assemblies.

Generalizing the results of SVER studies on the BFS and BN-350 critical assemblies, we can make the
following conclusions. The divergence between the experiment and calculations for the overall SVER reaches

TABLE 3. SVER in Model of BN-600 Reactor
without Boron Compensators

Position of sodium void	Vol. from which Na is removed, liters	Quantity of sodium removed, kg	Reactivity effect, 10⁻⁴ Δk/k	
			expt.	calc.
At center (h= 40 cm, 19 ports)	17,1	4,75	−1,09±0,06	−0,453
At center (h= H_core, 36 ports)	79,1	20,9	−6,30±0,35	−5,04
At periphery (h= H_core, 71 ports)	156,5	43,3	−10,0±0,4	−7,33

711

TABLE 4. SVER in BN-350 Reactor, 10^{-5} $\Delta k/k$

Site of measurement	Distance from center of core, cm	Expt.	Calc.	
			two-dimensional perturb. theory	perturb. theory*
Low-enrichment zone	9,85	—6,7±1,5	—3,0	—5,8
	19,7	—4,6±1,5	—3,4	—6,0
	39,4	—0,5±1,5	—5,5	—6,6
	54,6	—10,1±1,5	—8,1	—7,6
High-enrichment zone	59	—7,4±1,0	—9,6	—8,0
	69	—9,8±1,0	—13,1	—8,7
	78,7	—8,8±1,0	—7,1	—5,2
Shield	98,5	—1,8±1,5	—0,2	—0,2

*In the one-dimensional calculations a SVER correction for the end shields, obtained from direct two-dimensional calculations, was introduced.

30% and for the local coefficient it is 150-200%. The main cause of these differences is the consistent overestimation of the positive moderation component by the diffusion multigroup approximation. Some overestimation of the negative leakage component (see experiments on BFS-24 assembly) compensate for the overestimation of the positive part of the overall SVER for reactors of the BN-350 and BN-600 types. Obviously, for reactors with a large core volume, and especially with plutonium fuel, in which the moderation component will play the principal role, the difference between experiment and calculation in the overall SVER will exceed 30%. One of the main causes of the difference lies in the errors of the system of constants used. Thus, it was shown in [10] that the constant component of the error of SVER calculations with the BNAB-70 catalog is equal to roughly 0.5% $\Delta k/k$ in the overall SVER.

LITERATURE CITED

1. G. Khammel and D. Okrent, Reactivity Coefficients in Large Fast-Neutron Power Reactors [in Russian], Atomizdat, Moscow (1975).
2. I. P. Markelov et al., in: Papers on Programs and Methods of Physical Calculation of Fast Reactors [in Russian], NIIAR, Dimitrovgrad (1975), p. 34.
3. V. F. Khokhlov et al., in: Nuclear Constants, No. 8, Part 3 Izd. TsNIIatominform, Moscow (1972), p. 3.
4. V. V. Orlov et al., in: Fast Reactor Power Station, BNES, London (1974), p. 255.
5. A. I. Mogil'ner et al., At. Energ., 36, No. 5, 358 (1974).
6. A. A. Blyskavka et al., Preprint FÉI-201, Obninsk (1970).
7. V. V. Orlov et al., Preprint FÉI-306, Obninsk (1972).
8. V. V. Orlov et al., in: Proc. Int. Symp. on Physics of Fast Reactors, Tokyo, Oct. 16-19 (1973), Vol. 1, p. 571.
9. V. V. Orlov et al., At. Energ., 36, No. 2, 97 (1974).
10. A. A. Van'kov et al., in: Nuclear Constants [in Russian], No. 16, TsNIIatominform, Moscow (1974), p. 20.

MINIMIZATION OF LOSS OF ENERGY OUTPUT BY SYSTEM
OF REACTORS OPERATING WITH A VARIABLE LOAD SCHEDULE

V. I. Naumov and A. M. Zagrebaev UDC 621.039.516.2

The necessity for atomic power plants to operate with a variable 24-h load schedule [1] requires that a reactivity margin be reserved to compensate for transient xenon poisoning. The magnitude of that margin depends on the length of time for which the reactor must operate at reduced power W, on the degree of reactor power reduction $\varepsilon = W/W_n$ (where W_n is the nominal reactor power), and on other characteristics. In the point model of a reactor the reactivity margin ensuring that the plant operates at reduced power εW_n for any length of time is $\Delta\rho = x_{max} - x_r$, where x_r and x_{max} are the equilibrium and maximum (after the power reduction) concentrations of xenon, normalized to $\nu_f \Sigma_f / \sigma_x$ (σ_x is the xenon absorption cross section, Σ_f is the macroscopic fission cross section of the reactor core, and ν_f is the mean number of secondary neutrons per fission event).

Reservation of a reactivity margin for transient xenon poisoning results in a loss of energy output, $\Delta Q = Q_{max} - Q$, where Q_{max} and Q are the energy outputs of the reactor during operation according to the basic schedule and a variable 24-h load schedule, respectively. The energy output loss can be associated with the reserved reactivity margin by the linear relation [2] $\Delta Q = \Delta\rho/a$, where a is the burn-up rate at the end of the run.*

An atomic power plant may comprise several reactors with different characteristics (nominal electric power, burn-up rate, etc.). With a limited reactivity margin, e.g., for reactors with continuous fuel recharging or for reactors with discrete recharging at the end of a run, there arises the problem of optimizing the distribution of reactivity margins in the system of reactors in the power plant in order to minimize energy output losses while carrying out the given schedule of a daily reduction in the power of the plant.†

The problem is formulated as follows: find the distribution of the operational reactivity margins which minimize the linear form

$$\sum_{i=1}^{N} \Delta Q_i = \sum_{i=1}^{N} \Delta\rho_i/a_i = S \tag{1}$$

with the constraints

$$\sum_{i=1}^{N} \delta_i \varepsilon_i (\Delta\rho_i) = \alpha;$$

$$0 \leqslant \Delta\rho_i \leqslant \Delta\rho_{i\,max}, \tag{2}$$

where N is the number of reactors in the atomic power plant; δ_i, fraction of electric power from the i-th reactor; $\delta_i = W_{in}/\sum_{i=1}^{N} W_{in}$; ε_i, degree of power reduction in the i-th reactor; and α, prescribed degree of power reduction in the entire plant.

Note that optimization is possible only if $0 < \alpha < 1$ since for $\alpha = 0$ and $\alpha = 1$ the values of the operational reactivity margins are determined by $\Delta\rho_i = \Delta\rho_i\,max$ and $\Delta\rho_i = 0$. The effect from optimization, therefore, has its most pronounced impact in the middle part of the regulated range.

Figure 1 shows the plot of $\varepsilon(\Delta\rho)$ for various values of the nominal neutron flux densities with the assumption of an instantaneous reduction in reactor power. With a nominal neutron flux density $\sim 10^{13}$ neutrons/cm²·

---

*For a reactor with continuous fuel recharging, the quantity a is taken to mean the proportionality factor between the reactivity margin and the corresponding energy output loss.
†Modes of changes in the power of reactors operating in a system were optimized in [3] from the point of view of minimum absorption in xenon.

713
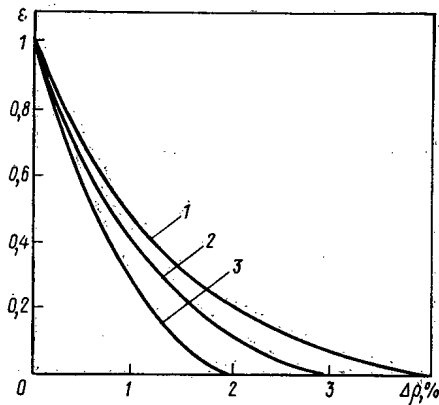
Fig. 1   Fig. 2

Fig. 1. Degree of reactor power reduction vs reactivity margin for neutron flux densities: 1) $\varphi = 5 \cdot 10^{13}$; 2) $4 \cdot 10^{13}$; 3) $3 \cdot 10^{13}$ neutrons/cm$^2 \cdot$ sec.
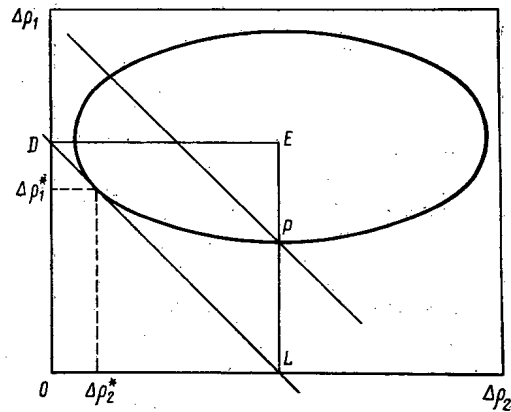
Fig. 2. Graphical interpretation of solution of optimization problem for system of reactors.

sec the $\varepsilon(\Delta\rho)$ relation is nonlinear. The optimization problem formulated belongs to the class of nonlinear programming problems and in the general case is solved numerically.

In order to obtain qualitative results we approximate $\varepsilon(\Delta\rho)$ with a polynomial of the second order. Numerical estimates show that the curves in Fig. 1 are approximated quite well by $\varepsilon = (1 - \Delta\rho/\Delta\rho_{max})^2$, where $\Delta\rho_{max} = C\varphi$ and C = const. Let us consider a system consisting of two reactors. In this case the problem can be solved analytically [4] and has a simple graphical interpretation (Fig. 2). The range of the variables $\Delta\rho_1$ and $\Delta\rho_2$ is the rectangle ODEL; the function being minimized, $S = \Delta\rho_1/a_1 + \Delta\rho_2/a_2$, is a straight line; the equation of the relation between the variables, reduced to a canonical form, is an ellipse:

$$\frac{(\Delta\rho_1 - \Delta\rho_{1}max)^2}{\varphi_1^2/\delta_1} + \frac{(\Delta\rho_2 - \Delta\rho_2 max)^2}{\varphi_2^2/\delta_2} = \alpha C^2. \tag{2a}$$

As follows from Fig. 2 (which, for definiteness, shows an ellipse with a semiaxis ratio of $\frac{\varphi_1^2}{\delta_1} / \frac{\varphi_2^2}{\delta_2} > 1$ and a straight line with a slope of $a_1/a_2 = 1$), the optimal solution is presented by either the case where the straight line is tangent to the ellipse, if the point of tangency belongs to rectangle ODEL, or the case in which the ellipse intersects the coordinate axis if the point of tangency does not belong to the range of definition. The coordinates $(\Delta\rho_1^*, \Delta\rho_2^*)$ of the tangency point are the optimal reactivity margins. Note that the maximum of the function is attained at the point P. By S_{min} and S_{max}, respectively, we denote the minimum and maximum values of the function. The effect due to the optimization will be estimated as $\Delta S = (S_{max} - S_{min})/(\Delta\rho_1 max + \Delta\rho_2 max)$.

To explain the physical aspect of the problem and to obtain estimates of the possible optimization effect we consider several concrete situations.

1. The reactors differ only as to the fraction of power $\varphi_1 = \varphi_2$, $a_1 = a_2$, $\delta_1/\delta_2 > 1$. The largest reactivity margin should be produced in the reactor with the highest power fraction (see Fig. 2). Indeed, the higher the power fraction of a reactor in the system, the lesser the extent to which a change in that power can ensure the required reduction of power in the system as a whole. In this case a smaller reactivity margin has to be reserved in the reactor with the high power (see Fig. 1), and this results in a reduction of the total energy output loss. The optimization effect for $\delta_1/\delta_2 = 2$ and $\alpha = 0.5$ is 30%.

2. The reactors differ only as to burn-up rate, $\varphi_1 = \varphi_2$, $\delta_1 = \delta_2$, $a_1/a_2 > 1$. In this case the equation associating the variables is the equation of a circle. Since the energy output loss is inversely proportional to the burn-up rate, it is clear that the highest reactivity margin should be reserved in the reactor with the highest burn-up rate. The effect from possible optimization when $a_1/a_2 = 2$ and $\alpha = 0.5$ is ~40%.

3. The reactors are identical in respect of all the parameters considered $\varphi_1 = \varphi_2$, $\delta_1 = \delta_2$, and $a_1 = a_2$. In this situation the reactivity margins are identical. The effect from the optimization is ~20%. For systems consisting of reactors with different parameters φ, δ, and a, an uneven reduction of power proves to be optimal.

714

Thus, the results given above indicate a possibility of obtaining a particular effect from the use of fuel with a systems approach to the analysis of the operation of an atomic power plant with a variable load schedule. In conclusion, let us point out that the converse problem of a maximum reduction of power from the atomic power plant with a given energy output loss is solved in much the same way.

LITERATURE CITED

1. A. P. Aleksandrov and I. A. Dollezhal', At. Energ., 43, No. 5, 337 (1977).
2. V. N. Vladimirov, Practical Problems of Nuclear Reactor Operation [in Russian], Atomizdat, Moscow (1976).
3. A. S. Gerasimov and A. P. Rudik, At. Energ., 42, No. 2, 143 (1977).
4. J. Headey, Nonlinear and Dynamic Programming [Russian translation], Mir, Moscow (1967).

EFFECT OF ENTRANCE CONDITIONS ON THE DEVELOPMENT

OF TURBULENT FLOW IN CIRCULAR PIPES

B. N. Gabrianovich, Yu. D. Levchenko,
Yu. P. Trubakov, and P. A. Ushakov

UDC 532.542.4

In reactor cores and in heat-exchanger equipment a region of hydrodynamically unstabilized flows of a coolant sometimes comprises an appreciable fraction of the channel length. This affects the temperature distribution in the elements of the power equipment and in-pile structures. The effect of the longitudinal variation of the heat flux on the temperature distribution can be taken into account by a Duhamel integral containing the so-called transient function. The calculation of this function requires quantitative data on processes in the inlet regions of the channels.

Calculations by various methods [1-4] generally give inlet lengths shorter than the experimental values. The inlet devices used in pipes (grids, washers, nozzles, diffusers, inlet from a large volume, etc.) distort the velocity profile at the inlet where the turbulence depends entirely on the prehistory of the flow. Experiment [5] shows that an initial level of turbulence intensity up to 3% does not affect the flow in the inlet region of a circular pipe. Other experiments [6-11] also do not show a dependence of the stabilization length on the form of the inlet conditions and the turbulence intensity at the pipe inlet. In the study of the damping of the turbulence of the inlet flow along a pipe in [12, 13] the effect of the initial turbulence on the stabilization of the radial profile of the mean longitudinal flow velocity was not investigated.

In the present paper we generalize the material of [6, 14, 15, 16] and present new experimental data on the stabilization length of the velocity profile in circular pipes as a function of entrance conditions. The experimental channel used was a machined pipe 145 mm in diameter consisting of 23 sections each 600 mm long. The sections were machined to second-class accuracy with an inner surface roughness of 0.32 (∇9). The individual sections were connected and centered by sleeves. Packing grease was applied to the outer surface of the pipe against the fittings. The experiments were performed with a confined stream of air at a Reynolds number of 285,000. The velocity profiles and turbulence intensity were measured by the hot-wire anemometer method using appropriate DIZA55M (Danish) equipment. The apparatus included a bridge with a constant temperature filament, an amplifier, a linearizer, and an RMS voltmeter.

A flat velocity profile at the pipe inlet was ensured by a nozzle with a Vitoshinskii profile having a 4.9 contraction ratio. A honeycomb and various inlet grids were placed in front of the nozzle. The velocity profile at the pipe inlet remained constant and the turbulence intensity varied from 0.7 to 7.1%. At the lower degree of turbulence (0.7%) the velocity profile at the pipe inlet was distorted by various kinds of contraction devices: washers of various diameters used both singly and in combinations, washers asymmetrically covering half the cross section of the pipe to a diameter. For each inlet condition the velocity and its fluctuations were measured along the pipe axis. In this way the "limiting" cases of the effect of inlet conditions on the development of flow characteristics along the pipe were investigated.

715

TABLE 1. Characteristics of Inlet Grids

No. holes	Diameter of holes	Porosity	Turbulence intensity at inlet,%
7	75	0,4	7,1
19	50	0,46	3,9
37	41	0,6	2,3
92	25	0,55	1,7
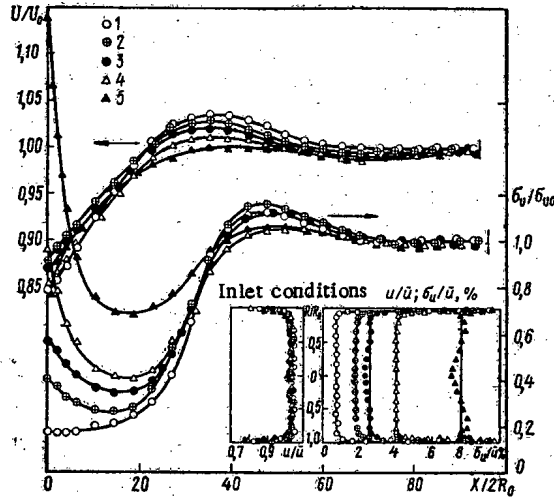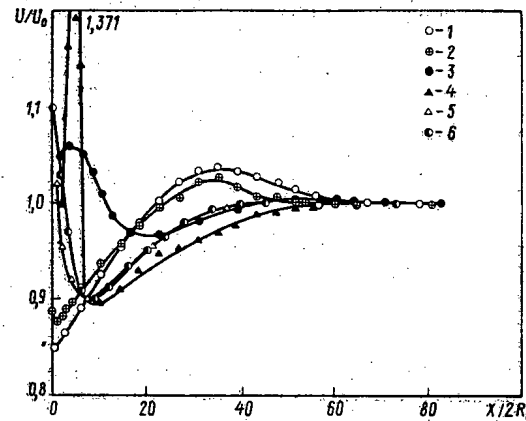
Fig. 1   Fig. 2

Fig. 1. Variation of longitudinal velocity U/U_0 and its fluctuations σ_u/σ_{u0} on pipe axis for various levels of initial turbulence: 1) screen 0.5 × 0.32 mm; 2) grid with 91 holes 25 mm in diameter; 3) grid with 37 holes 41 mm in diameter; 4) grid with 19 holes 50 mm in diameter; 5) grid with 7 holes 75 mm in diameter; Re=285,000.

Fig. 2. Variation of longitudinal velocity U/U_0 on pipe axis for various inlet conditions: 1-4) smooth profiled inlet; 2) inlet with 140 mm diameter washer; 3) inlet with five rings 133.6 mm in diameter; 4) inlet with washer covering half the cross section of the pipe, Re = 285,000 (our work); 5) inlet with diffuser; Re = 55,000 [9]; 6) inlet from a large volume; Re = 81,000 [6]; X, distance from channel inlet; R_0, pipe radius; $\bar{u}$, mean flow velocity; Re = $2R_0\bar{u}/\nu$.

The initial turbulence intensity at the pipe inlet was varied by metal grids placed behind the honeycomb in front of the nozzle. The holes in the grids were located at the vertices of equilateral triangles. The sizes of the vortices generated beyond the grid depended on the size and spacing of the grid holes. Therefore grids of various porosities were used (Table 1).

In this set of experiments measurements were made with a screen in front of the nozzle, which corresponded to a condition of smooth profiling of the inlet. The screen had a mesh size of 0.5 mm and the wires were 0.32 mm in diameter. The measured velocities and fluctuations along the pipe axis for various values of the initial turbulence intensity at the pipe inlet are shown in Fig. 1.

The mean velocity profiles in the inlet region of the pipe were linear for all the grids used in the experiments, and practically (within the ± 1% spread of the experimental data) identical with the velocity profile at the inlet cross section for a smooth profiled inlet. The radial profile of the intensity of turbulent velocity fluctuations at the inlet cross section of the pipe was also rather uniform over the cross section of the pipe. In the wall region the turbulence intensity was the same for all the grids, and was determined by the generation of turbulent fluctuations as a result of the velocity gradient in the boundary layer formed on the nozzle walls. In the central part of the flow the turbulence intensity was 0.7-7.1% for the various grids. To be sure that what was actually being measured was turbulence and not apparatus noise, the signal was fed into a 3348 Brueel and Kjaer spectrum analyzer and a DIZA 55D70 (Denmark) correlator. The velocity fluctuations at the pipe inlet were random and did not have a regular component in the 0-20-kHz frequency range.

Figure 1 shows that the increase in the initial level of turbulence intensity from 0.7 to 2.3% had practically no effect on the character of the development of velocity along the pipe axis. For a smooth profiled inlet the maximum axial velocity occurred at a distance of 40 diameters from the inlet. The maximum velocity decreased with increasing turbulence intensity in the inlet section of the pipe. For a turbulence intensity of 7.1% in the inlet section of the pipe there was a certain nonmonotonic character in the variation of the longitudinal velocity along the pipe. The minimum in the longitudinal flow velocity at a distance of 65 pipe diameters from the inlet became less noticeable with a decrease in the initial turbulence.

Turbulent velocity fluctuations produced by inlet grids were damped out at a distance of 20 diameters from the inlet where the minimum in the distribution of turbulent velocity fluctuations along the pipe was observed. The minimum velocity fluctuation on the pipe axis was proportional to the initial turbulence level. Experiments showed that the turbulence produced by a grid did not disappear completely before the turbulent vortices from the boundary layer began to reach the pipe axis. Downstream an increase in turbulence increased momentum transport in the radial direction, which prevented the formation of a velocity profile more elongated than the stabilized profile.

Thus, an increase in turbulence intensity at the pipe inlet led to a more monotonic development of the mean velocity and to a decrease in the stabilization length. Therefore the differences in the results obtained by different experimenters in the study of the development of velocity profiles in the inlet region of pipes may be due to the effect of the initial turbulence level.

A comparison of earlier results [6-12, 14-16] shows that different entrance conditions clearly affect the development of the hydrodynamic characteristics of the unstabilized part of the flow. The entrance conditions in circular pipes (grids, entrance from a large volume, diffusers, throttling washers) affect the contraction of the flow at the inlet. We have studied the effect of the contraction ratio at the inlet on the development of the flow along the pipe. The velocity profile, appreciably elongated close to the inlet because of the contraction of the stream, at a certain distance is first flattened, and then monotonically develops along the length to its stabilized form. The minimum velocity and the distance from the pipe inlet at which it occurs are determined by the type of inlet structure. The inlet structures used in the experiments included a 2 mm thick washer protruding 2.5 mm into the stream, a washer covering half the cross section of the pipe to a diameter, and a smooth profiled inlet.

Figure 2 shows the results of our measurements (curves 1, 2, 4) and data from [15, 9, 6] plotted on curves 3, 5, and 6 respectively. Figure 2 shows that the values of the velocity on the pipe axis for a smooth profiled inlet form an intersecting family of minima for other forms of pipe inlet. The stabilization length for all distortions of the flow at the inlet is practically unchanged.

Thus, the studies showed that at the same Reynolds number the stabilization length in circular pipes is weakly dependent on the contraction ratio of the flow at the inlet, and strongly dependent on the initial turbulence level.

<div align="center">LITERATURE CITED</div>

1. W. Szablewski, Ingenieur Arch., 21, 323 (1953).
2. G. V. Filippov, Zh. Tekh. Fiz., 28, 1823 (1958).
3. E. E. Solodkin and A. S. Ginevskii, Tr. TsAGI, 701, 26 (1957).
4. D. Bowlus and J. Brighton, Trans. ASME, 90D, 431 (1968).
5. J. Richman and R. Azad, Appl. Sci. Res., 28, 419 (1973).
6. L. N. Bibikov et al., At. Energ., 35, 19 (1973).
7. A. R. Barbin and J. B. Jones, Trans. ASME, 85D, 29 (1963).
8. M. Kh.-G. Ibragimov et al., Teplofiz, Vys. Temp., 12, 542 (1974).
9. I. Dalla Lana and S. Christiansen, Can. J. Chem. Eng., 45, 280 (1967).
10. G. A. Adamov and I. B. Idel'chik, Tr. No. 670, BNT MAP, 27 (1948).
11. J. Weir, A. Priest, and V. Sharan, J. Mech. Eng. Sci., 16, 211 (1974).
12. A. S. Sukomel et al., Inzh.-Fiz. Zh., 33, 816 (1977).
13. I. T. Shvets et al., Izv. Vyssh. Uchebn. Zaved., Energ., 8, 103 (1960).
14. V. I. Subbotin et al., "Investigation of the turbulent flow of air in the entrance region of a circular pipe," Preprint FÉI-699 (1975).
15. Yu. P. Trubakov, B. N. Gabrianovich, and Yu. D. Levchenko, Izv. Akad. Nauk BSSR, Ser. Fiz.-Energ. Nauk, No. 2, 89 (1976).

A GRAPHICOANALYTICAL METHOD FOR DETERMINING
THE LENGTH OF ELEMENTS ALONG THE HEIGHT
OF A MULTIELEMENT THERMOEMISSIVE ASSEMBLY

V. V. Sinyavskii

UDC 621.36

Theoretical [1-3] and experimental [4, 5] investigations of thermoemissive assemblies have shown that because of the nonuniformity of the heat generation along the height of the assembly q(z), there is a nonuniformity in the temperature of the emitters T_e of the individual elements of the assembly. If we have the restriction $T_e \leq T_{adm}$ (or $T_{e, adm} \leq T_{max}$), where T_{adm} is the limiting admissible temperature of the emitter, any nonuniformity in q(z) will reduce the output energy characteristics of an assembly with successively joined elements of equal length [1].

The efficiency of an assembly with nonuniform q(z) can be increased by redistributing the fissionable material along the height of the assembly (nuclear profiling [6]) or by an optimal distribution of the length of the elements along the height of the assembly (electronic or geometric profiling). For nonuniform q(z), geometric profiling has been investigated both theoretically [2, 7, 8] and experimentally [9]. The formulation of the problem and the numerical algorithm for determining $\{l_i\}^{opt}$ for nonuniform q(z) are given in [2]. However, it follows from general physical considerations that for the restriction $T_{e, max} \leq T_{adm}$, not only a nonuniformity in q(z) but also any nonuniformity in the parameters on which $T_{e, max}$ depends (e.g., the temperature T_c of the collectors, the pressure of the cesium vapors, etc.) will lead to a reduction of the output characteristics of an assembly with consecutively joined elements of equal length. In such cases, geometric profiling may be used effectively.

The proposed graphicoanalytical method for determining the optimal distribution function for the length of the elements along the height of the assembly, $\{l_i\}^{opt}$, is suitable for solving the problem of geometric profiling for any form of nonuniformity A(z) and restrictions of the type $R \leq R_{adm}$ (or $R \geq R_{adm}$). Before proceeding to describe the algorithm, we shall formulate a geometric-profiling problem somewhat more general than the one in [2].

We must determine the optimal number m^{opt} of consecutively joined thermoemissive electricity-generating elements (EGEs) and the optimal vector for the distribution of their lengths $\{l_i\}^{opt}$, $i \in [1; m^{opt}]$, along an assembly of height H with n distributed parameters of the form $A_j(z)$, $j \in [1; n]$, which, for k given limiting values R_p, $p \in [1; k]$, determining the resource, reliability, efficiency, technological quality, and other properties of the thermoemissive assembly, will realize the maximum useful electrical power (or total efficiency) of the assembly.

When the efficiency is maximized, the total thermal power is equivalent to the maximum useful electrical power for a given value of thermal power. It is possible to have a variant of the problem in which the assembly height H is optimized in addition to m^{opt} and $\{l_i\}^{opt}$.

The problem of geometric profiling, i.e., the actual determination of $\{l_i\}^{opt}$, can be solved by various methods. Thus, the authors of [2] give a variant of the geometric-profiling problem which is simpler but is most often encountered in practice, in which m is given, n = 1, k = 1, and, correspondingly, $A_1(z) \equiv q(z)$, $R_1 = T_{e, max}$.

A simple but effective graphicoanalytical method for determining $\{l_i\}^{opt}$ enables us to solve the problem in the most general formulation, with some distributed parameters and any number of restrictions. It is based on the use of V-q (voltage-heat) diagrams, which, for a given total current I, show in graphical form how the EGE voltage V varies with the density of the heat flux q_F per emitter (or the density of volumetric heat generation in the heat-generating core, q_V), the length l, the emitter temperature $T_{e, max}$, and, if necessary, other parameters (the collector temperature T_c, the pressure P_{Cs} of the cesium vapors, etc.). Such functional relationships for V (q, l, $T_{e, max}$) I = const are easily constructed from the volt-ampere characteristics of the EGEs
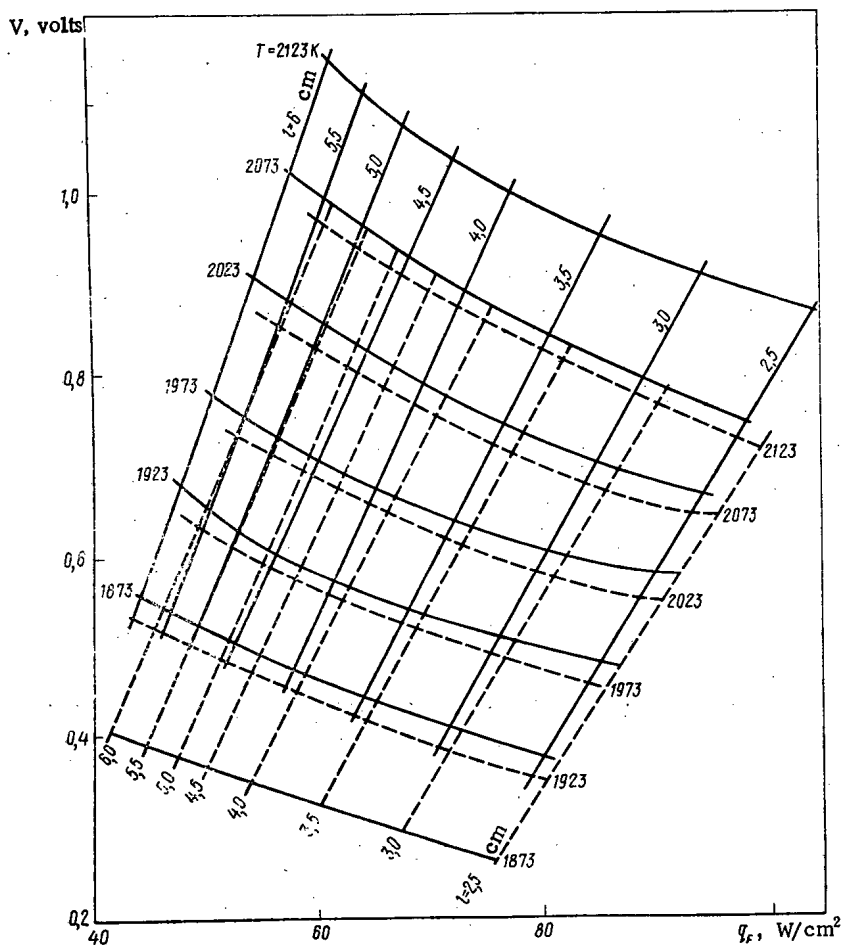
Fig. 1. Volt‑ampere (V‑q) diagram for profiling the length
of the elements, taking account of the nonuniformity of heat
generation and collector temperature and the restriction on
the maximum emitter temperature (I= 100 A).

at constant thermal power I (V)$_{q_F}$, l ... and constant emitter temperature I (V)$_{T_e, \, max}$ l ... . The volt‑ampere characteristics of the EGEs may be calculated with any accuracy by means of any algorithm. A typical V‑q_F diagram for determining $\{l_i\}^{opt}$ for two parameters q(z) and T_c(z) distributed along the height of the assembly and restrictions only on $T_{e, \, max}$ for I= 100 A are shown in Fig. 1. The volt‑ampere characteristics of the EGEs on which the diagram is based were calculated on a computer by the algorithm used in [1], taking account of the distributed nature of the heat fluxes entering the emitter jacket, the nonisothermal and nonisopotential nature of the electrodes, the thermal and electrical losses, and the effect of the nonoptimality of the collector temperature T_c. In order to keep the figure clear, the diagram shows the variation of V (q, l, T_c)$_I$ for three values of T_c: 900; 1000; and 1100°K. The working diagrams contain more detailed information on T_c. The coincidence of the characteristics for T_c = 900°K and 1100°K is a result of the experimentally observed specific variation of the isothermal thermoemissive transformations (TET) with T_c [10] which was used in calculating the EGEs.

From the V‑q diagrams for specific values of q_i, T_{c_i}, and if necessary, other values of A_i, we determine the l_i which for a given I yields the maximum value of V_i on condition that $T_{e, \, max} \leq T_{e, \, adm}$ and the other $R_j \leq R_{adm}$. Knowing all the V_i, we determine the total voltage $V_a = \sum_{i=1}^{m} V_i$, the total electrical power $W_a = V_a I$, and the efficiency of the assembly with the resulting $\{l_i\}$. If the dimensions l_i can vary continuously, then the profiling is carried out in such a way that $T_{e, \, max} = T_{e, \, adm}$ $i \in [1, \, m]$. This actually means that if we have only q(z), l_i is selected along the curve $T_{e, \, max}$(q) = $T_{e, \, adm}$, if we have the nonuniformities in q(z) and T_c(z), it is selected along the surface $T_{e, \, max}$(q, T_c) = $T_{e, \, adm}$, etc. If for a given $\{l_i\}$ we obtain an assembly height H* =

$= \sum_{i=1}^{m} (l_i + l_c)$, where l_c is the height of the switching connector, and this assembly height does not coincide with the given H, then we must make a correction to $\{l_i\}$ in such a way that H ≈ H*. This can be obtained by repeated determination of the vector $\{l_i\}$ from the V‑q diagrams for another value of m, another absolute q(z) (the rela-

tive distribution of $q(z)$ remains as before), or a reduction in the length of some of the EGEs (usually at the edges of the assembly) in such a way that $H \cong H^*$. It should be noted that in the last case the shortened EGEs will operate at $T_{e, max} < T_{adm}$. Naturally, in the absence of other considerations, we should select from the above methods the one which yields the maximum target function.

When we have thus determined $\{l_j\}$ for some values of I, we can construct the volt–ampere characteristic $I(V_a)$ $T_{e, max} \leq T_{e, adm}$, from which we can readily select the point, and consequently the $\{l_j\}^{opt}$ as well, for which we reach the maximum value of electrical power and satisfy restrictions of the form $R_p \leq R_{adm}$. At the same time as we optimize $\{l_j\}^{opt}$, we also optimize the number of successively joined EGEs in the assembly, m^{opt}, and its thermal power. /

Geometric profiling leads to some redistribution of the fuel along the height of the assembly, since for $\{l_i\}_{opt}$ the central EGEs are shorter than the peripheral ones, which must be taken into account in calculating the $q(z)$ and $T_c(z)$, and also in estimating the critical parameters of a system with profiled multielement assemblies.

Let us briefly consider some results obtained by means of the above method.

It has already been noted that $T_{e, max}$ is restricted; even a slight nonuniformity in $q(z)$ leads to a substantial reduction of the electrical power $W(K_z)$ in comparison with the power of an assembly with the constant heat generation, $W_0 \equiv W(K_z = 1)$ [1-3]. Thus, the authors of [1] obtained an empirical formula for determining the relative power of an assembly with elements of identical length for a cosinusoidal law of distribution of $q(z)$:

$$\bar{w}_q \equiv W(K_z)/W_0 \approx 2.52 - 1.52K_z,$$

which, e.g., when $K_z \equiv q_{max}/\bar{q} = 1.25$, yields $w_q \approx 0.6$. The individual EGEs operate at a $T_{e, max}$ almost 400°K higher than the maximum admissible value.

Geometric profiling of an assembly with nonuniform $q(z)$ and the restriction $T_{e, max} < T_{e, adm}$, for continuous variation of l_i, enables us to obtain electrical power values which are only a few percent lower than the power of an assembly with constant heat generation. Analogous results were obtained in [2, 7]. For a restricted number of typical dimensions of the EGEs, we also observe an increase in the output power of the assembly in comparison with an unprofiled one. However, since in this case some of the EGEs have a lower value of $T_{e, max}$, the power of the assembly is found to be lower than for continuous variation of l. If we assume discrete variation of l by a value which is a multiple of 0.5 cm, for the same conditions we have $w_q \approx 0.85$ when the $T_{e, max}$ values of individual EGEs differ from $T_{e, adm}$ by only 40°K.

The nonuniformity of $T_c(z)$ for constant $q(z)$ but with the restriction $T_{e, max} \leq T_{e, adm}$ also leads to considerable losses in electrical power $W(T_c)$ in comparison with the power of an assembly with constant $T_c = T_c^{opt}$. Thus, for $T_{c, max} - T_{c, min} \equiv 150°C$ and $T_{c, min} = T_c^{opt} w_c \equiv W(T_c)/W_0 \approx 0.8$ [1] with a difference of more than 100°C in the $T_{e, max}$ of individual EGEs. Geometric profiling with continuous variation of l_i increases w_c to 0.95 out of the optimal power value when all the EGEs have constant $T_{e, max}$ values. For same conditions when we have only two typical dimensions of the EGEs, $w_c \approx 0.9$.

The simultaneous effect of $q(z)$ and $T_c(z)$ on an unprofiled assembly yields an even lower relative power value, $w_{q, c} = W(K_z, T_c)/W_0$, where W_0 is the power of the assembly when $K_z = 1$ and $T_c(z) = T_c^{opt}$, i.e., even lower. For the conditions considered above, $w_{q,c} \approx 0.55$. Geometric profiling which takes account of the effect of $q(z)$ and $T_c(z)$ enables us to increase $w_{q,c}$ to ~ 0.9. When it is possible to have only discrete variation of l (by 0.5 cm), $w_{q,c} \approx 0.72$.

Thus, the algorithm worked out above enables us to determine $\{l_j\}^{opt}$ in a relatively simple manner for some parameters arbitrarily distributed along the height of the assembly and taking account of the restricted number of typical EGE dimensions that are actually possible. An important advantage of the method is that it can take account of any factors restricting the resource and operating capacity of the assembly. To do this, other boundary curves are drawn on the V–q diagrams in addition to the $T_{e, max}$ isotherms. The determination of the $\{l_j\}^{opt}$ is carried out in an analogous manner, but with all the R_{adm} restrictions taken into account.

LITERATURE CITED

1. Yu. A. Broval'skii et al., Teplofiz. Vys. Temp., 13, No. 1, 171 (1975).
2. V. M. Dmitriev and V. A. Ruzhnikov, Preprint FÉI-704, Obninsk (1976).
3. Yu. Ya. Kravehcnko and G. A. Stolyarov, Preprint IAÉ-1579, Moscow (1968).
4. E. S. Bekmukhambetov et al., At. Energ., 35, No. 6, 387 (1973).
5. B. A. Ushakov, V. D. Nikitin, and V. Yu. Korbut, At. Energ., 31, No. 5, 467 (1971).

6. E. S. Glushkov and N. N. Ponomarev-Stepnoi, At. Energ., 20, No. 6, 478 (1966).
7. E. Wolf and W. Haug, Atomkernenergie, 16, 213 (1970).
8. A. Schock, in: Proc 3rd Int. Conf. of Thermionic Electrical Power Generation. Julich, FRG (1972).
9. V. A. Kuznetsov et al., At. Energ., 36, No. 6, 450 (1974).
10. B. P. Baraksin et al., in: Reports of Soviet Scientists at the Second International Conference on the Thermoemissive Transformation of Energy [in Russian], VNIIT, Moscow (1969), p. 231.

FISSION NEUTRON DETECTORS

Z. A. Aleksandrova, V. I. Bol'shov,
I. E. Bocharova, K. E. Volodin,
V. G. Nesterov, L. I. Prokhorova,
G. N. Smirenkin, and Yu. M. Turchin

UDC 539.185

The average yield of neutrons per fission event $\bar{\nu}$ and their energy distribution N(E) are fission neutron characteristics that belong to the category of fundamental constants of breeder materials in reactors. Most practical problems can be solved using the well-known approximation of the fission neutron spectrum by the Maxwellian distribution

$$\chi(E, \theta) = (2/\sqrt{\pi\theta^3}) \sqrt{E} \exp(-E/\theta), \tag{1}$$

i.e., $N(E) = \bar{\nu}\chi(E, \theta)$. In such a case, knowing the average energy $\bar{E} = 3\theta/2$, or the so-called neutron temperature θ, it is possible to find the entire fission neutron spectrum. Thus, most experimenters focus their attention on the determination of the two first moments of the distribution N(E): the zero moment $\bar{\nu}$ and the first moment $\bar{\nu}\varepsilon$ (precisely speaking, their ratio $\bar{\varepsilon}$).

These fission neutron characteristics, and especially $\bar{\nu}$, are most frequently measured with the aid of detectors consisting of a hydrogeneous moderator and slow-neutron counters. The moderator is usually polyethylene and the slow-neutron detectors are BF_3 or ^3He counters. In such detectors, which in contrast to detectors that detect single events of microscopic interaction of fast neutrons with nuclei are called macroscopic detectors, neutrons live for tens of microseconds while being slowed down and scattered.

Since the moderation length $\sqrt{\tau}$ essentially depends on the energy of fast neutrons entering the moderator and since the spatial distribution of slow neutrons is a strong function of $t/\sqrt{\tau}$ (t being the distance to the neutron entry plane), the energy sensitivity of a slow-neutron counter can be varied within wide limits by changing its position in the moderator, its orientation with respect to the beam of incident neutrons, or the moderator configuration. Such an approach is frequently employed to fit the characteristics of the detecting system to the needs of the particular problem. Well-known examples of such detectors are the all-wave (long) counter [1], the isodose neutron detector [2], the Bramblett multispherical spectrometer [3], etc.

Here we report on certain new applications of the macroscopic method to the measurement of fission neutron characteristics. Three versions of the method are discussed: a macroscopic fast-neutron spectrometer (E detector), simultaneous measurement of the average yield and average fission neutron energy (νE detector), and a detector which measures $\bar{\nu}$ without being sensitive to the average fission neutron energy (ν detector).

Energy Dependence of Slow-Neutron Counters in Polyethylene

Moderator

The results reported in this paper are based on an investigation of the dependence of the sensitivity $\varepsilon(E, t_n)$ of slow-neutron counters in a polyethylene block on the energy of fast incident neutrons E and on the distance from the neutron incidence surface t_n. Although the measurement of these characteristics over an energy range from 0 to 15 MeV is rather difficult, no such difficulties exist when the characteristics are calculated theoretically. We have thus studied the sensitivity function $\varepsilon(E, t_n)$ by calculating its relative behavior by the Monte Carlo method and by normalizing it experimentally at several points taking into account the individual characteristics of the counters.

721
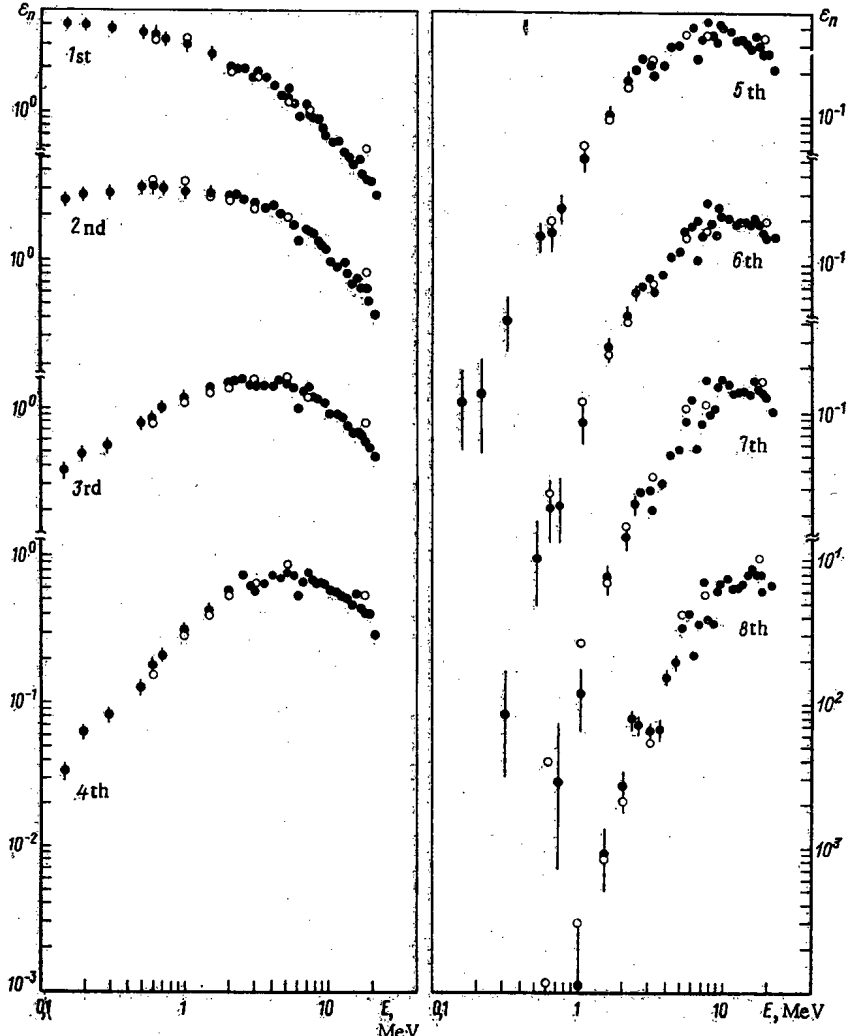
Fig. 1. Comparison of results obtained by the Monte Carlo method
(●) and experimentally (○) for the function $\varepsilon_n(E)$ [cm²] for one type
SN10NA counter.

Two basic "counter + moderator" arrangements are discussed: for measurements in the so-called good geometry when the detector registers source neutrons within a small solid angle, and for experiments in 4π geometry in which the detector monitors a considerable portion of space around the source. Good geometry is usually employed for studies of fission neutron spectra [3–6] and 4π geometry, for $\bar{\nu}$ measurements [7].

The first arrangement is most suitable for measurement of the sensitivity function $\varepsilon(E, t_n)$ with mono-energetic neutrons [6]. 4π detectors usually have a central channel reserved for a fission-fragment detector in coincidence with whose output pulses neutrons are registered by the coaxially positioned neutron counters.

The measured and calculated values of the function $\varepsilon_n(E) = \varepsilon(E, t_n)$ for a rectangular detector are shown in Fig. 1. The Monte Carlo procedure used in the calculations is described in [8]. Measurements were carried out for monoenergetic neutrons and for neutrons of radioactive (α, n) sources having a continuous energy spectrum.

The source of monoenergetic neutrons were T (p, n), D (d, n), and T (d, n) reactions taking place in an electrostatic generator with solid targets. Neutron yield was monitored with a thick-walled fission chamber with a ^{235}U layer placed near the neutron target within the same solid angle as the detector being calibrated. The measured $\varepsilon_n(E)$ functions were normalized with the aid of radioactive neutron sources consisting of a homogeneous mixture of ^{238}Pu with Li, F, B, and Be using the expression

$$(4\pi R^2/Q)\, M_n = \varepsilon_n(\bar{E})\ [\text{cm}^2],$$

where R is the distance between the source and the detector front surface (in the calculations and in all experiments R = 100 cm). The source yield Q was determined to within ~10%.

The measured and calculated results (Fig. 1) are seen to be in good agreement with each other indicating that the sensitivity of slow-neutron detectors depends strongly on their position within the moderator. The irregular structure of $\varepsilon_n(E)$, associated with resonances of the cross section of neutron scattering by carbon nuclei, manifests itself clearly at great depths t_n, viz., when $n > 3$.

The behavior of sensitivity $\varepsilon_n(E)$ weakly depends on the counter dimensions and on the distance R to the moderator surface as can be seen by comparing the functions $\varepsilon_n(E)$ calculated for a prism and for a 4π detector in which these parameters differ considerably. This is very fortunate from a methodological point of view since it allows one set of $\varepsilon_n(E)$ curves to be used without taking into account in the first approximation the geometric features of the detection system. It should also be noted that the resonance structure of $\varepsilon_n(E)$ is less prominent in 4π detectors because of the large spread of neutron "ranges" in the resonator. Similar tables of the function $\varepsilon_n(E, t_n)$ are given in [5] for a prism and in [7] for a 4π detector.

Stacked Macroscopic Spectrometer (E Detector)

The investigated detector has several advantages over the multispherical detector [3]. First of all, with a stacked structure there is no need to change the moderating envelopes and an entire set of readings for different moderator depths can be obtained simultaneously. Secondly, a stacked structure imposes no such strict constraints upon the dimensions of slow-neutron counters as a multispherical spectrometer making it possible to increase the sensitivity by one order of magnitude or more. Finally, in a stacked-counter spectrometer it is much easier to obtain an extensive set of $\varepsilon_n(E)$ functions. Thus, the family of $\varepsilon_n(E)$ curves of the multispherical spectrometer is covered by the characteristics of the first four rows of a stacked spectrometer. In other words, the later covers a wider dynamic range which is shifted towards higher energies, and this is one of the main factors that determine the accuracy of measurement of the parameter θ.

Let us consider the last problem in some more detail. Considering that the difference $|\Delta\theta| = |\theta - \theta_0| \ll \theta_0$ is small, the ratio R_n of the number of counts registered by counters of the n-th row of the spectrometer for two fission-neutron sources with the parameters θ and θ_0 can be written as a Taylor series

$$R_n = C \left[1 + \frac{\Delta\theta}{\theta_0} \left(\frac{\langle E \rangle_n}{\theta_0} - \frac{3}{2} \right) + \frac{1}{2} \frac{\Delta\theta^2}{\theta_0^2} \left(\frac{15}{4} - 5 \frac{\langle E \rangle}{\theta_0} + \frac{\langle E^2 \rangle_n}{\theta_0^2} \right) + \ldots \right] = C, \tag{2}$$

where $\langle E^k \rangle_n$ is the k-th moment of the neutron distribution $\chi(E, \theta) \varepsilon_n(E)$ registered by the n-th counter row, and C is the intensity ratio of the fission sources.

In a linear approximation, the desired quantity $\Delta\theta/\theta_0$ is the slope of the straight line $R_n = C(1 + \Delta\theta/\theta_0 x_n)$, where $x_n = \langle E \rangle_n/\theta_0 - 3/2$. The result can be easily made more accurate applying the method of successive approximations. Thus, since $\bar{E} = 3/2\theta$, the parameter x_n is the difference between the average energy of the register neutrons $\langle E \rangle$ and of the source neutrons $\bar{E}$ expressed in θ_0 units. Obviously, the greater the range of x_n the higher the accuracy with which $\Delta\theta/\theta_0$ can be determined. The sensitivity of the method and the applicability of the above approach to the processing of experimental results are well illustrated in [9] where the neutron spectra of ^{233}U, ^{235}U, and ^{239}Pu fission due to thermal neutrons were compared with those of spontaneous fission of ^{252}Cf (standard) to within 0.1–0.2% of the ratio θ/θ_0.

For the sake of convenience we have first considered relative measurements of θ/θ_0 even if the macroscopic spectrometer method makes it possible to find absolute values of the parameter θ. For this, the relation $M_n = c \int_0^\infty \chi(E, \theta) \varepsilon_n(E)\, dE$ is made to fit the experimental count readings M_n. Applying the method of least squares $\sum_n (M_n - \hat{M}_n)(\partial \ln M_n/\partial c) = 0$; $\sum_n (M_n - \hat{M}_n)(\partial \ln M_n/\partial\theta) = 0$ we obtain an expression from which θ can be found:

$$\left(\sum_n \hat{M}_n \right) \frac{\sum_n \int_0^\infty E\chi(E, \theta) \varepsilon_n(E)\, dE}{\sum_n \int_0^\infty \chi(E, \theta) \varepsilon_n(E)\, dE} - \sum_n \frac{\int_0^\infty E\chi(E, \theta) \varepsilon_n(E)\, dE}{\int_0^\infty \chi(E, \theta) \varepsilon_n(E)\, dE} \hat{M}_n = 0. \tag{3}$$

Expression (3) indicates that to find θ there is no need of knowing the absolute value of the sensitivity $\varepsilon_n(E)$ but only its dependence on the row number and energy, i.e., the neutron flux $Q/4\pi R^2$ incident on the detector does not enter the processing of experimental results. For relative measurement of θ/θ_0 one even needs not know the relation $\varepsilon_n(E)$ for the different detector rows: the result depends only on $\langle E \rangle_n$. Otherwise speak-

723
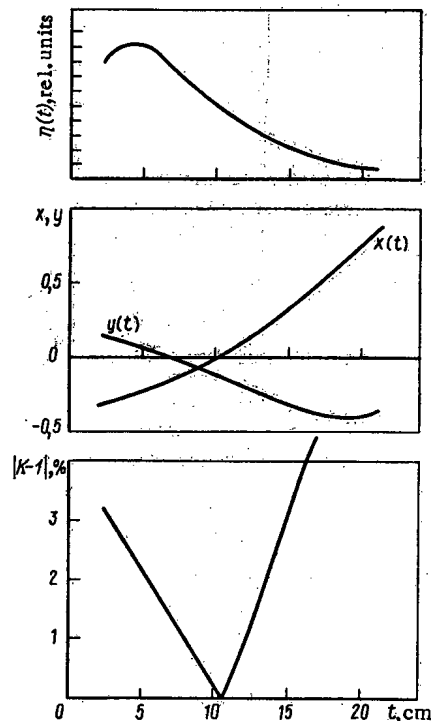
Fig. 2. Dependence of integral sensitivity to fission neutrons $\eta(t)$, of the functions $x(t)$ and $y(t)$, and of the correction factor $|k-1|$, on the distance t to the neutron incidence surface for a 4π detector.

ing, in this approach there is no need of calibrating $\varepsilon_n(E)$, all one has to do is to find the relative behavior of the sensitivity, e.g., by the Monte Carlo method.

Simultaneous Measurement of Average Yield and Average
Energy of Fission Neutrons (νE Detector)

The average yield of fission neutrons $\bar{\nu}$ is usually measured with the aid of 4π detectors operating in coincidence with fission-fragment detectors. The macroscopic spectrometer concept can be also realized within the scope of the structure and operating principles of 4π detectors [7]. This would allow simultaneous measurement of the two most important fission-neutron characteristics $\bar{\nu}$ and $\bar{E}$ (or θ).

The importance of such a 4π detector modification is due to the following reasons. Firstly, the applications of a good-geometry macroscopic detector is limited to neutron source intensities of $\gtrsim 10^3$ neutrons/sec. In many cases this condition can be satisfied only when a considerable amount of fissionable material is available, which appreciably restricts the experimental possibilities of the method. By increasing the method sensitivity by several orders of magnitude, the 4π detector eliminates these difficulties. Secondly, because of the energy dependence of the neutron detector efficiency, the results of measurement of the fundamental nuclear physics constant $\bar{\nu}$ must be corrected for the difference between the fission-neutron spectra of the measured isotope and the standard. The measured experimental ratio of the number of neutrons registered per one fission event can be written as

$$\rho = \frac{\bar{\nu}}{\nu_0} \frac{\int_0^\infty \chi(E,\,\theta)\,\varepsilon_n(E)\,dE}{\int_0^\infty \chi(E,\,\theta_0)\,\varepsilon_n(E)\,dE} = \frac{\bar{\nu}}{\nu_0}\,k, \tag{4}$$

where k is the correction mentioned above, and $\varepsilon_n(E)$ is the detector efficiency. Using expression (2), the factor k can be written as

$$k = 1 + \frac{\Delta\theta}{\theta_0}\,x_n + \frac{\Delta\theta^2}{\theta_0^2}\,y_n + \ldots, \tag{5}$$

724

indicating that its accuracy depends in a large measure on the ratio θ/θ_0. Unfortunately, this ratio is not very reliably known for thermal-neutron fission of even the most common reactor materials. In some cases the error of the correction factor is comparable with the correction proper $|k-1|$. Simultaneous measurement of $\bar{\nu}$ and θ eliminates this difficulty.

The method of simultaneous measurement of $\bar{\nu}$ and θ is implemented by placing in the moderator several concentric rows of counters and recording coincidences of their output pulses with the fission-fragments detector pulses. The ratio of the number of coincidences is used for finding θ and their sum, for measuring $\bar{\nu}$.

Detector for Measuring $\bar{\nu}$ Irrespective of the Average Fission
Neutron Energy $\bar{E}$ ($\bar{\nu}$ Detector)

Above we have discussed a method of relative measurement of $\bar{\nu}$ in which the correction for the difference between the fission-neutron spectra of analyzed object and the standard is determined experimentally. The dependence of the parameter x_n on the location of counters in the moderator [7] makes it possible to design a detector for which no correction is needed. However, the point is not a strict observation of the condition $k=1$, which is true only for all-wave detectors $[\varepsilon(E) = \text{const}]$, but the approximation

$$x = 0 \quad \text{or} \quad \langle E \rangle = \bar{E}, \tag{6}$$

to which corresponds the energy-dependent efficiency of the detector. The solution of (6) can be easily found from the function $x(t)$ for a 4π detector represented in Fig. 2. It is seen from the figure that condition (6) will be satisfied if the counters are placed at a distance $t_{opt} = 10.5$ cm from the inside surface of the moderator. Figure 2 also shows the parameter y, which defines the second-order term contribution in expression (5), and the difference between the factor k and unity for $x=0$, as functions of the distance t. It is seen that in the neighborhood of $t = t_{opt} \pm 0.5$ cm, the correction factor $|k-1|$ is less than the error in $\bar{\nu}_0$ for the standard ($\sim 0.3\%$) $\Delta\theta/\theta_0$ typical of the range of θ for heavy nuclei.

The realization of the condition $x=0$ by placing the counters precisely on the surface $t = t_{opt}$ is the simplest but not the only and best one since it limits the number of counters. One can make use of the fact that x has different signs to the right and left of $t = t_{opt}$, place the counters on both sides of the optimal surface, and complete the row of counters without violating the condition $x=0$. Detectors for measuring $\bar{\nu}$ described in literature satisfy rather the demand of maximum efficiency. Figure 2, in which the top curve represents the integral efficiency to fission neutrons $\eta(t) = \int_0^\infty \chi(E, \theta) \times \varepsilon(E, t)\, dE$, indicates that this demand does not coincide with the condition $x=0$.

CONCLUSIONS

The methods described in this article have been developed for studies of fission-neutron spectra. The range of problems that can be solved with their help can be greatly expanded. For example, a 4π detector similar to the one described here has been used to separate prompt and delayed fission neutrons and (γ, f) and (γ, n) neutrons [10].

Although macroscopic spectrometers are most effective in situations when the energy distribution can be represented in an easily parameterized form, their application is not at all limited to such cases. In the general case, the problem is solved using a group description of the distributions and reduces to a solution of a system of linear equations with experimentally determined left sides M_n.

LITERATURE CITED

1. A. Hanson and J. McKibben, Phys. Rev., 72, 673 (1974).
2. Kh. D. Androsenko and G. N. Smirenkin, Prib. Tekh. Eksp., 5, 64 (1962).
3. R. Bramblett, R. Ewing, and T. Bonner, Nucl. Instr. Methods, 9, 1 (1960).
4. V. I. Bol'shov et al., Preprint FÉI-578, Obninsk (1975).
5. Z. A. Aleksandrova et al., Preprint FÉI-866, Obninsk (1978).
6. V. I. Bol'shov et al., in: Proc. of the Conf. on Neutron Physics [in Russian], TsNIIatominform, part 4 (1977), p. 290.
7. V. I. Bol'shov et al., Preprint FÉI-865, Obninsk (1978).
8. I. E. Bocharova, L. I. Prokhorova, and G. N. Smirenkin, in: Nuclear Constants [in Russian], TsNIIatominform, Moscow (1974), p. 7.

725

9.   V. I. Bol'shov et al., in: Proc. of the Conf. on Neutron Physics [in Russian], TsNIIatominform, part 3, Moscow (1977), p. 284.
10.   J. Caldwell and E. Dowdy, Nucl. Sci. Eng., 53, 767 (1975); B. Berman and S. Fultz, Rev. Mod. Phys., 47, 713 (1975).

ANALYSIS OF THE RELIABILITY OF RADIOCHEMICAL
PLANTS WITH ELECTRON ACCELERATORS

V. M. Kshnyaskin and Yu. D. Kozlov   UDC 621.384.6:541.15

The reliability of radiochemical plants must be calculated at an early design stage [1-3]. The reliability of such plants significantly affects their economy during operation. Besides radiation physics parameters, the design of radiochemical plants requires the knowledge of the reliability of their units and elements.

Calculations of structural reliability are now an integral part of design in various fields of engineering, e.g., in reactor design [4]. The aim of this paper is the calculation of the reliability of component units of planned radiochemical plants with high-current electron accelerators and the evaluation of plant reliability as a whole. Since such plants are complex systems designed for long operating times, their reliability should be calculated in several stages [3].

The reliability of electron accelerators, radiochemical apparatus, and other technological and auxiliary equipment is calculated first. After the reliability indicators of these units have been analyzed and evaluated, the reliability of the radiochemical plant as a whole is calculated. The reliability of units composed of many components and linked by complex functional relations is calculated by the Monte Carlo method [1]. The combinatorial method [3, 4] is used to calculate the reliability of less complex units.

To analyze the reliability of radiochemical plants the latter are arbitrarily divided into individual units or elements in accordance with the following principles:

the failure of an element causes breakdown of the entire plant;

an element is a relatively independent functional or structural unit;

The number of elements in a plant should be minimal (if, e.g., the reliability indicators of both a plant unit and of its individual components are known, the calculations should be based on the entire unit);

if no reliability data are available, elements and units are combined if possible into one or two larger functional units whose reliability indicators are specified as a set of values for the given range of possible magnitudes. The reliability of each unit is calculated for all assumed values.

The reliability of radiochemical plants is analyzed with the aid of functional block diagrams of radiochemical apparatus and accelerators that specify the effect of failure of an element (unit) on the reliability of apparatus or accelerator.

To simplify the problem it is desirable to consider systems with instantaneous recovery in which the times of failure and recovery coincide [5]. An algorithm and program are designed for models with instantaneous recovery which compute the probability of no-failure operation $P(t)$, the failure flow parameter $\omega(t)$, the mathematical expectation of the number of failures in time t $H(t)$, and mean time between failures T [5].

Simulation of the operational process of a radiochemical plant with an electron accelerator consists in the following. The plant operation is considered either during its entire operating time or only during the principal operation period. The chosen operating time is split into intervals Δt and the flow of recovery of failed elements is implemented with the aid of random numbers. The duration of time intervals (Δt) should not be too long, on the one hand, so that typical variations of the flow are not smoothed, and not too short, on the other hand, so that insignificant properties of the flow are not manifested.
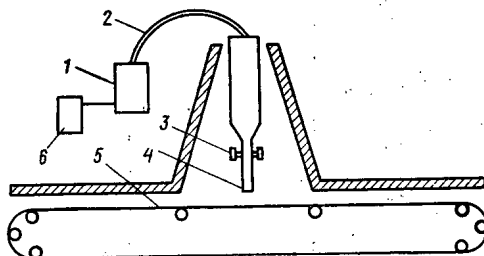
Fig. 1. Schematic drawing of radiochemical plant with electron accelerator: 1) high-voltage generator; 2) high-voltage cable; 3) vacuum system; 4) irradiator; 5) radiochemical apparatus (conveyer); 6) gas supply system.

It is known [6] that the input data on which an algorithm is based are the failure rate and the failure flow parameter (for nonrepairable and repairable units respectively) when the failure distribution is assumed to be exponential, and the mean time between failures, the time to failure, and dispersion when the assumed failure distribution is normal or lognormal.

It has been shown in [7] that failures of the cathode subassembly, the vacuum system, and the exit window have an exponential and normal distribution. The probability of no-failure operation of these units has the form

$$P(t) = e^{-\lambda} F(T - t/\sigma), \tag{1}$$

where t is the operating time, h; λ, failure rate due to transient defects, 1/h; T, time between failures due to wear, h; and σ, dispersion of the distribution of times between failures due to wear.

In simulation, the failures of elements and units caused by transient defects and wear are assumed to be a superposition of two parts: one with normally distributed and the other with exponentially distributed failures. Since the failures are independent, the exponential and normal parts are simulated separately. The model considers flows of failures of all units that enter into the failure flow of the radiochemical plant as a whole.

Thus, mathematical simulation consists of the following steps: repeated application of an algorithm describing the probabilistic model of the investigated process in individual units of the radiochemical plant; statistical processing of the obtained results and their analysis; calculation of the reliability of radiochemical apparatus, the electron accelerator, and of the plant as a whole (if necessary); setting up tables and graphs with recommendations as to the calculation of reliability of other similar units.

As an example of the application of the above technique consider the analysis of the reliability of a radiochemical plant with a high-current electron accelerator used for processing lumped (unmixed) systems. The radiation section consists of the electron accelerator, the radiochemical apparatus, and auxiliary equipment* (Fig. 1).

The kinetic energy of accelerated electrons is 0.08 pJ and the total irradiator current behind the exit window is about 50 mA. The high-voltage transformed [8] connected by a cable to the irradiator operates in a gas

---

*The reliability of only the radiation section of the plant is discussed. The technological equipment is the topic of another article.

TABLE 1. Reliability Parameters of Radiochemical Plant with an Electron Accelerator

Unit	Reliability parameter	
	ω (t), 1/h	T, h
High-voltage generator	$1,7 \cdot 10^{-3}$ $4,2 \cdot 10^{-4}$	600 2400
Gas supply system	$18,8 \cdot 10^{-5}$ $5,3 \cdot 10^{-5}$	5300 18000
Irradiator	$4,6 \cdot 10^{-5}$ $3,9 \cdot 10^{-5}$	21650 25500
Conveyer	$4,3 \cdot 10^{-4}$ $3,3 \cdot 10^{-4}$	} ~ 3000

727
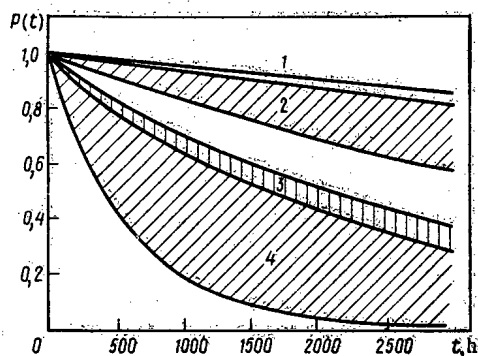
Fig. 2

Fig. 3

Fig. 2. Probability of no-failure operation of certain units of the accelerator and conveyer: 1) irradiator; 2) gas system; 3) conveyer; 4) generator.
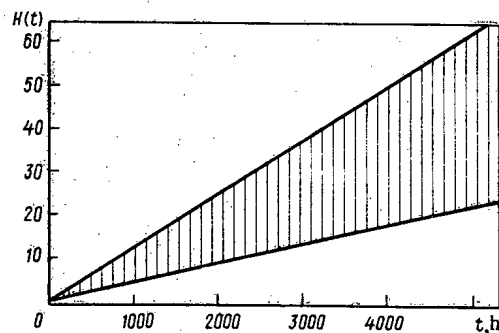
Fig. 3. Mathematical expectation of the number of failures H(t) in time t of the radiochemical plant with electron accelerator.

medium (electric gas). To take into account the reliability of operation of individual (smaller) components, the irradiator has been arbitrarily divided into four sections: the cathode subassembly, the vacuum system, the exit window, and the scanning system. The irradiator is located in a special radiation shield which can be dismounted in parts for servicing.

From the point of view of construction and number of components, the control console is similar to that of a typical radiochemical plant with an accelerator "Electron-3" whose reliability has been analyzed before in [7]. The conveyer is an electromechanical subassembly placed in an individual radiation shield. Its task is to transport in and out products to and out of the irradiation zone and consists of driving and tension drums, electric motor, various clutches, reducing gears, sprockets, chains, etc.

All elements of the plant and irradiator within the shield are in some measure affected by the action of electron and bremsstrahlung radiations and ozone. Thus, in analyzing the reliability of these units we have taken into account the possible radiation effects on these elements. For this we have calculated the γ radiation exposure dose rate for various parts of the structure within the biological shield. Using the data on radiation resistance of the materials and instruments [9] of which the radiochemical plant and irradiator are constructed, we have analyzed their usefulness for the given operating conditions and tentatively estimated the useful life of these elements equal to the time during which the allowable dose is absorbed.

The maximum and minimum failure rates for the components of the high-voltage generator, the gas supply system, and the radiochemical apparatus (conveyer) have been adopted from data published in [4, 10-12]. Table 1 lists the calculated reliability indicators of these units from which the curves of the probability of no-failure operation shown in Fig. 2 have been plotted. To evaluate the reliability of the plant as a whole, the results where supplemented by the reliability indicators of the cathode subassembly, the exit window, and the control console (Table 2) published before for "Elektron-3" radiochemical plant [7, 18].

The data in Tables 1 and 2 have been used as a basis for calculating the reliability indicators of the plant: operating time to failure, the mathematical expectation of failure in time t, and the failure rate under steady-state operating conditions. Considering the accuracy of statistical data used for calculating the reliability indi-

TABLE 2. Reliability Parameters of Certain Accelerator Components

Unit	Reliability parameter		
	$\lambda(t)$, 1/h	$\omega(t)$, 1/h	T, h
Cathode subassembly	$5,9 \cdot 10^{-3}$ $1,0 \cdot 10^{-1}$	—	170 1000
Vacuum system	—	$5,9 \cdot 10^{-4}$	2000
Exit window	$1,0 \cdot 10^{-2}$ $7,0 \cdot 10^{-3}$	—	100 150
Control console	—	$8,3 \cdot 10^{-4}$	1200

cators, the failure rate parameter of the system as whole was found to be 0.3 to $1.3 \cdot 10^{-2}$ per hour. The calculations were carried out by repeating the algorithm 1000 times with a time-to-failure error of about 3 h. The dependence of the mathematical expectation of the number of failures on operating time is shown in Fig. 3. The figure indicates that 25 failures can be expected to occur in the system in 2000 h and 63 failures, in 5000 h.

Thus, we have for the first time applied the method of mathematical simulation to the evaluation of the reliability of electrochemical plants at the design stage. The reliability indicators of component units of the plant and of the plant and electron accelerator as a whole have been calculated a priori. The results can be used for comparing the quantitative reliability indicators of individual units and (if necessary) for taking measures to improve their reliability. The obtained data can also be used for calculating the necessary margin of safety and for scheduling preventive maintenance of individual units or plants as a whole.

<div align="center">LITERATURE CITED</div>

1. V. M. Kshnyaskii et al., in: Proc. of All-Union Conf. on the Application of Particle Accelerators in the National Economy [in Russian], Vol. 1, Izd. NIIEFA, Leningrad (1976), p. 232.
2. V. M. Kshnyaskii, Yu. D. Kozlov, and L. V. Popova, in: Abstracts of Papers of the All-Union Scientific Engineering Seminar on the Application of High-Power Sources of Ionizing Radiation in Radiation Engineering [in Russian], VNIIRT (1976), p. 126.
3. Yu. D. Kozlov, K. I. Nikulin, and Yu. S. Titkov, Calculation of Parameters and Design of Radiochemical Plants with Electron Accelerators (Handbook) [in Russian], Atomizdat, Moscow (1976).
4. A. I. Klemin, Engineering Probability Calculations in Nuclear Reactor Design [in Russian], Atomizdat (1973).
5. L. G. Gorskii, Statistical Algorithms for Reliability Calculations [in Russian], Nauka, Moscow (1970).
6. B. P. Kredentser et al., Solving Reliability and Maintenance Problems with General-Purpose Digital Computers [in Russian], Sov. Radio, Moscow (1967).
7. Yu. D. Kozlov, At. Energ., 39, No. 4, 280 (1975).
8. E. A. Abramyan and V. A. Gaponov, At. Energ., 20, No. 5, 385 (1966).
9. N. A. Sidorov and V. K. Knyazev (editors), Radiation Resistance of Construction Materials in Radiation Engineering (Handbook) [in Russian], Sov. Radio, Moscow (1976).
10. A. M. Polovko, Principles of the Theory of Reliability [in Russian], Nauka, Moscow (1964).
11. B. S. Sotskov, Methodical Instructions and Reference Data for Calculating the Reliability of Components and Systems [in Russian], Moscow Aviation Institute (1964).
12. B. S. Sotskov, Principles of the Theory and Calculation of the Reliability of Components and Systems in Automation and Computers [in Russian], Vysshaya Shkola, Moscow (1970).
13. V. V. Akulov et al., see Ref. [1], p. 115.

NEW BOOKS

E. P. Anan'ev

ATOMIC PLANTS IN POWER ENGINEERING*

Reviewed by Yu. I. Koryakin

Monographs published by Atomizdat, which cover the various aspects of nuclear power engineering, go out of print quite rapidly indicating the growing interest to nuclear power industry. The reviewed book will help in satisfying this interest.

The book treats its subject on various levels and cannot be simply characterized. Nevertheless, one can distinguish two special features: 1) the material is based on experience gained in the Soviet Union and 2) the main stress is on advanced nuclear power technology. Both these qualities are attractive and important especially in conditions of intensive nuclear power plant construction.

Another important topic of the book is radiation safety which can be provided by a set of measures which are consistently and with deep insight presented by the author.

The author focuses his attention on channel and vessel reactors. Their evolution, present state, and technological problems concerning such reactors are the main subjects of seven (out of eight) chapters of the book. The author notes that large-scale solutions of problems make it possible to achieve new technological and economical levels of operation with these reactor types (especially with channel reactors), while on the other hand generating new technological problems. The author makes an attempt to estimate the scale and significance of certain socioeconomical factors associated with the development of nuclear power engineering. Unfortunately, this subject is barely touched upon. In view of its importance, the subject attracts widespread attention and heated discussions. Certain inaccuracies in the treatment of reactor physics must be mentioned. Possibly, they result from the attempt of the author to simplify the discussion and make it intelligible to less trained readers.

The book leaves a favorable impression. Notwithstanding certain minor weak points, the book is a valuable addition to the shelf of nuclear power engineering literature.

LETTERS TO THE EDITOR

EVALUATION OF THE SELECTIVITY OF ELECTROCHEMICAL REACTOR-FUEL RECOVERY ON THE BASIS OF THERMODYNAMIC DATA

V. A. Lebedev   UDC 669.536.7

The separation factors of uranium and rare earths, uranium and zirconium, uranium and plutonium, and uranium and thorium have been determined from thermodynamic data. The elements listed above have similar oxidation–reduction potentials in chloride melts and thus determine the efficiency of electrochemical recovery of reactor fuel. The separation factor Q was calculated from the expression [1]

$$\lg Q = \frac{(n-m)\,FE + mFE_2^* - nFE_1^*}{4.575\,T} + \lg \frac{\gamma_1}{\gamma_2}\,, \tag{1}$$

where E_1^*, E_2^* are relative standard potentials Me_1/Me_1^{n+}, Me_2/Me_2^{m+} [2, 3]; γ_1, γ_2 are the activity factors of Me_1 and Me_2 in a liquid metal electrode [4]. If $n = m$, the separation factor is independent of the melt potential E. For $n \neq m$ the calculations were made for two-phase (L+compound) melts of electropositive metal (Me₂) with a 1 mole % concentration of its ions in the electrolyte (c₂).

The comparative efficiency of various solvents salts used in separation was evaluated from

$$\lg Q/Q' = \frac{nF}{4.575\,T}(E_2^* - E_1^{*''} - E_2^{*'} + E_1^{*'}). \tag{2}$$

The error in log Q estimated from Eq. (1) is ± (0.3 to 0.6) and from Eq. (2), ± (0.2 to 0.4). The initial data and the obtained results are listed in Tables 1 and 2.

The separation factor of uranium and lanthanum increases regularly when the solvents are light metals located higher and to the right in the periodic system. The factor is close to one for thallium electrodes, $10–10^2$

TABLE 1. Separation Factors of Me₁ and Me₂ in Liquid Metal Me–KCl melt–LiCl System Containing Me_1^{n+} and Me_2^{m+} Ions

Me_1^{n+}	Me_2^{m+}	Me	$\lg \gamma_1 = A + BT^{-1}$		$\lg \gamma_2 = A + BT^{-1}$		$\lg Q = A + BT^{-1} + \frac{n-m}{m}\lg c_2$		Q	
			A	-B	A	-B	A	B	800	1000
La³⁺	U³⁺	Zn	5,05	12475	2,44	3685	2,14	586	750	535
		Cd	4,16	9738	3,03	885	0,66	523	20	15
		Al	3,01	9892	3,84	7505	−1,30	6994	—	5·10⁵
		Ga	4,72	13333	1,38	4984	2,87	1023	1,4·10⁴	8·10³
		In	2,73	9508	2,36	2033	−0,10	1901	189	63
		Tl	2,36	8153	0,49	−2678	1,40	−1455	0,4	0,9
		Sn	4,26	13377	1,97	4546	1,82	545	318	232
		Pb	−0,07	6618	2,97	2360	−3,51	5118	770	41
		Bi	0,94	11158	1,05	4328	−0,58	2546	400	92
Pu³⁺	U³⁺	Zn	5,38	9770	2,44	3685	−1,03	2489	107	25
		Cd	4,44	6354	3,03	885	−2,61	3105	19	3
		Al	3,26	9050	3,84	7505	−4,60	7029	—	270
		Bi	1,40	8284	1,05	4328	−3,67	4618	121	9
U³⁺	Zr⁴⁺	Zn *	0,56	0,374	7,66	10164	−2,26	8150	2·10⁶	2·10⁶
Th⁴⁺	U³⁺	Zn *	4,78	9511	0,79	0,559	−0,03	−213	0,10	0,11
		Al *	3,83	9470	0,65	0,307	−1,20	3002	—	14
		Ga *	2,29	8710	0,53	0,195	0,33	822	5	3
		In *	0,77	3850	0,43	0,256	−2,52	2028	0,24	0,10
		Sn *	0,46	6459	0,67	0,288	−2,60	3123	4,4	0,8
		Pb *	1,14	3620	0,41	0,253	−2,74	2457	0,5	0,1
		Sb *	−0,02	9830	0,82	0,226	−1,24	2773	—	8
		Bi *	1,33	7430	0,475	0,157	−0,11	904	2,8	1,4

*The column log γ_U shows for these systems the coefficients of the equations $E_2 = A + B \cdot 10^{-3}\,T$ [4], where E_2 is the emf between the metal and its two-phase (L+compound) melt.

731

TABLE 2. Ratio of Separation Factors of the Elements Me_1 and Me_2 Obtained with KCl—NaCl Melt (Q) and Other Solvent Salts (Q')

Me_1^{n+}	Me_2^{m+}	MeCl	$E_1^* = A + B \cdot T$		$E_2^* = A + B \cdot T$		$\lg Q/Q' = A + B \cdot T^{-1}$		Q/Q'	
			$-A$	$B \cdot 10^4$	$-A$	$B \cdot 10^4$	A	B	1000	1100
U^{3+}	Zr^{4+}	LiCl	2,83	6,0	2,40	6,0	0,30	−1227	0,12	0,5
		NaCl	2,99	6,7	2,58	6,7	0,30	−907	0,25	0,30
		NaCl—KCl	3,01	6,6	2,66	6,8	0,00	0,00	1,0	1,0
		KCl	3,12	7,1	2,82	7,7	−0,61	756	1,4	1,2
		CsCl	3,18	7,4	2,88	7,7	−0,14	756	4,2	3,5
Pu^{3+}	U^{3+}	LiCl	3,46	9,4	2,83	6,0	1,06	907	1,4	1,7
		NaCl	3,60	9,8	2,99	6,7	0,61	605	1,0	1,1
		LiCl—KCl	3,57	9,7	2,84	5,4	−2,42	−2420	1,0	0,6
		NaCl—KC	3,58	9,3	3,01	6,6	0,00	0,00	1,0	1,0
		KCl	3,76	10,8	3,12	7,1	1,51	1059	2,8	3,6
		CsCl	3,87	11,6	3,18	7,4	2,27	1815	2,8	4,2
Th^{4+}	U^{3+}	LiCl	2,90	6,0	2,83	6,0	0,40	202	4,0	3,9
		NaCl	2,98	5,9	2,99	6,7	−1,21	1815	3,4	2,8
		LiCl—KCl	3,00	6,0	2,84	5,4	1,61	−1613	1,2	1,4
		NaCl—KCl	3,09	6,4	3,01	6,6	0,00	0,00	1,0	1,0
		KCl	3,17	6,7	3,12	7,1	−0,40	605	1,5	1,4
		CsCl	3,25	6,9	3,18	7,4	−0,61	202	0,4	0,4

for cadmium, lead, and indium electrodes, 10^2–10^3 for bismuth and zinc electrodes, and 10^4–10^5 for gallium and aluminum electrodes. Considering the results of separation of rare-earth metals with liquid metal electrodes [1, 5], one should expect that the separation factors of uranium and cerium (neodymium, praseodymium) will be similar to, of uranium and dysprosium (erbium, yttrium) by 1 order of magnitude greater than, and of uranium and samarium (ytterbium) by 2–3 orders of magnitude greater than, the separation factors of uranium and lanthanum. The separation factor of uranium and plutonium varies within 2 orders of magnitude depending on the nature of the liquid metal solvents employed, increasing in the order Cd, Zn, Bi, and Al and reaching 10^2–10^3 for aluminum electrodes.

Zinc electrodes are efficient separators for uranium and zirconium. With zinc, indium, and lead electrodes one should expect enrichment of the metal phase with thorium, and of the KCl—NaCl melt with uranium. No significant separation of these elements should be expected with tin and bismuth electrodes. Preferential accumulation of uranium should be observed on gallium, antimony, and aluminum electrodes. Selection of the liquid metal solvent makes it possible to change the separation factor of uranium and thorium within more than 2 orders of magnitude.

Less marked is the effect of the solvent salt on the selectivity of electrochemical processes in the liquid metal—salt system (see Table 2). The effect becomes appreciable only when the ions of elements being separated have markedly different z/r parameters. For example, in the solvent series from lithium chloride to cesium chloride, the separation factors of uranium and zirconium decrease, and of thorium and uranium increase by more than 1 order of magnitude as a result of more intense complexing in the salt melt and stronger complexing bonds of Zr^{4+} ($z/r = 4.88$) and Th^{4+} (4.21) in comparison with U^{3+} (2.88) ions. Higher temperatures, as a rule, reduce the selectivity, particularly with bismuth (Pu—U) and zinc (U—Zn) electrodes.

It is interesting to compare the electrochemical separation factors of elements in metal—salt systems with those obtainable in well-known separation processes (e.g., by extraction). The separation factors of ions of the above-considered elements by extraction of 0.3 M by tertiary amine solutions out of 2 M HNO_3 are as follows [6]: 4 for U^{4+}/Th^{4+}, 2 for $Th^{4+}/U(VI)$, 10^3 for $Pu^{4+}/U(VI)$, 10^2 for Pu^{4+}/U^{4+}, $4 \cdot 10^4$ for U^{4+}/Sm^{3+}, $5 \cdot 10^3$ for $U(VI)/Sm^{3+}$, $4 \cdot 10^4$ for U^{4+}/Zr^{4+}, $3 \cdot 10^3$ for $U(VI)/Zr^{4+}$. It is seen that the selectivity of electrochemical processes in liquid metal—salt systems is similar to that of extraction by organic solvents.

The above results indicate the possibility in principle of separation of uranium from fission products, plutonium, and thorium by electrochemical methods, and the considerable effect of the nature of metal solvent salts and temperature on the process selectivity.

LITERATURE CITED

1. V. A. Lebedev et al., Zh. Fiz. Khim., 46, No. 9, 2356 (1972).
2. M. V. Smirnov, Electrode Potentials in Molten Chlorides [in Russian], Nauka, Moscow (1973).
3. V. I. Silin and O. V. Skiba, Preprint NIIAR P-118, Dimitrovgrad (1971).
4. V. A. Lebedev, At. Energ., 41, No. 1, 33 (1976).

5. A. V. Kovalevskii, V. A. Lebedev, and I. F. Nichkov, Tsvetnye Met., No. 11, 45 (1973).
6. Oke W. Hultgren, in: Reprocessing of Power Reactor Fuels [in Russian], Atomizdat, Moscow (1972), p. 103.

DETERMINATION OF NEUTRON AND RADIATION COMPONENTS
OF ENERGY RELEASE IN BORON-CONTAINING RODS USING
GRAY CHAMBERS

V. P. Polionov, Yu. G. Pashkin,
and Yu. A. Prokhorov

UDC 621.039.562.24

Well-known methods based on reaction speed and calorimetric measurements were used to determine the energy release in boron-containing fuel rods in the PF-4F8 critical assembly [1-3] in which the ionization method using a Gray chamber was also tested. Unlike the methods used in [1, 2], the ionization method makes it possible to find the neutron and radiation components of energy release which is important for design purposes. The method is quite simple and provides reliable results with an acceptable accuracy. Its sensitivity is approximately 10 times the sensitivity of the calorimetric method [2] and amounts to $\sim 10^{-7}$ W/g for natural boron.

The determination of energy release in boron-containing material is based on the well-known Bragg—Gray principle [4] which establishes the relation between the measured ionization of a gas confined in a cavity of a solid body and the release of energy in the walls of the body.

The energy release per unit volume of the medium is given by

$$Q = Wf = \frac{n_{sol}}{n_{gas}} \frac{\Delta U (C_c + C_{mi})}{t V_c e N} K\eta,$$ (1)

where W is the average energy of ion pair production in gas; f, ratio of stopping powers of the chamber material and the gas per electron; n_{sol} and n_{gas}, number of electrons per unit volume of the solid body and the gas, respectively; ΔU, change of chamber potential during irradiation time t with a power N; C_c and C_{mi}, capacity of the chamber and the measuring instrument, respectively; V_c, chamber volume; e, electron charge; η, ion collection efficiency in the gas gap of the chamber; and K, an extrapolation factor described below. The term $\Delta U(C_{mi} + C_c)/t$ is henceforth called the chamber current.

Measurements were conducted with plane-parallel chambers. The gas gap was formed between the faces of two boron carbide cylinders 20 mm in diameter which are a part of the boron rod. The chamber is fitted with a device for varying and monitoring the gas gap.

If a chamber with a gas gap δ is placed in a reactor radiation field, the current I_δ flowing in it is given by

$$I_\delta = I_\alpha + I_{Li} + I_{B,c} + I_e + I_{lk},$$ (2)

where I_α, I_{Li}, and $I_{B,C}$ are neutron components due, respectively, to the products of (n, α) reactions in ^{10}B and to recoil nuclei of boron and carbon produced by their interaction with neutrons, the latter component being negligible in comparison with the first one; I_e is the radiation current component measured with a special boron carbide chamber in which the gas cavity is shielded by an aluminum foil from the (n, α) reaction products, and I_{lk} is a leakage current determined in the absence of reactor radiation and found to amount to only 3% in our conditions.

For a "zero" gas gap, for which Eq. (1) is true, the chamber current components differ from currents flowing in the chamber with a finite gas gap for the following reasons: the Bragg—Gray condition [4] that the fraction of particles entering the gas gap with a residual range less than the gap length is negligible is not completely satisfied; the neutron flux on the inner surfaces of chamber electrodes increases in the presence of a gas gap; an edge effect takes place in which a fraction of charged particles, mainly from the edges of electrodes, emerges at an angle to the chamber axis and leaves the sensitive volume of the chamber without fully

733

TABLE 1. Energy Release in Boron Rod Measured by Different Methods

Method	Energy release, 10^{-6} W/g	
	neutron component	total energy release
Ratio of reaction speeds [1]	1.34 ± 0.03	—
Calorimetric [2]	—	1.43 ± 0.16
Ionization	1.30 ± 0.09	1.43 ± 0.1

spending their energy. These effects diminish with decreasing gas gap and vanish completely in a "zero" gap. In this case, the chamber current satisfies all conditions of the Bragg—Gray equation [4].

To find the chamber current at "zero" gap, we have subtracted from the currents obtained with 0.07 and 0.5 mm gas gaps the radiation current component and the leakage current at these gaps. Then, we have determined the parameter x in expression (3) which describes the current in a plane-parallel chamber due to α particles and lithium nuclei taking into account the gas gap dimensions expressed in α particle track lengths:

$$I \approx \left\{ \frac{7}{11} \left[1 - \frac{x}{2} \left(1 + \ln \frac{1}{x} \right) \right] + \frac{4}{11} \left[1 - \frac{kx}{2} \left(1 + \ln \frac{1}{kx} \right) \right] \right\}, \tag{3}$$

where k is the ratio of track lengths of α particles and lithium nuclei. This expression has been obtained for a small gap assuming an isotropic angular distribution of reaction products: helium and lithium nuclei. Next we have determined the neutron component of the chamber current for a "zero" gap which is 1.13 times the current for a 0.07-mm gap. The obtained data are listed in Table 1.

The results confirm that the measurements are correct and indicate the possibility of using the ionization method for measuring the energy release components in boron rods in low-power critical assemblies with an accuracy acceptable for practical purposes. The method is quite simple and easy to implement. The reactor power was measured by the frequency method by S. A. Morozov to whom the authors express their gratitude.

LITERATURE CITED

1. V. A. Kuznetsov et al., At. Energ., No. 5, 926 (1972).
2. A. S. Zhilkin et al., At. Energ., 42, No. 6, 502 (1977).
3. A. I. Mogil'ner et al., At. Energ., 24, No. 1, 42 (1968).
4. J. Hein and H. Brownell (editors), Radiation Dosimetry [Russian translation], IL, Moscow (1958).
5. A. I. Mogil'ner et al., Preprint FÉI-98, Obninsk (1967).

PHOTOPRODUCTION OF NEUTRONS IN A THICK LEAD TARGET

V. I. Noga, Yu. N. Ranyuk,
and Yu. N. Telegin

UDC 621.384.64.038.624:539.125.5.03

The purpose of the paper is a study of the yield of neutrons from a thick lead target bombarded by 230- and 1200-MeV electrons in linear accelerators of the Physicotechnical Instutute of the Academy of Sciences of the Ukrainian SSR. The experiment was staged as follows. A beam of electrons hit a lead target in the form of a 0.2- to 8-cm-thick cylinder with a diameter of 2.5 cm. Neutrons were counted by the method of radioactive indicators [1]. Neutron detectors (aluminum samples) in the form of 0.5-cm-thick disks 3 cm in diameter were placed at a distance of 15 cm around the lead target at definite angles with respect to the electron beam direction. The activity induced by the ^{27}Al(n, p)^{27}Mg reaction was measured with a γ spectrometer consisting of a Ge(Li) detector and a "Langur" spectrometer. The spectrometer was connected to an M-6000 digital computer which recorded and processed the spectra.

The various reactions of neutron–nuclei interaction used for neutron detection by the method of induced activity result in the production of radioactive nuclides. Most suitable for this purpose under conditions of γ background are (n, p) reactions for which the background process is the photoproduction (γ, π^+). Since the photoproduction process is about 140 MeV, γ quanta do not contribute to the measured activity below this energy, while for $E_\gamma > 140$ MeV their contribution is negligible because of the small photoproduction cross sections of π mesons as compared with the (n, p) reaction cross section. However, the use of (n, p) reactions leads to practical difficulties associated with the need of a monoisotopic detectors. The ^{27}Al(n, p)^{27}Mg reaction used by us is one of the most suitable reactions for practical applications.

The angular distributions of neutron yield obtained for different target thickness and electron energies are nearly isotropic indicating that evaporation is the main neutron production mechanism. The integral neutron flux was calculated from

$$f_n = 4\pi k R / \sigma_{\text{ef}},$$
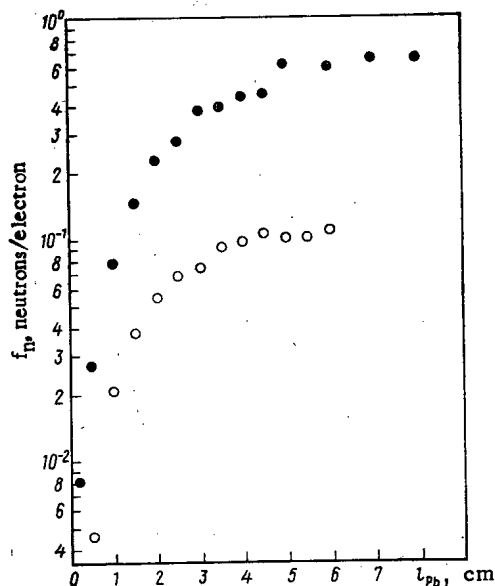
Fig. 1. Neutron yield f_n as a function of target thickness l_{Pb} at 230 (O) and 1200 MeV (●).

735
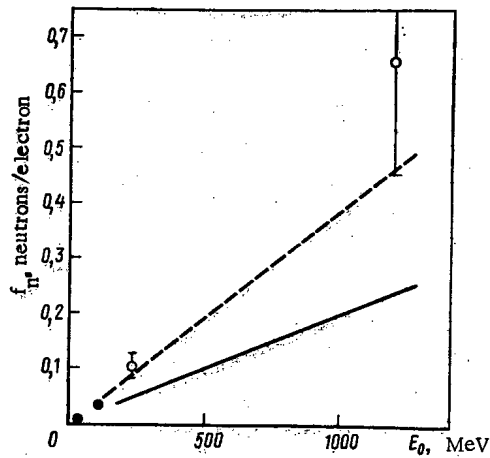
Fig. 2. Neutron yield f_n as a function of electron energy E_0 under saturation conditions: results of [3, 4] (●), our results (O); — — — calculated in [5], ——— calculated in [6].

where k is a factor accounting for neutrons with an energy below the reaction threshold, and R is an activation integral (cm^2/sr · electron) [1]. The neutron production cross section was described by the single-step function

$$\sigma_n(E_n) = \begin{cases} 0 & \text{for } E_n < Q_{ef}; \\ \sigma_{ef} & \text{for } E_n \geqslant Q_{ef}, \end{cases}$$

where Q_{ef} and σ_{ef} are, respectively, the effective threshold and the effective threshold cross section. In our case $Q_{ef} = 4$ MeV and $\sigma_{ef} = 30$ mb. To find k the neutron spectrum was represented by the expression

$$\varphi(E_n) \sim E_n \exp(-E_n/T),$$

where E_n is the neutron kinetic energy and T is a constant. The constant T was calculated from experimental data on the spectrum of neutrons from a tantalum target obtained for a maximum bremstrahlung beam energy of 140 MeV [3]. The estimated error of f_n is ±30%. Absorption of neutrons in the lead target was neglected.

Data shown in Fig. 1 as well as similar results of other works [4] indicate that the behavior of $f_n(\ell_{Pb})$ is the same for different electron energies E_0 and is characterized by the fact that neutron yield saturation begins at a certain target thickness. The minimum target thickness ℓ_{min} corresponding to saturation depends on E_0. The thickness ℓ_{min} shifts toward greater thickness with increasing E_0. This must be taken into account in selecting optimum target dimensions for a given initial energy.

Of special interest is the dependence of neutron yield on electron energy since there is a practical possibility to vary this yield in particular when the accelerators employed have a high upper energy limit. Figure 2 shows the available calculated and experimental data concerning the dependence of the yield of neutrons from a lead target on E_0. To within an acceptable error the results obtained in [5] agree with experimental results. The results calculated in [6] are considerably lower than other data. It can be assumed that the discrepancy is a result of the fact that the processes leading to neutron production were not fully accounted for. This is particularly important at energies exceeding the pion photoproduction threshold.

LITERATURE CITED

1. E. A. Kramer-Ageev, V. S. Troshin, and E. G. Tikhonov, Activation Methods of Neutron Spectrometry [in Russian], Atomizdat, Moscow (1976).
2. C. Burgart et al., Nucl. Sci. Eng., 42, 421 (1970).
3. R. Alsmiller and M. Moran, Nucl. Instrum. Methods, 48, 109 (1967).
4. W. Barber and W. George, Phys. Rev., 116, 1551 (1959).
5. W. Swanson, SLAC-PUB-2042 (1977).
6. J. Levinger, Nucleonics, 6, No. 5 (1950).

MATHEMATICAL MODEL FOR CALCULATING FISSION
PRODUCTS CONCENTRATION AND ENERGY RELEASE
IN CIRCULATING NUCLEAR FUEL

L. I. Medvedovskii, E. S. Stariznyi,
V. A. Cherkashin, V. A. Rudoi,
and K. I. Stepanova

UDC 621.039.55

The solution of certain problems associated with the design and application of uranium radioactive loops requires calculation of fission products concentration and of the three-dimensional distribution of γ- and β-radiation energy release and its spectral composition in circulating nuclear fuel. Methods and results for calculating these characteristics in nuclear reactors with noncirculating fuel have been published in several works [1-3]. Design works, as a rule, do not take into account isomeric transitions, direct generation of nuclides in chains, and burnup of active nuclides. We have designed a mathematical model of the accumulation of fission products in circulating nuclear fuel and devised a method for calculating the radiation characteristics of uranium radioactive loops (distribution of the power of γ and β radiation and their spectral composition in the uranium radioactive channel). This mathematical model can also be employed for calculating the radiation characteristics of fission products in pulsed reactors, in which burnup of fission products is especially high, and in nuclear reactors with fixed fuel.

Consider all possible transmutations of fission product nuclei. A nucleus (including isomers) can be generated directly in fission, as a result of neutron capture by an isotope of lower mass, as a result of decay of its
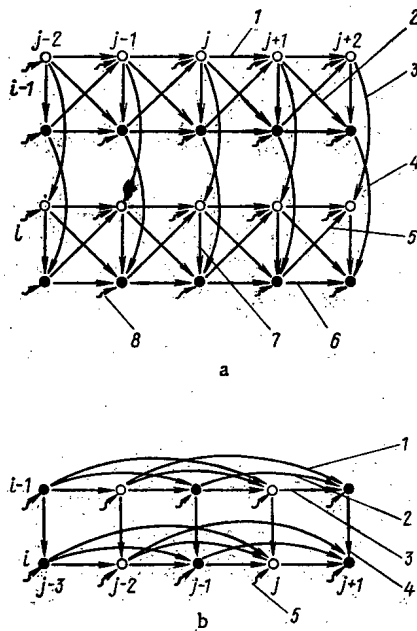
Fig. 1. Initial (a) and linearized (b) chains (O, isomer; ●, ground state): a: 1) $(1-\alpha^I_{i-1j}-\beta^I_{i-1j})\lambda^I_{i-1j}A_{i-1j}$; 2) $\alpha^I_{i-1j+1}\lambda^I_{i-1j+1}A^I_{i-1j+1}$; 3) $\sigma^I_{i-j+2}\Phi A^I_{i-j+2}$; 4) $\sigma_{i-1j+2}\Phi A_{i-1j+2}$; 5) $(1-\alpha_{ij+1})\lambda_{ij+1}A_{ij+1}$; 6) $\alpha_{ij+1}\cdot\lambda_{ij+1}A_{ij+1}$; 7) $\beta^I_{ij}\lambda^I_{ij}A^I_{ij}$; 8) $y_{ij-1}\Sigma_f\Phi$; b: 1) $\lambda_{3i-1j-2}A_{i-1j-2}$; 2) $\lambda_{2i-1j-1}\cdot A_{i-j-1}$; 3) $\lambda_{1i-j}A_{i-j}$; 4) $\sigma_{i-1j+1}\Phi A_{i-1j+1}$; 5) $Y_{ij-1}\Sigma_f\Phi$.

737
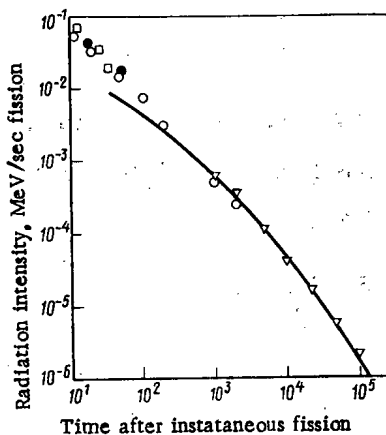
Fig. 2. Comparison of results obtained by the proposed method with experimental data: □) data [2], ○) data [4], ▽) data [5], ●) data [6], ⟶) our results.

isomer (if the nucleus is not an isomer), and as a result of decay of an isobar and of an isomer of isobar with smaller nuclear charges. The generated nucleus can capture a neutron, pass into a ground state (if the nucleus is an isomer), into an isobar next in the chain, and into an isomer of the isobar next in the chain. All these processes are reflected in the following system of differential equations:

$$\begin{cases} dA_{ij}/dt = y_{ij}\Sigma_f\Phi - \lambda_{ij}A_{ij} - \sigma_{ij}\Phi A_{ij} + \alpha_{ij-1}\lambda_{ij-1}A_{ij-1} + \\ + \alpha'_{ij-1}\lambda'_{ij-1}A'_{ij-1} + \beta'_{ij}\lambda'_{ij}A'_{ij} + \sigma_{i-1j}A_{i-1j}; \\ dA'_{ij}/dt = y'_{ij}\Sigma_f\Phi - \lambda'_{ij}A'_{ij} - \sigma'_{ij}\Phi A'_{ij} + (1-\alpha'_{ij-1} - \\ -\beta'_{ij-1})\lambda'_{ij-1}A'_{ij-1} + (1-\alpha_{ij-1})\lambda_{ij-1}A_{ij-1} + \\ + \sigma'_{i-1j}\Phi A'_{i-1j}, \end{cases} \tag{1}$$

where A_{ij} is the concentration of the j-th nucleus in the i-th chain; y_{ij}, probability of output in fission; Σ_f, nuclear fuel fission macro cross section; Φ, thermal neutron flux density; λ_{ij}, decay constant; σ_{ij}, neutron capture micro cross section; α and β, probability coefficients (Fig. 1a); quantities marked with strokes correspond to isomers.

To simplify the solution let us arrange isomers with ground states in one chain numerating them so that a nucleus with a higher number cannot turn into a nucleus with a lower number; transitions take place between nuclei with numbers differing by not more than three. The concentration A_{ij} of isotope (i, j) in the mixture can then be described by a single equation (see Fig. 1b):

$$dA_{ij}/dt = Y_{ij} - \Lambda_{ij}A_{ij} + \rho_{i-1j} + A_{i-1j} + \lambda_{3ij-3}A_{ij-3} + \lambda_{2ij-2}A_{ij-2} + \lambda_{1ij-1}A_{ij-1};$$
$$A_{ij}(0) = B_{ij}, \tag{2}$$

where

$$Y_{ij} = y_{ij}\Sigma_f\Phi; \quad \rho_{ij} = \sigma_{ij}\Phi; \quad \Lambda_{ij} = \lambda_{ij} + \rho_{ij};$$
$$\lambda_{kij-k} = \lambda_{ij-k}\alpha_{ij-kj}; \quad \sum_{k=1}^{3} \alpha_{ijj+k} = 1.$$

Here α_{ijj+k} is the probability of transition of nucleus (i, j) into the nucleus (i, j + k).

Since nuclear fuel in a uranium radioactive loop enters the neutron field periodically, for each elementary volume we have

$$\Phi(t) = \begin{cases} \Phi_0 & \text{if } 0 \leqslant t < t_p; \\ 0 & \text{if } t_p \leqslant t < t_p + t_y; \end{cases}$$
$$^{n+1}A_{ij}(0) = {}^nA_{ij}(t_p + t_y), \tag{3}$$

where t_p is the time nuclear fuel spends in the reactor core; t_y, time nuclear fuel is outside the core; $^nA_{ij}(t)$, concentration of the (i, j) isotope in the n-th cycle of the uranium radioactive loop operation. Under condition (3), the solution of system (2) is

738

$$
{}^nA_{ij}(t) = \begin{cases} A^0_{ij} + \sum\limits_{k=1}^{i} \sum\limits_{l=1}^{j} {}^nA^{kl}_{ij} \exp\left(-\Lambda_{kl}t\right) \\ \text{if} \quad 0 \leqslant t < t_p; \\ \sum\limits_{l=1}^{j} {}^nC^l_{ij} \exp\left(-\lambda_{il}t\right) \quad \text{if} \quad t_p \leqslant t < t_p + t_y, \end{cases}
$$

where

$$
\begin{cases}
\text{if} \quad A^0_{ij} = (Y_{ij} + \rho_{i-1j}A^0_{i-1j} + \lambda_{3ij-3}A^{0\mathbf{3}}_{ij-3} + \\
\qquad + \lambda_{2ij-2}A^0_{ij-2} + \lambda_{1ij-1}A^0_{ij-1})/\Lambda_{ij}; \\
{}^nA^{ij}_{ij} = {}^nB_{ij} - A^0_{ij} - \sum\limits_{k=1}^{i-1}\sum\limits_{l=1}^{j}{}^nA^{kl}_{ij} - \sum\limits_{l=1}^{j-1}{}^nA^{kl}_{ij}; \\
(k,\ l) \neq (i,\ j):\ {}^nA^{kl}_{ij} = (\rho_{i-1j}{}^nA^{kl}_{i-1j} + \lambda_{3ij-3}{}^nA^{kl}_{ij-3} + \\
\qquad + \lambda_{2ij-2}{}^nA^{kl}_{ij-2} + \lambda_{1ij-1}{}^nA^{kl}_{ij-1})/(\Lambda_{ij}-\Lambda_{kl}); \\
{}^nC^0_{ij} = A^0_{ij} + \sum\limits_{k=1}^{i}\sum\limits_{l=1}^{j}{}^nA^{kl}_{ij}\exp\left(-\Lambda_{kl}t_p\right); \\
{}^nC^j_{ij} = {}^nC^0_{ij} - \sum\limits_{l=1}^{j-1}{}^nC^l_{ij}; \\
(l < j):\ {}^nC^l_{ij} = (\lambda_{3ij-3}{}^nC^l_{ij-3} + \lambda_{2ij-2}{}^nC^l_{ij-2} + \\
\qquad + \lambda_{1ij-1}{}^nC^l_{ij-1})/(\lambda_{ij}-\lambda_{kl}); \\
{}^{n+1}B_{ij} = \sum\limits_{l=1}^{j}{}^nC^l_{ij}\exp\left(-\lambda_{il}t_y\right).
\end{cases}
\tag{5}
$$

The specific power of gamma and beta radiation of fission products arranged into r chains of length s each amounts at the instant t in the n-th cycle to

$$
{}^nW(t) = \sum_{i=1}^{r}\sum_{j=1}^{s}{}^nA_{ij}(t)\lambda_{ij}E_{ij} = \begin{cases}
P + \sum\limits_{k=1}^{r}\sum\limits_{l=1}^{s}{}^nU_{kl} \times \\
\times \exp\left(-\Lambda_{kl}t\right) \\
\text{(inside core)}; \\
\sum\limits_{k=1}^{r}\sum\limits_{l=1}^{s}{}^nV_{kl} \times \\
\times \exp(-\lambda_{kl}t) \text{ (outside)}.
\end{cases}
$$

Here

$$
P = \sum_{i=1}^{r}\sum_{j=1}^{s}A^0_{ij}\lambda_{ij}E_{ij}; \qquad
{}^nU_{kl} = \sum_{i=k}^{r}\sum_{j=l}^{s}{}^nA^{kl}_{ij}\lambda_{ij}E_{ij}; \qquad
{}^nV_{kl} = \sum_{j=l}^{s}{}^nC^l_{kj}\lambda_{kj}E_{kj},
$$

where E_{ij} is the γ (β) radiation energy of isotope (i, j).

The reliability of the results thus obtained depends to a large extent on the fullness and accuracy of initial data. The lack of comprehensive data about short-lived fission products considerably impairs the accuracy of calculations for short circulation periods (on the order of minutes).

Using the above procedure we have computed the dependence of γ radiation power of the products of instantaneous fission on the holding time. The results obtained are in good agreement with known experimental data [2, 4-6] for holding times exceeding ~1000 sec (Fig. 2).

LITERATURE CITED

1. J. Perkins and R. King, Nucl. Sci. Eng., 3, 726 (1958).
2. M. Ramakrishna and A. Ganguly, in: Proc. 3rd Int. Geneva Conf., No. 28/P/792 (India) (1964).
3. N. G. Gusev et al., Radiation Characteristics of Fission Products (Handbook) [in Russian], Atomizdat, Moscow (1974).
4. F. Meienschein, in: Proc. 2nd Geneva Conf., Vol. 2, Atomizdat, Moscow (1959), p. 297.
5. L. Bunnej and D. Sam, Nucl. Sci. Eng., 39, 81 (1970).
6. P. Fisher and L. Engle, Phys. Rev., 134, B796 (1964).

LETTERS TO THE EDITOR

A POSSIBILITY OF REDUCING THE DOUBLING TIME
FOR THERMAL LIQUID-SALT BREEDER REACTORS

V. L. Blinkin   UDC 621.039.542.4

Conditions of expanded breeding can be attained in liquid salt uranium—thorium thermal reactors (LSR) upon continuous extraction of fission products and protactinium from the fuel salt circulating through the active zone [1]. Under such operating conditions a breeding coefficient BC = 1.064 is achieved in an MSBR-1000 reactor, along with a specific fissionable material charge of G_{sp} = 1.5 kg/MW (el.) and $T_2 \approx 20$ years [2]. An increase in the power capacity and the dimensions of the reactor permits increasing somewhat the breeding coefficient (to 1.08-1.085) and reducing G_{sp} to 0.8-0.9 kg/MW (el.), which permits providing $T_2 < 10$-12 years [2-3]. However, such an increase in the efficiency of an LSR is associated with an increase in the temperature of the fuel salt is is limited by the heat resistance of the construction materials. One can improve the neutron balance in a reactor by limiting the continuous extraction of the transmutation products of ^{233}U from the fuel salt. In the neutron balance of an MSBR ~ 4% of all the neutrons is absorbed by ^{234}U nuclei, and the entire chain of transmutations of nuclides under the action of neutrons from ^{234}U to ^{242}Pu has an effective number of secondary neutrons $\eta = 0.877$ in the MSBR spectrum [4]. If one excludes ^{234}U and all subsequent nuclides from the fuel composition of an MSBR, then its breeding coefficient is increased to 1.086, G_{sp} is reduced to 1.26 kg/MW (el.), and T_2 is reduced to 13.4 years.

Continuous extraction of ^{234}U from the fuel salt of an LSR can be accomplished in a special installation which separates ^{233}U and ^{234}U. A mixture of uranium isotopes in the form of UF_6 extracted from the fuel salts by the method of fluorination enters this installation. Such extraction is provided for in the design of the fuel reprocessing system of an MSBR prior to the entry of the fuel salt into the extractor system. The uranium extracted from the fuel salt in the form of UF_6 is returned to the loop, being reduced in advance to UF_4 in a hydrofluorinator.

Of course, the isotope separation system leads to an increase in the cost of an LSR. However, the improvement in the neutron balance, and as a result of this the increase in the breeding of excess ^{233}U, can compensate for the cost of the separation operation. The total costs of the fuel cycle are determined by the expression

$$C_T(x) = C_{T0} - \Delta C_T [1 + F(x)], \tag{1}$$

where C_{T0} represents the costs of the MSBR fuel cycle, which comprise the costs of the components of the fuel composition, continuous reprocessing of the fuel, and periodic replacement of the graphite moderator and ΔC_T is the value of the excess amount of ^{233}U made in the MSBR (without extraction of ^{234}U):

$$F(x) \equiv \frac{\Delta C(x)}{C_U \Delta G_0} = \frac{\Delta G(x)}{\Delta G_0} - 1 - \varepsilon \frac{D_p}{\Delta G_0}, \tag{2}$$

where $\Delta G(x)$ is the amount of excess ^{233}U made in the LSR per unit time with an equilibrium ^{234}U concentration x in the mixture of ^{233}U and ^{234}U in the composition of the fuel salt, $\Delta G_0 \equiv \Delta G(x_0)$, $x_0 = 0.258$ is the equilibrium concentration of ^{234}U in the MSBR in the absence of isotope separation in the fuel cycle, $\varepsilon = C_{u.s.o.}/C_U$, $C_{u.s.o.}$ is the cost of a unit separation operation, C_U is the cost of unit mass of ^{233}U, $\Delta C(x)$ is the change in the value of the excess ^{233}U produced upon extraction of ^{234}U, and $D_p = D_p(x, x_p, x_w)$ is the separating capacity of the stage, which depend on the flows in the separation stage and on the concentrations x, x_p, x_w of ^{234}U in the supply, extraction, and return (to the fuel salt loop) flows, respectively [5].

The quantity $\Delta G(x) = \Delta G(x, x_p)$ depends both on the equilibrium ^{234}U concentration x and on the losses of the ^{233}U extracted from the system in the composition of the flow enriched in ^{234}U with concentration $1 - x_p$ of ^{233}U. The function F depends on three independent variables, for which it is convenient to select x, x_p and x_w. These variables uniquely determine the values of the total flows in the separation stage and the fraction γ of the flow of uranium isotopes removed into the bypass loop of the isotope separation system. In addition, the
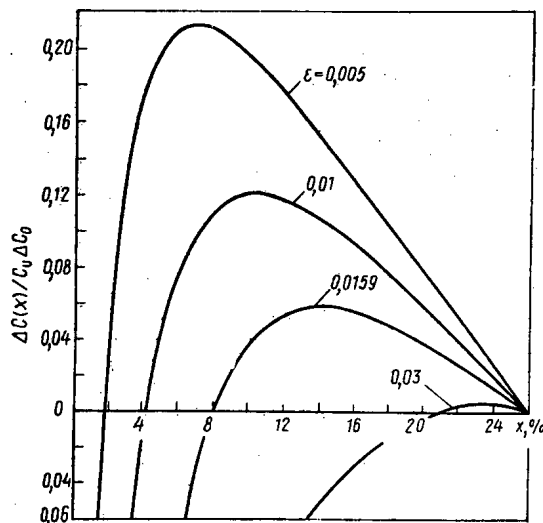
Fig. 1. Dependence of the relative variation of the cost
of excess ^{233}U on the equilibrium concentration of ^{234}U in
the fuel salt of an LSR.
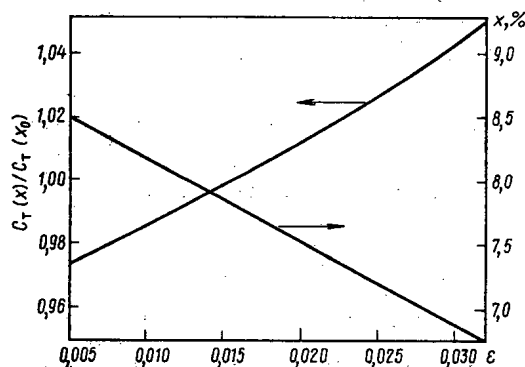
Fig. 2. The effect of ε on the fuel component of the cost
of electric energy $C_T(x)$ and on the equilibrium ^{234}U con-
centration x in the mixture of uranium isotopes in the fuel
salt of an LSR upon the extraction from the LSR of ^{234}U
under conditions providing for $T_2 = 15$ years.

function $F(x, x_p, x_w)$ depends on ε (as on a parameter). It follows from Eqs. (1) and (2) that minimal costs of
the fuel cycle are achieved when $F(x, x_p, x_w)$ has the maximum value determined by the conditions:

$$\partial F / \partial x_w = 0; \quad \partial F / \partial x_p = 0; \quad \partial F / \partial x = 0. \tag{3}$$

The first of the conditions (3) gives $x_w = x$. However, it is evident from the balance conditions of the
flows in the separation stage that it is impossible to realize such conditions with a nonzero productivity of
the stage. Therefore we restrict ourselves to the requirement that $(x - x_w)/x \ll 1$. The second condition de-
termines the dependence $x_p = x_p(x)$ which provides a local maximum of F with respect to x_p. The dependence
of the function $F(x)$ optimized with respect to x_w and x_p is given in Fig. 1 for the parameters of an MSBR [2. 4]
for four values of ε. The value $\varepsilon = 1.59 \cdot 10^{-2}$ corresponds to assumed values of C_U and $C_{u.s.o}$ for 1980 ($C_U =$
\$680/kg, $C'_{u.s.o} = \$120$/unit separation operation for the separation of ^{235}U and ^{238}U, and $C_{u.s.o} = 9\,C'_{u.s.o} = 1080$
dollars/unit separation operation for the separation of ^{234}U and ^{233}U [3]). For $\varepsilon = 1.59 \cdot 10^{-2}$ the function $F(x) \geq 0$
when $x = 0.08$. Consequently, according to (1) the total costs of the fuel cycle are not increased upon the ex-
traction of ^{234}U. At the same time for $x = 0.08$ and $T_2 = 15$ years the reactor produces an additional 13.3 kg/
year of ^{233}U, the separating capacity of the stage is 1050 unit separation operations/yr, and the concentration
of ^{234}U in the enriched flow extracted from the system amounts to 0.983.

When $x = 0.02$, $T_2 = 13.8$ years, but $F(x) < 0$ and the costs of the fuel cycle increase by 10%. However, if
$\varepsilon = 5 \cdot 10^{-3}$ (i.e., if $C_{u.s.o.}$ becomes less in proportion to the improvement in isotope separation technology),
then $x = 0.02$ is attained with $F(x) = 0$, and the costs of the fuel cycle are not increased. On the other hand, the

value of $C_{u.s.o.}$ of a small-capacity (~1000 unit separation operations/yr) separation facility can be larger by several times than for full-scale separation plants. It is shown in Fig. 2 how the costs of the fuel cycle depend on ε when $T_2 = 15$ years is provided for by the extraction of ^{234}U. The values of C_{T_0} and ΔC_T entering into Eq. (1) were taken as follows [3]: $C_{T_0} = 3.67$ dollars/kWh and $\Delta C_T = 0.47 \times 10^{-3}$ dollars/kWh. It follows from Fig. 2 that when $\varepsilon = 0.03$, which corresponds to $C_{u.s.o} = 2160$ dollars/unit separation operation, the fuel component increases by only 5% in comparison with its value for an MSBR in the absence of ^{234}U extraction and with $T_2 = 20$ years.

It is important to note that the condition $(x - x_w)/x \ll 1$, which provides for a maximum of F with respect to x_w, is satisfied with $\gamma = 1.5 \cdot 10^{-5}$ — the fraction of the flow of uranium extracted from the fuel salt of an MSBR reactor in the fuel-reprocessing loop. Therefore, the extraction of ^{234}U does not require additional expenditures on the fluorination of uranium to UF_6 and its subsequent reduction. A separation facility can be placed directly in the loop for the return of uranium to the fuel salt, which is provided for in the design of an MSBR.

Thus, the continuous extraction of ^{234}U from a type MSBR reactor permits reducing T_2 from 20 to 14-15 years without an appreciable increase in the cost of the fuel cycle and without increasing its power capacity if the ratio of the unit separation operation cost to the cost of unit mass of ^{233}U does not exceed 0.03. A further increase in ε leads to an almost proportional increase in the cost of the fuel cycle.

LITERATURE CITED

1. V. L. Blinkin and V. M. Novikov, Liquid-Salt Nuclear Reactors [in Russian], Atomizdat, Moscow (1978).
2. E. Bettis and R. Robertson, Nucl. Appl. Tech., 8, No. 2, 190 (1970).
3. L. Reichle, in: Proc. of Int. Conf. on Nuclear Power and Its Fuel Cycle, IAEA-CE-36/424, Salzburg, May 2-13, 1977.
4. M. Effantin et al., Reacture a Sels Founds. Filier "Sels Found." Dossier Technique, Coeur, 1, CEA/DEDR/DEMT R-76-16 (1976).
5. M. Benedict and T. Pigford, Nuclear Chemical Engineering, McGraw-Hill (1957).

A POSSIBILITY FOR THE USE OF HIGHLY ACTIVE FUEL REGENERATION WASTES OF FAST POWER REACTORS

E. M. Vetrov and E. M. Ikhlov

UDC 621.039.77

Processes have been developed for chemical production with the use of γ radiation, which permits reducing the number of processing stages of the raw materials and in the end gives an economy of raw materials and energy [1]. The realization of such processes in industry depends on the degree of "readiness" of the γ sources and the level of expenditures on γ radiation. The concept of the readiness of radiation sources for industrial purposes includes how well the principal parameters of the sources correspond to the requirements of radiation chemistry technology (e.g., with respect to strength and degree of uniformity of the adsorbed dose), the safety of operation of the cources to the population and the environment, and the presence in industry of an increasing reserve for expanded production of sources. Standard productivity in workshops with radiation chemistry technology is provided by a γ power from tens to hundreds of kilowatts.

The production of ^{60}Co γ sources for radiation chemistry in an amount of more than 30-50 kW/yr is associated with the problem of the construction of specialized establishments. At the same time provisions are made in a nuclear power system for the processing of highly active fuel regeneration wastes (FRW) of fast reactors (FNR) of significantly greater total γ power. The potential possibilities of FRW as sources of radiation for radiation chemistry productions are discussed with application to the physical characteristics of borosilicate glass, whose composition is recognized as one of the most promising for the extended storage of hardened fission products [2-5]. This glass is also assumed to be suitable for the fixation of FRW of fast neutrons. For FRW with a holding time of from 3 months to 30 years the γ activity of such glass amounts to

from 0.25 to 25 g. equiv. Ra/cm^3 for the optimal content of fission products (~16 mas %). Within these limits of holding time the effective coefficients of true absorption of γ radiation of a mixture of fission products in water-equivalent media and iron-based construction materials are practically constant. Taking account of the recommended geometry of containers for the storage of vitrified FRW (solid and hollow cylinders up to 200 and 1200 mm, in diameter, respectively), the following working dimensions of γ sources are assumed: Diameter of solid cylinders of 60-200, hollow-600 × (5-10), and height of 200-400 mm. The efficiency of the sources (in containers made of stainless steel up to 2 mm thick) is 0.75-0.5. When the efficiency of devices for γ radiation ~0.2, the expected strengths of the absorbed dose amount to 5-500 rad/sec, depending on the holding time of the FRW. The radiation of FRW with a holding time less than 3 years should be used at the site of their production, but with a longer holding time they can be used in installations situated outside a radiochemical establishment. The suggested dimensions of the sources permits operating them with the use of systems of equipment which are inexpensive in comparison with the unloading machines of reactors and which have been developed for radioisotope γ-facilities [6] in connection with a specific γ strength of the same order as the fuel unloaded from reactors.

Conditions with a temperature difference less than 600°C, which are safe for vitrified FRW, are expected in the presence of the compulsory gas or water cooling in the irradiators of nuclear installations [7]. In emergency situations vitrified FRW, being appreciably more resistant to leaching, pose less danger of radioactive contamination of the environment than materials of ^{60}Co and ^{137}Cs sources. The cost of γ radiation sources based on FRW can be determined as the fraction of the expenditures in nuclear power which is necessary for vitrification and sealing up of FRW.

The acquisition of FRW by the chemical industry will provide an economy for nuclear power in the construction and operation of specialized storage facilities for highly active hardened wastes.

Expansion in production of the strengths of γ radiation of FRW, which is estimated to be proportional to the anticipated increase in nuclear power capacities, makes it advisable to create in the near future an experimental industrial facility with a γ capacity of the order of several tens of kW, and in the long term – the construction of a number of facilities with a capacity of hundreds of kilowatts in a design for transportable FRW with a holding time of only 2-3 years.

The data given here permit consideration of the problem of the necessity for an all-round development of vitrification technology and the application in the national economy of the radiation of hardened highly active wastes of fast reactor (FNR) fuel regeneration.

LITERATURE CITED

1. Radiation Chemistry [in Russian], Atomizdat, Moscow (1972).
2. In: Proc. IAEA Symp. "Management of radioactive wastes from nuclear fuel cycle," Vienna (1976).
3. V. B. Shevchenko (editor), Reprocessing of the Fuel of Power Reactors [Russian translation], Atomizdat, Moscow (1972).
4. N. E. Brezhnev et al., [2], Vol. II, p. 85.
5. G. B. Poluéktova, Contemporary State of the Problem of the Processing and Disposal of Highly Active Wastes [in Russian], TsNIIatominforma, Moscow (1976).
6. E. E. Kulish et al., Design and Construction of Radioisotope Radiation Chemistry Facilities (Handbook) [in Russian], Atomizdat, Moscow (1975).
7. N. Mifsuishi and K. Ishiguma, J. Nucl. Sci. Tech., 13, No. 4, 215 (1976).

743

USE OF A CRYSTAL SYNCHROTON TARGET
TO OBTAIN A POSITRON BEAM

V. G. Potemkin and S. A. Vorob'ev

UDC 539.124.6

It is known that if the energy of an electron beam is high enough its interaction with a single crystal oriented in a definite way exhibits interference effects. The use of this phenomenon is of interest for increasing the intensity of a positron beam with an angular spread smaller than the critical channeling angle. In view of this, experiments were performed on the effect of the shape of the energy spectrum of a collimated beam of bremsstrahlung photons of a synchrotron on the double differential positron yield $d^2N^+/dE^+d\Omega e^+/e^-$ (MeV $\cdot$ sr)$^{-1}$ from an amorphous converter.

The bremsstrahlung beam, which had an angular spread of $0.8 \cdot 10^{-3}$ rad, was obtained from the slowing down of accelerated electrons in internal targets of the Sirius synchrotron [1]; in a tantulum target $0.4 \cdot 10^{-3}$ m ($0.1X_0$) thick, and in a diamond target $(10 \times 6 \times 2) \cdot 10^{-3}$ m ($1.52 \cdot 10^{-2}X_0$) thick.

The diamond target was located so that the angle between the [110] crystallographic axis and the momentum of the electron beam P_0 was $\beta = 1°$ 59', and the angle between the (001) crystal plane and P_0 was $\alpha = 76°$ 50'. The bremsstrahlung beam from this target was $\sim 40\%$ linearly polarized in the horizontal plane for the first interference maximum, which corresponds to a photon energy $K = E_\gamma/E_0 = 0.33$ for $E_0 = 800$ MeV. Figure 1 shows spectra of bremsstrahlung beams from diamond and tantalum targets measured by a magnetic pair spectrometer with an energy resolution of $\sim 3\%$ for the conditions described in [2]. The total energy of the bremsstrahlung beam from the tantalum target was 1.4 times as large as that from the diamond, but in the range of photon energies corresponding to the first maximum the intensity of the photons from the diamond target was 1.3 times as large as that from the $0.4 \cdot 10^{-3}$ m thick tantalum target.

Positrons were produced by the bremsstrahlung beam in copper converters $0.22X_0$ and $0.44X_0$ thick. The photon beam reached the converter after penetrating a $3 \cdot 10^{-3}$ m thick duralum plate in the connecting tube of the accelerator vacuum chamber and a layer of air, which altogether amounted to $0.095X_0$.

The yield of positrons at an angle $\theta \approx 0°$, where θ is the angle between the direction of the photon beam and the positron momentum P_+ (MeV/c), was measured directly in the experiment. Positrons were recorded by the telescope of 2X scintillation detectors. The resolving time of the recording system was $0.7 \cdot 10^{-6}$ sec, the error was $\sim 1.3\%$ for fewer than $\sim 10^4$ positrons/pulse, the duration of the synchrotron radiation pulse was 20 msec, and the current of accelerated electrons was $(20-30) \cdot 10^{-3}$ A. The positron energies were analyzed by a magnetic spectrometer on a SP-57-1-A base with pole pieces having an angular aperture of 38° and a resolution of 5.8% [3]. The results of the measurements were normalized to the readings of a thin-walled ionization chamber-monitor [4]. The total error of the measurements did not exceed ± 20%. The measured values of $d^2N^+/dE_+d\Omega$ from beams of bremsstrahlung photons with various energy spectra are shown in Fig. 2.

The appearance of a peak on the curve for the positron yield, $d^2N^+/dE_+d\Omega = f(E_+)$ at $\theta \approx 0°$ can be explained by the contribution to the bremsstrahlung intensity by coherent bremsstrahlung photons of the first interference maximum. The latter are radiated into a small angular cone substantially smaller than that formed by the system of collimators. According to our investigation the intensity and monochromaticity of the positron beam produced by coherent photons of the first interference maximum depend on these same parameters of a beam of bremsstrahlung photons with a quasimonochromatic spectrum. For more complete collimation, when the angle $\theta_{col} < m_0c^2/E_0$, the natural angle of emission of bremsstrahlung photons, the incoherent bremsstrahlung intensity is decreased, and the effect under discussion is more pronounced. The positron yield at $\theta \approx 0°$ thus depends not only on the thickness of the amorphous converter for $E_{\gamma max} \approx E_0 = const$, but also on the thickness and orientation of the single crystal relative to P_0. The experimental data obtained are in satisfactory agreement with the results of theoretical calculations of $d^2N^+/dE_+d\Omega$ performed by the Monte Carlo method using a program [5] for a photon beam with a quasimonochromatic spectrum (cf. Fig. 1), but without taking account of the polarization of the photons. The effect of linear polarization of bremsstrahlung photons on the positron yield was not investigated.
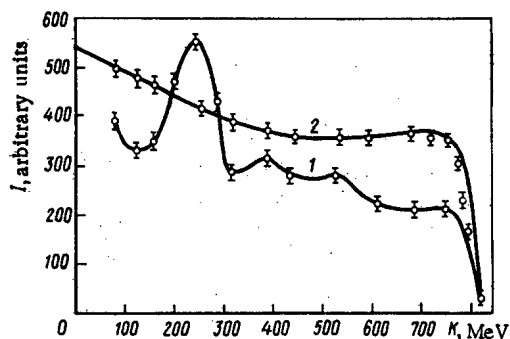
Fig. 1

Fig. 2

Fig. 1. Bremsstrahlung spectra from 1) a crystal and 2) an amorphous target normalized to the same number of dumped electrons.
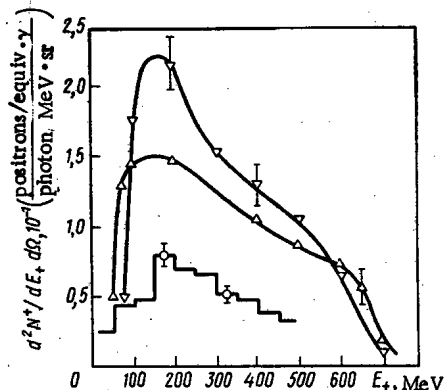
Fig. 2. Positron yield $d^2N^+/dE_+d\Omega$ from beams of bremsstrahlung photons with various energy spectra for a copper target $0.22X_0$ thick; Δ, yield of positrons produced by bremsstrahlung from an amorphous target; ∇, the same from a crystal target; O, calculated by Monte Carlo method with program in [7]. Measured and calculated data normalized to an equivalent γ photon.

According to our data a beam of positrons can be obtained in a given range of angles and energies with a monochromaticity and intensity determined by the corresponding parameters of the first interference maximum. The position of the positron beam and its intensity can be changed by varying the angles of orientation and thickness of the single crystal while maintaining constant values of the parameters of the beam of accelerated electrons generating coherent bremsstrahlung. The single crystal used is optimum from the point of view of the amplitude of the interference maxima, since it has the greatest close-packed structure with a fcc lattice. The orientation of the crystal was chosen so as to achieve maximum polarization for performing experiments on the photoproduction of mesons. The class of orientations in which the contributions to the interference maximum give some points of the reciprocal lattice of the single crystal, and the photon beam has a smaller polarization but higher intensity, is much preferable for this purpose. From this point of view, the expedient orientation of a single diamond crystal is $\beta \neq 0$, $\alpha = 0$. An appreciably larger increase in the positron yield for a converter thickness close to the optimum of $\sim 0.5X_0$ can be achieved for an energy $E_+ < 0.35 E_{\gamma max}$. The angle of collimation of the photon beam and the spread of the positron beam remain the same as in experiments with a beam of photons from an amorphous target. The system combining an internal crystal target with an amorphous converter is of practical interest for experiments imposing restrictions on the size or angular spread of the positron beam.

In conclusion, the authors thank Prof. A. N. Didenko and senior scientist V. M. Kuznetsov for making it possible to perform the measurements.

LITERATURE CITED

1. A. A. Vorob'ev et al., The 1.5-GeV TPI Synchrotron [in Russian], Atomizdat (1968).
2. V. M. Kuznetsov et al., Prib. Tekh. Eksp., No. 3, 24 (1973).
3. V. N. Kuz'min et al., in: Proc. of Sixth Interuniversity Conference on Electron Accelerators [in Russian], Énergiya, Moscow (1968), p. 37.
4. G. V. Potemkin, Deposited Article No. 747-75, VINITI, Moscow (1975).
5. V. A. Tayurskii, At. Energ., 42, 317 (1977); F. M., Izrailev et al., Preprint Inst. Yad. Fiz. 63-73, Novosibirsk (1973).

GAS-CHROMATOGRAPHIC APPARATUS FOR DETERMINING
CARBON IN URANIUM AND URANIUM DIOXIDE PELLETS
WITH SERIAL LOADING OF SPECIMENS

V. A. Nikol'skii, V. K. Markov,   UDC 546.264
A. S. Panov, and B. S. Valyunin

The allowable carbon content in metallic uranium and uranium dioxide pellets is determined by the conditions under which these materials are used in nuclear power engineering: The more stringent the conditions of the application of these materials, the higher the requirements as to their purity. For example, in order to avoid carbonization of the fuel-element can the carbon content in UO_2 pellets should not exceed thousandths of a percent.

The methods described in [1-4] for determining carbon in metals, methods based on burning the analyzed material in a stream of oxygen, have the major drawback that only one boat with the specimen under analysis is loaded into the tube for combustion. Since the apparatus is opened to load a specimen, air with carbon-containing gases enter. This results in a higher correction for the blank test (one for each determination) and, therefore, a higher limit for carbon detection. Thus, low carbon contents in materials are made with large (1-5 g) specimens [3, 4] which is extremely undesirable for actinides because of safety considerations.

Small weighed portions (10-50 mg) are used in conductometric techniques [5, 6] for determining carbon in uranium but the necessity, after each specimen, to check the airtightness of the instrument and to eliminate from it CO_2 which may have entered with air stretches each determination out to 1 h or more.

A rapid, highly sensitive gas-chromatographic method is proposed for determining carbon in metallic uranium and UO_2 pellets: By burning the analyzed material in a stream of oxygen and then concentrating and measuring the liberated CO_2 with a KhL-4 chromatograph.

A distinctive feature of the apparatus (Fig. 1) is the combustion unit consisting of a quartz tube 8 to length 1-1.2 m and diameter 20-25 mm, moving on rails along the tube of the furnace 11 with Silit rods. Before the operation begins the furnace is moved to the extreme right-hand position, the ground-glass joint is removed from the tube, and a number (up to 20) of boats 9 with specimens are loaded into the cold zone at one time. Behind the first boat, counting from the furnace, a magnet places a steel ball 10 whose mass and diameter allow
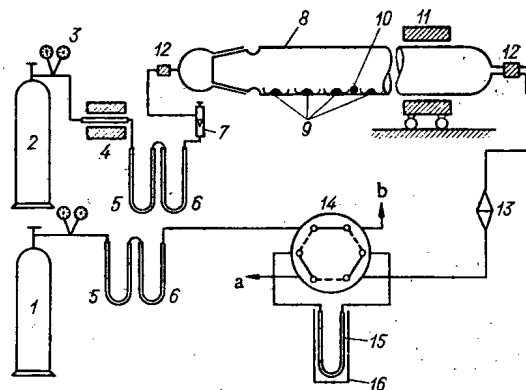

Fig. 1. Gas-chromatographic apparatus for determining carbon in uranium and UO_2 pellets with serial loading of specimens: 1, 2, 4-6, 8-11, 13-15) see text; 3) reducers; 7) rotameter (PS-3A with lightened float); 12) vacuum hoses; 16) Dewar flask with cooling mixture; a) to atmosphere; b) to chromatograph.

TABLE 1. Determination of Carbon in Uranium Specimens

Metallic uranium		Uranium dioxide	
weighed portion, mg	carbon content, %	weighed portion, mg	carbon content, %
11,4	0,119	30,7	0,0059
20,3	0,112	58,3	0,0052
59,7	0,109	150,4	0,0058
200,3	0,110	300,2	0,0055
400,7	0,112	600,4	0,0054
1050,4	0.111	—	—
2052,2	0,109	—	—

the boat to be moved (pulled) along the tube by means of an external magnet. The diameter of the tube is chosen so that the ball would pass above the boat. After the loading and a blank test combustion is begun: The ball is used to move the first boat to the edge of the furnace, the ball is then returned to the cold zone and placed behind the second boat, and the hot furnace is pulled onto the first boat. After the combustion of the first specimen the furnace is moved to the extreme right-hand position, the second boat is moved up against the first, the ball is placed behind the third boat, and the furnace is moved onto the second boat and the entire series is analyzed in this way.

The CO_2 is concentrated in a U-shaped trap 15 (metal of length 0.5-0.6 m and diameter 4 mm, filled with silica gel particles of diameter 1-0.5 mm). During concentration of CO_2 the trap is cooled with a mixture of acetone or alcohol with dry ice. As the CO_2 is flushed out the trap is heated with water.

To purify the oxygen 2 and helium 1 from CO_2 impurity and water vapor the apparatus is furnished with two traps: Metal tubes of length 1 m and diameter 18-20 mm with activated molecular sieves 5 and Ascarite 6. The oxygen is furthermore passed through a furnace 4 with CuO, heated to 700-750°C in order to oxidize the carbon-containing gases (including CO) to CO_2.

The streams of oxygen and helium are switched by using a six-position valve 14 which can take two positions. In the first position (solid lines) oxygen passes through trap 15 and in the second position (dashed line), helium passes.

In order to purify the oxygen coming out of the combustion tube from sublimates, dust, and aerosols the apparatus is provided with a trap 13 (a tube filled with fiberglass and a Petryanov cloth membrane). The technique of the analysis as a whole reduces to the following. Once the chromatograph has reached operating conditions a series of boats containing the specimens to be analyzed are loaded into the combustion tube 8 and a blank test is performed. When the apparatus has been found to be airtight and the oxygen and helium have been found to be purified well from carbon-containing impurities (according to the data of the chromatograms of the blank test) analyses are begun: The furnace, which has been heated to the desired temperature, is moved onto the first boat; after the time established for complete combustion of the carbon from the specimen valve 14 is switched and trap 15 is heated; the CO_2 travels from the trap to the chromatograph, whose signal is recorded on a recorder chart.

The apparatus can be used to analyze radioactive materials (metals, alloys, oxides), from which carbon is extracted quantitatively in the gaseous phase as CO_2 at a temperature no higher than 1200°C. It was discovered that carbon is burned out of uranium metal shavings completely at a temperature of no less than 900°C in 1 min with an oxygen flow rate of 100-150 cm^3/min.

Determination of carbon in UO_2 is carried out at a temperature no lower than 1000°C. According to our data and those of [7], the separation of any gas mixture concentrated in the trap is advisably carried out in a silica gel column of length 1 m at room temperature with a carrier-gas (He) flow rate of 120 cm^3/min.

Table 1 gives the results of the determination of carbon in metallic uranium and its dioxide; it is seen that for such analysis it is sufficient to have weighed portions of 20-30 mg. The limit of detectability of carbon with a weighed portion of 300 mg is $2 \cdot 10^{-4}$ wt. %. However, in analysis of UO_2 containing less than $3 \cdot 10^{-3}$% carbon the result may be overestimated owing to sorption of CO_2 from the air by the carbon dioxide. The duration of a single determination of carbon is 7-10 min in the case of uranium and 10-15 min in the case of UO_2 pellets.

The reproducibility of the method in determining 0.11%, 0.048%, and 0.02% carbon in uranium is characterized by a variation coefficient of 6%, 11%, and 18%, respectively, and in determining 0.01% and 0.006% carbon in UO_2 pellets, 11% and 17%, respectively.

LITERATURE CITED

1. L. L. Kunin, E. D. Malikova, and B. A. Chapyzhnikov, Determination of Oxygen, Carbon, Nitrogen, and Hydrogen in Alkali and Alkaline-Earth Metals [in Russian], Atomizdat, Moscow (1972).
2. P. Ya. Yakovlev, E. F. Yakovleva, and A. I. Orzhekhovskaya, Determination of Carbon in Metals [in Russian], Metallurgiya, Moscow (1972).
3. All-Union State Standards (GOST) 12344-66 and 12365-66 (Alloy and High-Alloy Steels. Methods of Chemical Analysis) [in Russian], Standartizdat, Moscow (1967).
4. Production Group, U. K. Atomic Energy Authority, Report No. 400 (S) (1963).
5. V. K. Markov et al., in: Uranium. Methods of Determination [in Russian], Atomizdat, Moscow (1964), p. 431.
6. D. I. Ryabchikov and M. M. Senyavin (editors), Analytic Chemistry of Elements, Uranium [in Russian], Izd. Akad. Nauk SSSR, Moscow (1962).

α PARTICLE RECORDING WITH RF-3
FILM TRACK DETECTORS

I. V. Zhuk, A. P. Malykhin,   UDC 539.1.074.88
L. P. Roginets, and O. I. Yaroshevich

Increasing attention is recently being given to the use of solid track detectors for recording α particles [1].

Here we present the principal results of a study of the detection of α particles with the aid of triacetate substrates of various photographic materials: type "FOTO" amateur film, "MIKRAT-200" and "MIKRAT-300" industrial film, MZ-3 positive film, x-ray film, multipurpose cinefilm, and RF-3 fluorographic film.* Most suitable for detection purposes was found to be the substrate of RF-3 film which after etching preserves a clean surface and a uniformly transparent layer, and has minimum natural background ($\sim 5 \cdot 10^2$ tracks/mm^2). Unlike tracks with "ragged" edges which form in the substrate of "FOTO" and x-ray films, the tracks formed in the RF-3 film substrate have a regular form of circles or slightly elongated ellipses, detection taking place preferentially on the surface which has been covered with emulsion. For similar processing conditions, the tracks formed on this surface are more prominent and somewhat sharper. Accordingly, the RF-3 film was studied in detail. Figure 1 shows the average track diameter as a function of etching time and of the density of aqueous solution of NaOH. The film was processed at 60°C since higher temperatures impair the detector surface and lower temperatures require a longer processing time. The α particle source was a thick (as compared with the mean free path) 0.1-mm layer of uranium with a 90% enhanced content of ^{235}U. The principal emitter was ^{234}U with $E_\alpha = 4.8$ MeV which was in close contact during exposure with the substrate of RF-3 film from which the emulsion was washed away. After exposure the detectors were placed in a NaOH solution of the investigated density and etched at 30 min intervals. After each 30-min interval the detectors were dipped in a fixing bath (10% solution of acetic acid), vigorously flushed in water, dried, and photographed under a microscope always on one and the same portion of the surface. The average diameter for a group of 50 tracks was determined from enlarged photographs. Increasing the etching time caused a deterioration of the detector surface and of the track quality, whereas a reduction of the etching time and of the NaOH solution density led to the need of longer detector processing. Increasing the solution density increases the track growth rate and necessitates tighter processing time and solution density control. The optimal detector processing conditions were found to be etching of the detector for about 4 h in NaOH solution of a density equal to 1.2 g/cm^3.

The effect of etching time on the detection of α particles of different energies was investigated for the selected solution density. In this case the α particle source was a thin reference source (OSAI) of ^{239}Pu ($E_\alpha = 5156$ keV) with several collimating diaphragms with a 3-mm aperture. The energy of α particles passing through a layer of air and incident on the detector was determined to within 60 keV from well-known relations [2] between the measured air density and the distance from the source to the detector.

---

*The films were kindly provided by the V. V. Kuibyshev Kazan Chemical Plant.
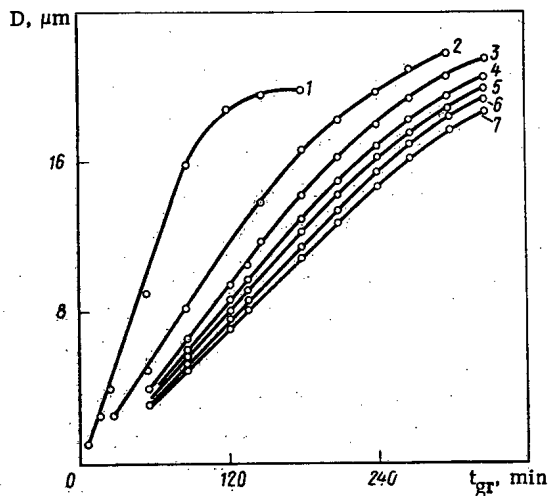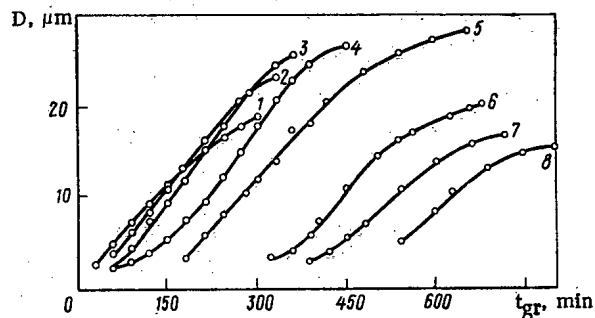
Fig. 1   Fig. 2

Fig. 1. Average diameter of α-particle tracks recorded in a 2π geometry as a function of etching time for NaOH solution densities of 1.305, 1.26, 1.22, 1.18, 1.17, 1.15, and 1.11 g/cm^3 (curves 1-7, respectively).

Fig. 2. Average diameter of tracks produced by α particles normal to the detector as a function of etching time in NaOH solution of a density 1.2 g/cm^3 for E_α = 0.98, 1.44, 1.81, 2.20, 2.45, 2.92, 3.77, and 3.36 MeV (curves 1-8, respectively).

The obtained results (Fig. 2) show that the track diameter is not a monotone function of α-particle energy and that direct α-particle spectrometry on the basis of track diameters in RF-3 substrate is possible only within a relatively narrow energy range.

By increasing the etching time it was possible to detect α particle of higher energies which penetrated deeper into the detector. This indicates that only the ends of α-particle tracks are detected where dE/dx is maximum. The detection of α particles with an energy of ~2.5 MeV becomes difficult, and with energies > 3.5 MeV practically impossible, since the long etching time needed for such energies makes the detector surface too irregular. To detect α particles with energies of 2.5 MeV or higher normally incident on the detector surface, the particles must be first moderated by an air layer or by thin foils (films).

To test operation in neutron fields, the detectors were irradiated in the BTS-2 critical assembly [3] with an average neutron spectrum energy of ~600 keV; the density of secondary background tracks on the detector surface due to neutrons was $(1.33 \pm 0.11) \cdot 10^{-6}$ tracks/neutron. Irradiation in the thermal spectrum produced practically no additional background.

The obtained data lead to a conclusion that the substrate of RF-3 film from which the emulsion is washed off makes a good α-particle detector. The found dependence of track diameters on the processing conditions and α-particle energy make it possible to select an exposure dose such that the filling factor of the detector surface by tracks does not exceed about 0.4 below which track overlapping and count errors associated with it are insignificant.

LITERATURE CITED

1.   Nucl. Instrum. Methods, 147, No. 3-4 (1977).
2.   O. F. Nemets and Yu. V. Gofman, Nuclear Physics Handbook [in Russian], Naukova Dumka, Kiev (1975).
3.   N. M. Grusha et al., Izv. Akad. Nauk BSSR, Ser. Fiz.-Energ. Nauk, No. 1, 20 (1974).

IDENTIFICATION AND ESTIMATE OF TRITIUM
CONTENT IN VVR-M REACTOR WATER

A. M. Drokin, V. K. Kapustin,
V. P. Korotkov, V. V. Leonov,
V. K. Mironov, and Yu. P. Saikov

In 1976 water from the dump tanks of the VVR-M JINR reactor which had been treated at the special water purification plant was found to contain a radionuclide with a low-energy (below 20 keV) β decay. Somewhat earlier a similar source had been found in the water of the primary loop of the reactor. It was assumed that this radionuclide was tritium. Information on the assumulation of tritium in ordinary water used as a coolant in nuclear reactors is available in [1-3]. The main purpose of the present work is to confirm the validity of the assumption that the activity is due to tritium and to estimate the tritium content in the reactor water. The accumulation of tritium in this water may be of fundamental importance both during its deactivation and in the reactor operation plan.

This liquid-scintillation method was employed to identify and estimate the tritium content in the reactor water. The measurements were made with an "Isocap 300" instrument. The counting rate from the radionuclide in the sample was recorded simultaneously in low-energy channel A and high-energy channel B. Channel A (2-18 keV) was used to measure tritium, and Channel B (20-1500 keV) to monitor the presence of other radionuclides in the sample. The samples counted were made by mixing 13.5 ml of liquid scintillator ZhS-8 and 1.5 ml of the water being investigated. The effect of the quenching of scintillations in the sample was monitored by an external standard. Even after storage the water of the primary loop has a complex radionuclidic composition. Therefore, in the measurements the possibility of filling channel A by recording β particles from radionuclides other than tritium is not excluded. In addition, if the β decay is accompanied by the emission of γ rays, there is a possible contribution to the observed counting rate from Compton electrons produced by the absorption of γ rays in the scintillation material. To eliminate these undesirable phenomena and to identify tritium in the water of the primary loop the coolant was distilled and then purified by using KU-2 and AV-17 ion-exchange resins. The removal of radionuclides interfering with the determination of tritium was considered complete when the counting rate of the sample in channel B corresponded to the background, within the limits of statistical error. To reduce the contamination of the measuring cells in experiments with water of the primary loop the coolant was stored for two weeks and then diluted ten fold with distilled artesian water having a tritium content of 10^{-10} Ci/liter. The radioactive purity of the equipment and materials was monitored at all stages of the purification. To this end the experimental equipment was first flushed with distilled artesian water, and after each stage of purification samples were removed for analysis. The prepared samples were considered "background." The experimental results are listed in Table 1. Analysis shows that the source of the low-energy β radiation is a long-lived nuclide with a half-life or more than 2 years. In its decay no β particles or γ rays with energies above 20 keV are emitted. Neither distillation nor ion-exchange purification removes this source. The observed difference in counting rates after KU-2 and AV-17 ion-exchange purification is accounted for by dilution, since the resins were prepared for the experiments with distilled artesian water. The source could not be removed by coprecipitation with iron hydroxide.

The combination of these characteristics of the behavior of the source of low-energy β radiation in the experiments performed on the purification of the water of the primary loop with other of its properties (half-life, energy of β radiation, absence of γ radiation) led to the conclusion that the radionuclide being studied was tritium. This is indicated also by the results of check experiments on the identification of tritium in the water of the primary loop performed by the radioactive gas chromatographic method as in [4]. The water was dissociated by aluminum carbide, and after gas chromatographic detection by thermal conductivity the methane formed was measured in a flow counter. These experiments showed conclusively that the water of the primary loop contained tritium.

TABLE 1

Analyzed object — water of the primary loop after tenfold dilution	Measured channel	Counting rate, pulses/min			
		primary loop of water after two-week exposure		primary loop of water after 6-month exposure	
		cell 1	cell 2	cell 1	cell 2
Before distillation	A	15879 (21)	16528 (23)	15998 (23)	16345 (21)
	B	2073 (22)	2164 (24)	135 (19)	147 (23)
After distillation	A	15113 (19)	15332 (18)	15657 (18)	15960 (20)
	B	24 (21)	22 (22)	16 (26)	11 (24)
After distillation and ion-exchange purification by KU-2	A	13174 (19)	12497 (24)	13051 (19)	12541 (18)
	B	25 (25)	32 (25)	30 (22)	24 (24)
After distillation and ion-exchange purification by KU-2 and AB-17	A	10685 (23)	10664 (23)	10601 (26)	10637 (18)
	B	28 (23)	20 (24)	28 (20)	31 (23)

The parentheses indicate the counting rate with respect to the background object.

A quantitative estimate of the tritium content in the reactor water was made by determining its registration efficiency in the form of HTO on the Isocap 300 counter. Tritiated water obtained from the Institute of Water Problems, Academy of Sciences of the USSR was used as a standard. As a check the standard used was compared with a tritiated water standard obtained from the Radium Institute. The difference between the standards was 3.4%. The concentration of tritium in the water of the primary loop of the VVR-M reactor as of Dec. 9, 1976, was $(1.3 \pm 0.1) \cdot 10^{-4}$ Ci/liter, in purified water from the reactor dump tanks as of June 2, 1976 $(1.2 \pm 0.1) \cdot 10^{-5}$ Ci/liter. From the radioactive gas chromatographic measurements the concentration of tritium in the water of the primary loop as of Dec. 9, 1976 was $(2.0 \pm 0.4) \cdot 10^{-4}$ Ci/liter, which, within the limits of twice the error of the measurements, agreed with the tritium concentration as measured by the liquid-scintillation method.

It is difficult to substantiate the observed tritium content in the VVR-M reactor water because of the lack of reliable data on its entrance into the coolant from fuel elements, boron control rods, and the beryllium reflector where it is produced.

Since the reactor systems were designed to operate with a coolant containing radioactive products, one should expect that the observed tritium content in the water of the primary loop, which is comparable with that of the fragment radionuclides I, Sr, and Ba, will not lead to any further complications except the purification of reactor discharge water containing tritium in amounts exceeding the yearly average admissible concentration in water. Therefore, in processing radioactive water the rate of its entry into the special water purification plant is regulated in such a way that the tritium concentration in the purified water does not exceed the level permitted by health regulations.

LITERATURE CITED

1. Tritium (a thematic collection of translation). AINF 149 (P) TsNIIAtominform (1971).
2. Yu. P. Abolmasov, At. Energ., 41, 215 (1976).
3. A. I. Lur'e, At. Energ., 41, 258 (1976).
4. V. V. Leonov, E. N. Sinotova, and M. V. Korsakov, Radiokhimiya, 16, 564 (1974).

CALCULATION OF X-RAY AND γ-RAY PHOTOELECTRIC ATTENUATION FACTORS FOR STATISTICAL MODELING OF TRANSPORT PROCESSES

O. S. Marenkov and T. V. Singarieva

UDC 539.12.04

In the numerical modeling of photon transport in matter by the Monte Carlo method, it is expedient to represent the functional dependence of the partial integrated cross sections for elementary interaction pro-

TABLE 1. Coefficients τ_i for Calculating Macroscopic Cross Sections (cm^2/g) in the Range $E \geq E_K$ and the Error of the Approximation δ

Element	E_{max}	$-\tau_0$	τ_1	$-\tau_2$	τ_3	$-\tau_4$	δ, %
Hydrogen	10	.2645E—02	.7086E—01	.7487E+00	.5575E+01	—.1936E+01	0,3
Helium	30	.2154E—02	.1413E+00	.3322E+01	.4893E+02	—.1576E+02	2,5
Lithium	40	.3411E—02	.3088E+00	.1009E+02	.2076E+03	—.4091E+02	2,2
Beryllium	60	.3142E—02	.4216E+00	.2014E+02	.5918E+03	—.4857E+02	2,8
Boron	80	.3267E—01	.5682E+01	.3483E+03	.1326E+05	.3243E+03	2,6
Carbon	100	.3172E—02	.6921E+00	.5340E+02	.2610E+04	.2941E+03	2,7
Nitrogen	150	.1991E—02	.6169E+00	-6514E+02	.4259E+04	.8060E+03	3,3
Oxygen	150	.2663E—02	.8397E+00	.9179E+02	.6634E+04	.1906E+04	2,4
Fluorine	150	.3038E—02	.9836E+00	.1128E+03	.9171E+04	.3414E+04	1,7
Neon	200	.1806E—02	.7942E+00	.1218E+03	.1307E+05	.5600E+04	2,0
Sodium	200	.2205E—02	.9767E+00	.1520E+03	.1740E+05	.9889E+04	1,8
Magnesium	300	.1134E—02	.7194E+00	.1514E+03	.2298E+05	.1398E+05	1,9
Aluminum	300	.1267E—02	.8192E+00	.1770E+03	.2913E+05	.2154E+05	1,5
Silicon	300	.1336E—02	.8981E+00	.2042E+03	.3824E+05	.3247E+05	2,7
Phosphorus	300	.1443E—02	.9891E+00	.2304E+03	.4603E+05	.4555E+05	0,9
Sulfur	400	.8812E—03	.8023E+00	.2325E+03	.5733E+05	.6273E+05	1,4
Chlorine	400	.9405E—03	.8955E+00	.2701E+03	.7466E+05	.9110E+05	2,0
Argon	400	.8683E—03	.8412E+00	.2571E+03	.7510E+05	.1040E+06	0,9
Potassium	500	.6035E—03	.7416E+00	.2648E+03	.9423E+05	.1366E+06	1,5
Calcium	500	.6762E—03	.8461E+00	.3039E+03	.1144E+06	.1881E+06	1,2
Scandium	600	.5544E—03	.8225E+00	.3227E+03	.1332E+06	.2494E+06	1,1
Titanium	600	.5721E—03	.8169E+00	.3121E+03	.1411E+06	.2765E+06	1,2
Vanadium	600	.5121E—03	.8087E+00	.3208E+03	.1595E+06	.3435E+06	1,1
Chromium	800	.3713E—03	.7421E+00	.3119E+03	.1855E+06	.4368E+06	1,0
Manganese	800	.3784E—03	.7792E+00	.3356E+03	.2075E+06	.5247E+06	1,0
Iron	800	.4010E—03	.8505E+03	.3624E+03	.2401E+06	.6564E+06	0,9
Cobalt	800	.4083E—03	.8019E+00	.3752E+03	.2660E+06	.7842E+06	0,9
Nickel	1000	.3261E—03	.8645E+00	.3757E+03	.3078E+06	.9667E+06	0,9
Copper	1000	.3311E—03	.8949E+00	.3807E+03	.3292E+06	.1125E+07	0,8
Zinc	1000	.3370E—03	.9448E+00	.3319E+03	.3667E+06	.1322E+07	0,9
Germanium	1500	.1996E—03	.8264E+00	.3379E+03	.4263E+06	.1720E+07	1,1
Arsenic	1500	.2091E—03	.8853E+00	.3399E+03	.4687E+06	.2009E+07	0,9
Selenium	1500	.2143E—03	.9275E+00	.3395E+03	.5030E+06	.2290E+07	0,9
Molybdenum	3000	.1224E—03	.1154E+00	.1235E+03	.9589E+06	.6408E+07	1,5
Palladium	4000	.8518E—04	.1262E+01	—.1309E+03	.1234E+07	.9640E+07	1,9
Silver	4000	.9806E—14	.1383E+01	—.1556E+03	.0331E+07	.1092E+08	1,7
Cadmium	4000	.9996E—04	.1437E+01	—.2013E+03	.1391E+07	.1193E+08	1,6
Tin	4000	.1157E—03	.1579E+01	—.3248E+03	.1545E+07	.1406E+08	1,5
Antimony	5000	.7005E—04	.1494E+01	—.5211E+03	.1610E+07	.1486E+08	2,1
Iodine	5000	.7997E—04	.1685E+01	—.6670E+03	.1804E+07	.1798E+08	1,7
Barium	5000	.8762E—04	.1924E+01	—.9389E+03	.2072E+07	.2284E+08	1,5
Tungsten	10000	.3494E—14	.3526E+01	—.5065E+04	.4282E+07	.6975E+08	1,4
Platinum	10000	.2472E—04	.3976E+01	—.6563E+04	.4837E+07	.8563E+08	1,3
Gold	10000	.2542E—04	.4150E+01	—.7005E+04	.4987E+07	.8642E+08	1,2
Mercury	15000	.2533E—04	.4276E+01	—.7435E+04	.5080E+07	.8815E+08	1,3
Lead	15000	.2409E—04	.4545E+01	—.8196E+04	.5399E+07	.1006E+09	1,2
Radium	15000	.1984E—04	.5442E+01	—.1124E+05	.6210E+07	.1252E+09	0,9
Thorium	15000	.1833E—04	.5802E+01	—.1236E+05	.6537E+07	.1410E+09	1,0
Uranium	15000	.1256E—04	.6068E+01	—.1368E+05	.6798E+07	.1517E+09	1,1
Plutonium	15000	.7086E—05	.6388E+01	—.1530E+05	.7048E+07	.1585E+09	1,6

cesses on the photon energy E by simple expressions which are convenient for computer calculations. The question of the analytic approximation of the energy dependence of the photoelectric absorption cross sections of photons $\tau(E)$ was discussed in [1, 2] where it was shown on the basis of theoretical [3] and semiempirical [4] data that the relation $\tau(E)$ for any element can be approximated by a polynomial in inverse powers of the energy with an error of no more than 3%

$$\tau(E) = \sum_{i=0}^{4} \tau_i E^{-i} \tag{1}$$

in the energy range $E_K \le E \le E_{max}$, with the value of E_{max} for each element given by the condition

$$\frac{\mu(E_{max})}{\tau(E_{max})} > 100,$$

where $\mu(E)$ is the total interaction cross section. In the energy range $E \le E_K$ Eq. (1) is simplified [1, 5]. The semiempirical values of the photoelectric cross sections [4] were obtained by the subtraction method

$$\tau(E) = \mu(E) - [\sigma_{coh}(E) + \sigma_{incoh}(E)]. \tag{2}$$

Here $\mu(E)$ was determined from empirical data, and the cross sections for coherent $\sigma_{coh}(E)$ and incoherent $\sigma_{incoh}(E)$ scattering were calculated theoretically [6]. However, for $E \gg E_K$ the subtraction method becomes incorrect for all elements because of the small contribution of the photoelectric absorption cross section τ to the total interaction cross section μ [7-9]. Therefore data on photoelectric cross sections from [4] and the corresponding coefficients τ_i in Eq. (1) of [2, 5] can be recommended for use in simulation calculations only in the energy region of characteristic x-ray and low-energy γ radiation. We note that the maximum value of the energy in [4] is 10^3 keV. In modeling the transport of intermediate and high-energy photons, taking account of photoelectric absorption, one should prefer systematic theoretical data on photoelectric cross sections [3, 10].

The theoretical values of the photoelectric cross sections of 100 elements were obtained in [3] by quantum mechanical calculations in which various models of the screened potential were employed for various energy ranges. The cross sections were not calculated for each element; interpolations were performed in the atomic number. In [10] the cross sections for the photoelectric absorption of photons were calculated and tabulated for 100 elements in the energy range from 1 to 1500 keV by using the Hartree−Slater relativistic model. The comparison of semiempirical [4] and theoretical [10] data on photoelectric cross sections made in [8] showed that in the energy range for which the data in [4] are completely correct the divergence does not exceed 10%, and for the most part is from 1 to 5%.

Taking account of the energy restrictions on the use of the tables in [4], interpolation equation (1) was employed for 100 elements solely on the basis of theoretical papers [3, 10]. Data from [10] were used in the energy range from 1 to 1500 keV for elements from hydrogen through bromine. For krypton and elements of higher atomic number these data were supplemented by values of the photoelectric cross sections for $E > 1500$ keV from [3].

The present article lists results for 50 elements most frequently encountered in problems of applied and technical atomic physics. The coefficients τ_i, calculated by the method of least squares, are listed in Table 1. The energy range for elements from hydrogen to neon is $(1 - E_{max})$ keV; for sodium and elements of higher atomic number the range is $(E_K - E_{max})$ keV. The maximum error of the approximation δ observed at one or two points in the pertinent energy range for each element does not exceed 3.3%, and in most cases is 1-2%.

LITERATURE CITED

1. O. S. Marenkov, At. Energ., 33, 987 (1972).
2. O. S. Marenkov and B. G. Komkov, At. Energ., 43, 30 (1977).
3. E. Storm and H. Israel, Nucl. Data Tables, A7, No. 6, 565 (1970).
4. W. Veigele, At. Data Tables, 5, No. 1, 51 (1973).
5. O. S. Marenkov and B. G. Komkov, Apparatus and Methods of X-Ray Analysis [in Russian], Vol. 21 (1978), p. 103.
6. J. Hubbell et al., J. Phys. Chem. Ref. Data, 4, No. 3, 471 (1975).
7. R. Pratt, A. Ron, and H. Tseng, Rev. Mod. Phys., 45, No. 2, 273 (1973).
8. J. Hubbell and W. Veigele, U.S. Dept. Commer. NBS Tech. Note No. 901, 41 (1976).
9. J. Hubbell, U.S. Dept. Commer. NBS Special Publication No. 461, 3 (1977).
10. J. Scofield, Report UCRL-51326 LLL (1973).

PURIFICATION OF IRON FROM U AND Ra
MICROIMPURITIES BY ZONE MELTING

I. R. Barabanov, L. P. Volkova,
V. N. Gavrin, V. I. Glotov,
D. S. Kamenetskaya, L. L. Koshkarov,
I. B. Piletskaya, and V. I. Shiryaev

Zone melting is one of the most efficient methods of obtaining pure substances, especially iron. It is important to ascertain, however, whether there is a minimum initial concentration of impurities at which redistribution under zone melting no longer occurs. Such a limiting concentration of impurities has been established, e.g., for Ge and CdTe [1].

In the present paper we study the possibility of purifying iron from U and Ra microimpurities by crucibleless electron-beam zone melting. Purification from these impurities is required in connection with the use of iron in the fabrication of counters with a low intrinsic background for astrophysical and nuclear research. In order to reduce the background of a gas-discharge counter with a volume of about 1 cm^3 to 1 count per day, the concentration of uranium in equilibrium with the elements of its radioactive series should not exceed $\sim 10^{-8}\%$ in the structural materials of the counter. In the initial (carbonyl) iron the uranium content, as shown by measurements of the surface α-activity, is tens of times higher than the value indicated.

The radium concentration and its redistribution during the zone melting were measured by the emanation method [2]. The "clean" and "dirty" halves of iron bars subjected to fourfold zone melting at a speed of $v = 136$ mm/h were measured, with the radium content in each half being averaged. Notwithstanding this averaging, a difference was detected in the radium concentration in the clean and dirty halves of the rods: $0.35 \cdot 10^{-14}$ and $0.72 \cdot 10^{-14}$ at.% Ra, respectively ($1.2 \cdot 10^{-8}$ and $2.6 \cdot 10^{-8}$ at.% when converted to equilibrium U content).

Of particular interest was the study of the character of the distribution of radioactive impurities along the rods. The neutron-activation method [3] was used to analyze iron specimens cut from various segments of the rod subjected to zone melting with $v = 136$ mm/h (9 passes). The distribution found confirmed the efficiency of zone melting for purification of iron from uranium, notwithstanding its low initial concentration (Fig. 1).

The solubility of uranium in bcc δ-iron near its melting point is not known, i.e., the main parameter determining the efficiency of purification by zone melting is not known. The character of the uranium distribution curve (see Fig. 1) indicates that the uranium concentration in δ-Fe in equilibrium with the melt is considerable. The distribution coefficient K can be approximated by calculating the diagram of equilibrium of the melt with the bcc solid solutions of Fe in γ-U and δ-Fe from the known segments of that diagram.

Approximate thermodynamic calculation with the use of the model of regular solutions [4, 5] allowed the mixing energy of the Fe−U melt to be found from the known liquidus of the melt and the bcc solid solution of Fe in γ-U, yielding a value of about 25,000 J/mole (−6000 cal/mole). On the basis of data concerning the temperature and entropy of the melting of iron in uranium (1812 and 1404°K and 2 and 3.28 cal/mole · deg, respectively) for the calculated interaction parameter of the melt and the known part of the liquidus of the melt and the bcc solid solution of uranium in δ-Fe, we determined values of K (0.16) and the uranium concentration on the solidus at 1773°K (0.7 at.% at a uranium concentration of 4.5% in the melt). More efficient purification of iron from uranium might be expected with such a K. Complete purification is associated with diffusion of impurities from the unmelted part of the rod and in the absence of equilibrium at the interface between the solid and liquid phases at the given rate of advance of the liquid zone. The ratio of the uranium concentration in the unmelted part of the rod adjacent to the last liquid zone to the concentration in the last liquid zone (~ 0.13) is in quite satisfactory agreement with the calculated distribution coefficient (0.16).
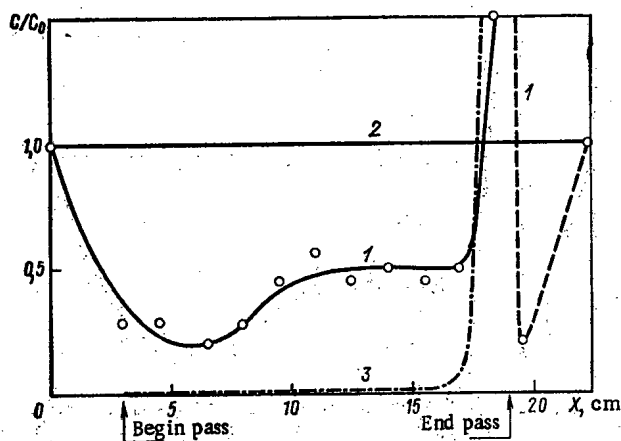
Fig. 1. Curve of uranium distribution along iron rod after nine passes of liquid zone with speed of 136 mm/h (1); 2) initial distribution; 3) calculated curve of limiting distribution for $K = 0.15$.
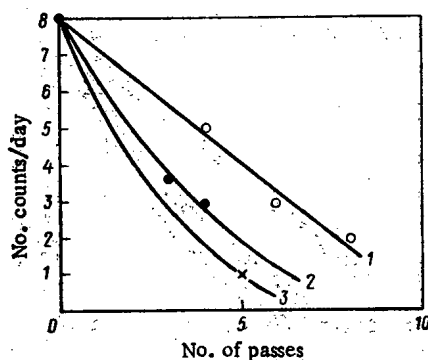
Fig. 2. Background of counter with casing (cathode) made of iron vs number of passes of liquid zone at various rates of advance of the zone: 1) 204 mm/h; 2) 136 mm/h; 3) 60 mm/h.

The results of measurements of the total background of a proportional counter with a volume of 0.5 cm³, made of iron, purified by the zone-melting method, are given in Fig. 2. It is seen that the maximum degree of purification under our conditions can be obtained after tens of passes of the liquid zone at a speed of about 60 mm/h.

LITERATURE CITED

1. O. A. Matveev, E. N. Arkad'eva, and L. A. Goncharov, Dokl. Akad. Nauk SSSR, 221, No. 2, 325 (1975).
2. I. R. Barabanov et al., in: Proc. Int. Conf. on Low Radioactivity Measurements and Applications, Bratislava (1977), p. 37.
3. L. I. Genaeva et al., Cosmic Rays [in Russian], Nauka, Moscow, No. 11 (1969), p. 182.
4. V. I. Danilov and D. S. Kamenetskaya, Zh. Fiz. Khim., 22, 69 (1948).
5. L. Kaufman and Ch. Bernstein, Computer-Assisted Calculation of State Diagrams [Russian translation], Mir, Moscow (1972).

RELIABILITY OF DETECTION OF SODIUM BOILING
BY CORRELATION OF ACOUSTIC AND NEUTRON NOISE

B. V. Kebadze and K. A. Aleksandrov   UDC 621.039.534.6

A promising method of detecting sodium boiling in the core of a fast reactor is that of recording acoustic and neutron noise. Since the statistical characteristics of these signals, taken separately, may change for other reasons (apart from boiling), the reliability of registration of the fact of boiling is enhanced by employing the method of cross-correlating the signals [1]. Let us evaluate the statistical reliability of detection of boiling (the probability of failure to record boiling and of spurious response), taking account of the statistical error of measurement of the cross correlation owing to uncorrelated background noise.

In our estimates we use the results of experiments on a BOR-60 reactor [2] in which sodium boiling was effected throughout the entire volume of the fuel assembly (FA) as the result of γ-ray heating of tungsten rods. The neutron flux fluctuations were measured with an ionization chamber set up 2.5 m from the core; the acoustic signals were measured with an inserted piezoelectric transducer at a distance of ~30 cm from the place where bubbles collapsed. For correlation with the noise of the neutron flux we formed the envelope of the acoustic signal with a rectifier and a filter with a time constant of ~30 msec. Figure 1 shows the statistical character- istics of the noise in the frequency range; these characteristics were obtained by Fourier transformation of the estimates of the correlation functions. The duration of the procedure (T = 10 min) and the frequency resolution selected (~0.1 Hz) ensure measurement of the spectral densities to within 10-15%. A distinctive feature of the spectra are peaks at a frequency of about 1 Hz which are absent under conditions without boiling.

Experiments on stands and calculations showed [3, 4] that the existence of resonances is characteristic of the process of sodium boiling. This is due to either the periodic formation and collapse of a vapor bubble during local boiling under the conditions of partial blockage or oscillations of the vapor volume when vapor covers the entire cross section of the FA; the boiling mode in the BOR-60 experiments in analogous to the latter. The possibility of detecting boiling from the periodic component of the neutron noise was considered in [3] but the problem of correlation differences between the signals was not considered there.
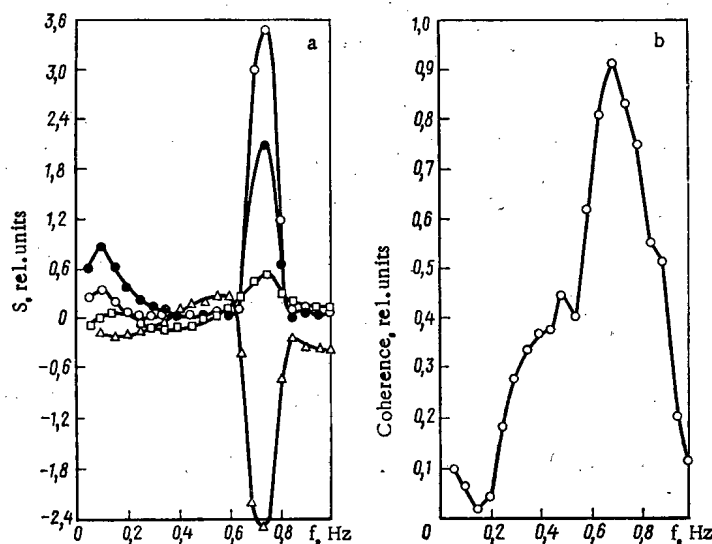

Fig. 1. Statistical characteristics of noise during sodium boiling in BOR-60 reactor: a) spectral densities (S), neutrons (N), and en- velope of acoustic (A) signals; O) S_{NN}; ●) S_{AA}; □) Re S_{NA}; △) Im S_{NA}; b) function of coherence of acoustic and neutron signals.
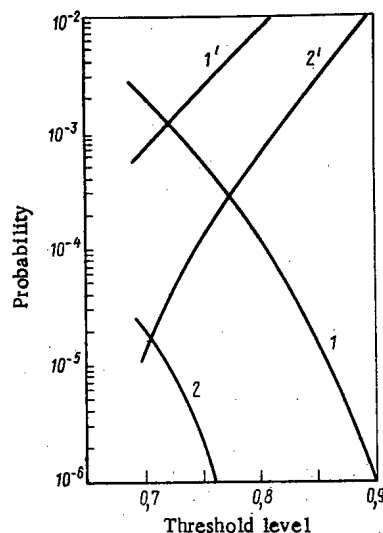
Fig. 2. Probability of transmission of malfunction signal (1', 2') and spurious response (1, 2) as function of threshold level for C F: 1, 2) n = 8 and 12 with $\gamma^2 = 0$; 1', 2') $\gamma^2 = 0.92$ and 0.95 with n = 8.

In view of the periodic character of the process it is expedient to characterize the degree of correlation by a coherence function (C F)

$$\gamma^2 (\omega) = \frac{|S_{xy} (\omega)|^2}{S_{xx} (\omega) S_{yy} (\omega)},$$

which was $\geqslant 0.9$ in the given experiments. The advantage of using C F, from the point of view of realization of a detection system, consists in its being independent of the transmission coefficient of the measuring channels.

Let us consider the problem of the statistical reliability of detection. We assume that the system is actuated when the coherence function exceeds some threshold level L. Since the frequency of the periodic component is not known in advance, it is necessary to monitor over some range Δf which, according to the data of [2] and other sources [1, 3] is 1-10 Hz. Under steady-state conditions of boiling the periodic signal is quite narrow-band, fractions of a hertz (see Fig. 1). However, bearing in mind that with the development of boiling, e.g., as the power varies, the oscillation frequency can change, we choose a resolution band B = 1 Hz, thus splitting the range of detection into 10 channels. In evaluating the probability of errors, we use a well-known [5] relation for the distribution density of sampled C F for two random processes with a normal distribution law:

$$C = (n - 1) (1 - \gamma^2)^n (1 - y)^{n-2} F (n, n; 1; \gamma^2 y),$$

where γ^2 and $y = \gamma^2$, respectively, are the true and sampled value of the coherence function, n = BT is the number of degrees of freedom determined by the resolution band B and the measuring time T, and F is a hypergeometric function of four arguments.

Let us evaluate the probability of spurious response by the system, taking account of the fact that in the absence of boiling the C F is zero. For this case the distribution function is of the form

$$C_0 = (n - 1) (1 - y)^{n-2}.$$

The probability of the threshold level L being surpassed in one frequency interval is

$$\Phi (> L) = \int_L^1 C_0 dy = (1 - L)^{n-1} = p.$$

The probability of a spurious response, i.e., the threshold being overcome in at least one interval, is

$$\Phi_\Sigma = 1 - (1 - p)^m.$$

The probability of the transmission of a signal of a malfunction situation, characterized by some nonzero value of the CF, is defined as

$$\Phi_{tr} = \int_0^L C dy.$$

757

In our numerical calculations we used the following series expansion of F:

$$F(a, b; c; z) = 1 + \frac{ab}{c} z + \frac{1}{2!} \frac{a(a+1)b(b+1)}{c(c+1)} z^2 + \cdots$$

for $z < 1$.

The calculations of the probabilities of spurious response and transmission of a signal for several values of the parameters n and γ^2, given in Fig. 2, show that even with comparatively large coherence values and an appropriate threshold level a realization time in excess of 10 sec is required to obtain roughly one spurious response per year. In this case a quite low probability of transmission of a malfunction can be ensured by the choice of threshold.

Under the conditions of this experiment the ratio of the boiling and background is more favorable for neutron noise than for acoustic noise. When account is taken of the spectral density of the neutron flux fluctuations in the region of resonance without as well as with boiling and the distribution of their estimates χ^2 [3, 5], it can be shown that for given values of B, T, Δf, and m the choice of threshold level makes it possible to ensure a probability of errors of the first and second kinds that is less than 10^{-6}. Obviously, in the given case the use of the spectral density along with the CF allows the characteristics of the detection system to be improved. This is attained primarily by reducing the probability of spurious response. The choice of detection threshold and the set of the parameters monitored (spectra, CF) should be made in each concrete case with allowance for the real signal-to-noise ratios.

It must be pointed out that the estimates presented in this paper presume the existence of stationary random processes with a normal distribution law. The periodic fluctuations during boiling often constitute not a narrow-band random process but rather natural oscillations against the background of random noise. This increases the reliability of detection. In a high-power fast reactor, because of the large distance of the acoustic transducers from the site of boiling and the smaller reactivity effects the ratio of the background and the boiling noise may prove to be not as favorable as in the case considered above, thus resulting in a reduction in the detection reliability.

LITERATURE CITED

1. S. Wright, R. Albrecht, and M. Edelmann, Ann. Nucl. Energy, 2, 367 (1975).
2. V. A. Afanasiev et al., Preprint Zkf-344, Dresden (1977).
3. J. Erhardt, Nucl. Technol., 31, No. 1, 123 (1976).
4. J. Van Erp et al., Nucl. Eng. Design, 15, No. 4, 441 (1972).
5. J. Bendat and A. Piersol, Measurement and Analysis of Random Data, Wiley, New York (1966).

CALCULATION OF SANITARY-PROTECTIVE
ZONES AROUND ACCELERATORS

Yu. A. Volchek

The operation of accelerators is usually accompanied by an increased background of ionizing radiation in the adjacent territory. This necessitates the creation of a sanitary-protective zone between the source of radiation and objects not associated with the operation of the facility. As a result of theoretical and experimental studies of scattered radiation beyond the shielding of accelerators a method has been developed for predicting the radiation environment on the territory of planned accelerators [1]. It must be pointed out, however, that economic factors have not been taken into account.

In two earlier papers [2, 3] a technique was proposed for determining the optimal shielding parameters from the point of view of economy and it was shown that in the construction and operation of accelerators a combination of a structural method of protection and a sanitary-protective zone can yield a substantial economic effect. The relation for the optimal thicknesses x and y of the side and top shielding, respectively, as a function of the radius r of the sanitary-protective zone is quite simple and as applied to point sources of radiation with a scattered-neutron yield $\gtrsim 10^{11}$ neutrons/sec is of the form [3]:

$$x = \frac{1}{\Sigma_1} \ln (A\beta_1)/(D_2 R^2), \tag{1}$$

$$y = \frac{1}{\Sigma_2} \left(\ln \frac{B\beta_2}{D_1 r^2 - \frac{D'\beta_3}{.2} - R^2 D_2 e^{-\Sigma_1' r}} - \Sigma_2' r \right); \tag{2}$$

$$r^3 + r^2 \frac{sd + \alpha - b \frac{\Sigma_2'}{\Sigma_2}}{2c_1} - r \left(\frac{D'\beta_3}{s^2 D_1} + \frac{b}{c_1 \Sigma_2} \right) - \left(sd + \alpha - b \frac{\Sigma_2}{\Sigma_2} \right) \frac{D'\beta_3}{2D_1 c_1 s^2}$$

$$\overline{r \frac{R^2 D_2}{D_1} + \frac{R^2 D_2}{2D_1 c_1} \left[\frac{b}{\Sigma_2} (\Sigma_1' - \Sigma_2') + sd + \alpha \right]} = e^{-\Sigma_2' r}. \tag{3}$$

Here A and B are quantities proportional to the yield of the leading groups of radiation through the surface of the side and top shielding, respectively; D', a quantity proportional to the concentration of the radioactive air ejected through the ventilation pipe; Σ_1 and Σ_2, effective cross sections for the introduction of the leading groups of direct and scattered radiation into the material of the shielding; Σ_1' and Σ_2', analogous quantities for air; β_1 and β_2, factors for converting the radiation flux density into dose rate; β_3, a factor for converting the concentration of radioactive isotopes in the air into dose rate; s, a turbulence coefficient depending on the relief and development of the site; c_1, expenditure for the land for the sanitary-protective zone; α, expenditure for the construction of engineering supply lines; d, expenditure per meter of ventilation pipe; D_1 and D_2, maximum possible dose rates at the limit of the sanitary-protective zone and the outer surface of the side shielding, respectively; R, radius of the accelerator building; and b, expenditure per meter of upper-shielding thickness.

In the development of the technique for optimizing the shielding parameters the spread of the scattered radiation for distances of more than 50 m from the source was approximated by [4]

$$\varphi(r) = \frac{q}{4\pi r^2} \exp(-\Sigma_r r), \tag{4}$$

where φ is the neutron flux density; q, source strength (neutrons/sec); and Σ_r, cross section for the removal of fast neutrons, taken to be equal to 0.005 m^{-1}.

In [5] Thomas presented the empirical relation

$$\varphi(r) = \frac{Bq}{4\pi r^2} (1 - e^{-r/\mu}) e^{-r/\lambda}, \tag{5}$$

where B = 2.8 and $\mu = 56$; for $\lambda = 267$ m this formula approximates, to within 6%, the experimental data around an accelerator without top shielding or with a thin top cover [6]. The lower limit could be assumed to be $\lambda = 224$ m, the value obtained for fission neutrons. For accelerators with "good" top shielding the value of λ should be large. In measurements of the radiation fields in the proton synchrotron at Brookhaven the value of
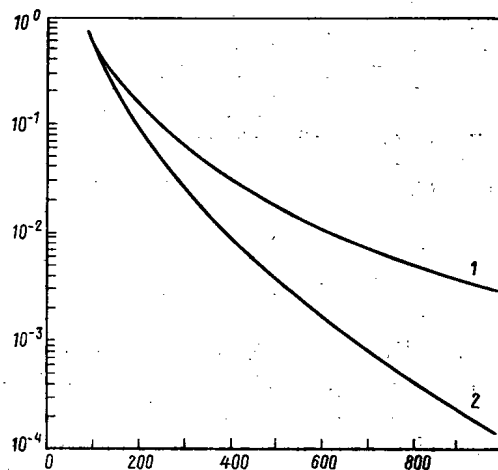

Fig. 1. Neutron flux density vs distance to accelerator
for: 1) $\Sigma'_2 = 0.00117$ m^{-1}; and 2) $\Sigma'_2 = 0.0046$ m^{-1}.

λ was 600 m [7] whereas for attenuation of neutrons generated in the Berkeley betatron and synchrocyclotron the value is $\lambda = 850$ m [6]. For neutrons with E > 100 MeV the value of λ is 850 m. This value was obtained for strongly interacting particles which are part of extensive air showers of cosmic radiation [6].

Let us assume that the limits of variation of the parameter Σ_T, corresponding to the limits of variation of λ from 224 to 850 m ($\Sigma_T = 0.0046-0.00117$ m$^{-1} = \Sigma'_2$). From the data given in Fig. 1 it follows that the values of the flux density of the scattered neutrons at a distance of 800 m with Σ'_2 varying over the range indicated can differ by a factor of 10 (curve 1 is characteristic of accelerators with "good" top shielding and curve 2, accelerators without top shielding).

Let us consider a cyclical proton accelerator with a scattered neutron B of 10^{10}-10^{13} neutrons/sec. For such an accelerator we have $\Sigma'_1 = 1.25 \cdot 10^{-3}$ m^{-1} [3], $D_1 = 0.28$ mrem/h; $\beta_2 = 0.135$ (mrem/h)/neutrons/cm$^2 \cdot$ sec, $\beta_3 = 5.5 \cdot 10^2$ mR $\cdot$ m^3/h $\cdot$ mCi [3], R = 16 m, and h = 20 m; depending on the concrete conditions the parameters s, b, Σ_2, c, and α can vary within the following limits: s (0.03-0.2 [8]), b ($9 \cdot 10^4$-10^6 rubles/m), Σ_2 (5.3-12.7 m^{-1}), c (0.1-100 rubles/m^2), and α (100-400 rubles/m).

Calculations with Eqs. (2) and (3) showed that the variations in Σ'_2 in the established interval have an insignificant effect on y and r. Thus, for B = 10^{10} neutrons/sec and s_1, b_1, $\Sigma_{2(1)}$, c_1, and α_1 corresponding to the lower limiting value y and r change by less than 10-15%, with the larger values of r corresponding to $\Sigma'_2 = 0.0045$ m^{-1}. With an increase in the scattered-radiation yield and the absolute values of s, b, Σ_2, c, and α, a change in the parameter in the interval indicated displays a diminishing effect on the values of y and r and for B = 10^{12}-10^{13} neutrons/sec and s, b, Σ_2, c, and α equal to the upper limiting values amounts to < 1%. This can be explained by the fact that with an increase in the scattered radiation yield greater than 10^{11} neutrons/sec, the formation of a radiation field on the territory begins to be affected by the radioactive air ejected into the atmosphere, and at high values of B the effect of Σ'_2 on the size of the sanitary-protective zones begins to fall off.

Since a change in Σ'_2 in the limit established has an insignificant effect on the optimal values of y and r (< 10-15%), in estimation of the shielding parameters by the optimization method Σ'_2 may be assumed to be constant. A study of the expenditures for protective measures with Σ'_2 varying from 0.00117 m^{-1} to 0.0046 m^{-1} showed that the absolute minimum expenditure c_{opt} (x, y, r) is attained for $\Sigma'_2 = 0.0046$ m^{-1}; however, since for a concrete facility Σ'_2 can assume any intermediate value in this interval, it is expedient to recommend the value $\Sigma'_2 = 0.00117$ m^{-1} for estimation by the optimization technique. In this case the optimal expenditure for protective measures, c_{opt}, increases by no more than 10-15% in comparison with c_{opt} for $\Sigma'_2 = 0.0046$ m^{-1}.

LITERATURE CITED

1. L. N. Zaitsev et al., JINR Preprint 16-6185, Dubna (1972).
2. Yu. A. Volchek et al., in: Trudy GIPRONII (Proc. All-Union State Design Institute of Scientific-Research Institutes and Laboratories of the Academy of Sciences of the USSR and Academies of Sciences of the Union Republics), "Design and Construction of Buildings and Equipment for Scientific Research" [in Russian], Nauka, Moscow (1973), p. 112.
3. Yu. A. Volchek and A. Ya. Yakovlev, At. Energ., 39, No. 4, 281 (1975).

4.   B. S. Sychev and V. P. Sidorin, in: Problems of Dosimetry and Radiation Protection [in Russian], No. 5, Atomizdat, Moscow (1966), p. 138.
5.   R. Thomas, in: Engineering Compendium on Radiation Shielding, Vol. 1, Springer-Verlag, Berlin (1968), p. 23.
6.   A. Rindi and P. Thomas, Part. Accel., 7, No. 1, 23 (1975).
7.   C. Distenfeld and R. Colvett, Nucl. Sci. Eng., 26, 117 (1966).
8.   V. M. Krupchatnikov, Ventilation in Working with Radioactive Substances [in Russian], Atomizdat, Moscow (1964).

SYSTEMATICS OF (n, p) AND (n, α) CROSS SECTIONS

V. N. Levkovskii   UDC 539.172.4

In the theory of nuclear reactions the (n, i) cross section, independently of the reaction mechanism assumed, is represented as the product

$$\sigma_{n,i} = \sigma_n \alpha_i, \tag{1}$$

where σ_n is the cross section for the nonelastic interaction of a neutron with the nucleus, and $\alpha_i = \Gamma_i/\Sigma\Gamma_i$ is the probability that as a result of the interaction particle i (in our case a proton or an alpha particle) will be emitted. It is known that σ_n varies slowly with neutron energy, and for energies > 1 MeV is practically equal to the geometrical cross section

$$\sigma_n = \pi r_0^2 (A^{1/3} + 1)^2; \quad r_0 = 1.4 \cdot 10^{-13} \text{ cm.} \tag{2}$$

It was shown earlier [1-3] that for the (n, p) and (n, α) reactions at neutron energies of 14-15 MeV α_i is quite satisfactorily described by the simple relation

$$\alpha_i = K_{1(i)} \exp\left[-K_2 (N-Z)/A\right], \tag{3}$$

where K_1 and K_2 are constants: $K_{1(p)} = 0.73$, $K_{1(\alpha)} = 0.29$, $K_2 = 33$.

Since the maximum of the excitation functions of the (n, p) and (n, α) reactions generally lies in the 14-15-MeV neutron energy range, the natural assumption was made in [3-5] that Eq. (3) approximately represents the limiting maximum possible probabilities of the emission of charged particles. Consequently, the maximum values of α_i can be considered as specific characteristics of the atomic nucleus, and their study is clearly of great theoretical and practical interest.

Equation (3) correctly (to within 10-30%) describes about 200 (n, p) and (n, α) cross sections, including those for nuclei with a magic number of neutrons or protons, but does not confirm the presence of striking "shell effects" predicted by theory and postulated by many authors. In the overwhelming majority of cases, Eq. (3) correctly predicts the ratios of emitted particles and the nature of the variation of the cross sections in series of isotopes of a single element, i.e., the so-called isotope effect first established in [1, 6, 7]. However, in a number of cases the difference between the calculated and experimental values clearly exceeds the experimental errors. As a rule these nuclei lie far from the stable nuclide curve; in a series of isotopes the calculated cross sections for the lightest isotope are frequently 1.5-2 times smaller, and those for the heaviest isotope 1.5-2 times larger than the experimental values, and thus the isotope effect (i.e., the decrease of α with increasing A) predicted by Eq. (3) is smaller than the experimental value for certain medium-weight and heavy nuclei.

The graphs in Figs. 1 and 2 show the dependence of the natural logarithm of α_p on the mass number of the target nucleus for all published data on (n, p) cross sections. The dependence of ln α_p on A is well approximated by sets of straight lines for a series of isotopes (Z = const), and for isotopes (N = const) and nuclei with the same neutron excess (N − Z) = const. The isotopic and isotonic dependences clearly do not exhibit either shell or even−odd effects; the (N−Z) dependence is also uniform over a wide range of Z values, but in the Z = 36-40 and Z = 52-56 ranges sharp bends are observed in the straight line N−Z dependences, possibly related to the structural rearrangements of nuclei near the filled neutron shells N = 50 and 82. It should be noted, however, that the monotonic N−Z dependence by no means repeats the behavior of the thermal effects of reactions (Q) whose variation in (N−Z) series is far from monotonic and uniform, and the sharp bends in the straight line (N−Z) dependence do not correspond to the jumps in Q values at magic nuclei.

A least squares analysis established that the (N−Z) dependence is best approximated by a series of straight lines converging to a point in the A = 196-246 region:

$$\ln \alpha_p = K_1 + K_2 A + K_3 (N-Z) A - (N-Z). \tag{4}$$
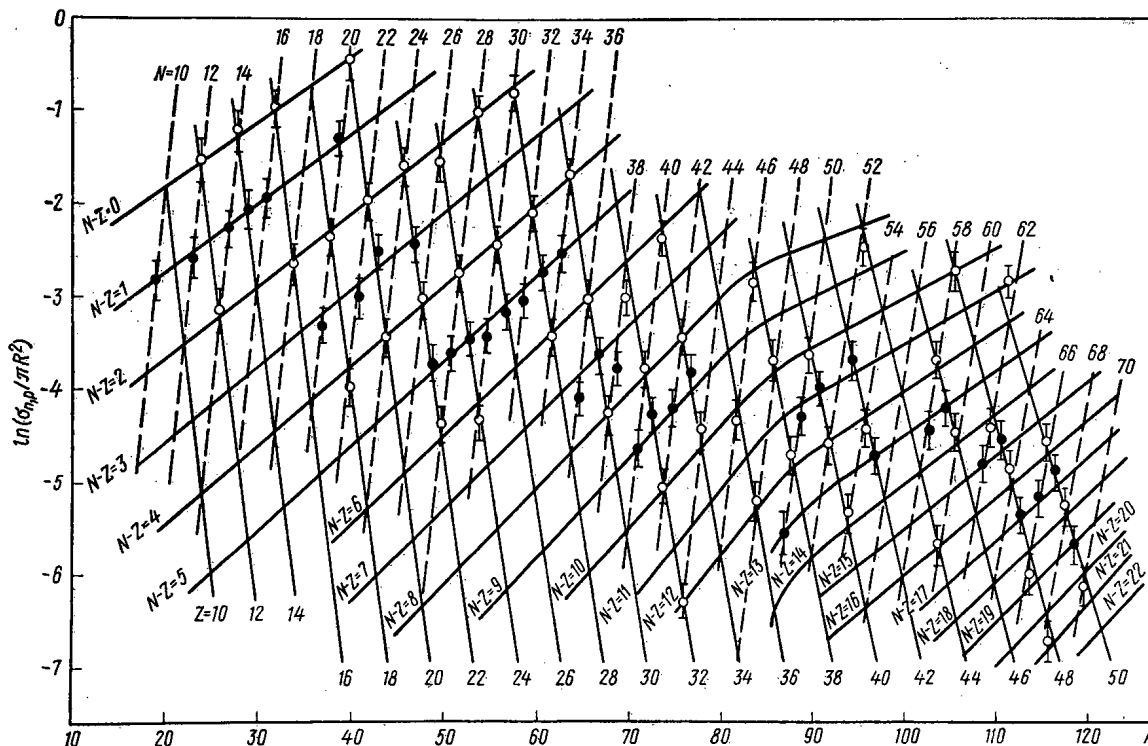
Fig. 1. $\ln \alpha_p$ as a function of A (Z = 9-50): $\circ$) even–even; $\bullet$) odd–odd and even–odd (Z even, A odd) nuclei.
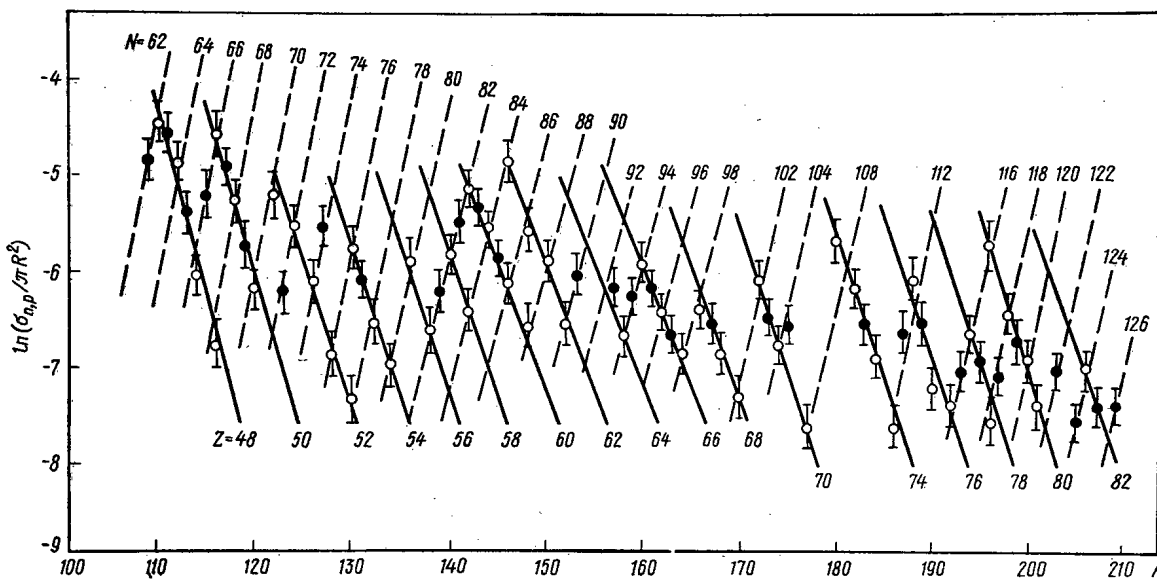
Fig. 2. $\ln \alpha_p$ as a function of A (Z = 48-83). Notation same as in Fig. 1.

In the Z = 9-38 range K_1, K_2, and K_3 are equal, respectively, to −3.2, 0.069, and 0.00405; in the Z = 38-52 range (up to N = 76) 1.8, 0, 0.00510; in the Z = 52-62 range (up to N−Z = 28) 9.8, −0.0506, and 0.00460.

Since Eq. (4) is in appreciably better agreement with experiment than Eq. (3), it is preferable to use it to estimate unknown (n, p) cross sections, particularly for nuclei with unusually small or large values of the asymmetry parameter (N−Z)/A in the given Z range. Like Eq. (3), Eq. (4) can clearly be used in traditional theoretical studies as normalizing functions for fitting the mathematical form and parameters of models of nuclear reactions ("pairing corrections," "shell corrections," "isospin potentials," "nuclear temperatures," etc.), but it is believed that at the present time a greater contribution to the theory would be made by broadening the experimental research on excitation functions and ratios of emitted particles over a wide range of energies and methods of exciting atomic nuclei. Probably the general relations shown in Figs. 1 and 2 are not specific characteristics of only (n, p) and (n, α) reactions. There are, unfortunately, very incomplete data on

763

(n, 2n), (n, 3n), (n, 4n), (n, np), (n, T), (n, $n_x p_x$), (γ, p), (α, p), and (α, np) cross sections and excitation functions, in particular the appearance in these reactions of regular isotope effects, N−Z dependence, and constancy of the ratios of emitted particles, indicating that the phenomenon described manifests itself in various nuclear reactions, and further study of it will lead to a better understanding of the mechanism of nuclear reactions and its relation to the structure of the atomic nucleus.

LITERATURE CITED

1. V. N. Levkovskii, Zh. Eksp. Teor. Fiz., 33, 1520 (1957).
2. V. N. Levkovskii, Zh. Eksp. Teor. Fiz., 45, 305 (1963).
3. V. N. Levkovskii, Yad. Fiz., 18, 705 (1973).
4. B. Bayhurst and R. Prestwood, J. Inorg. Chem., 23, 173 (1962).
5. S. Pearlstein, J. Nucl. Energy, 27, 81 (1973).
6. V. N. Levkovskii, Zh. Eksp. Teor. Fiz., 31, 360 (1956).
7. D. Gardner, Nucl. Phys., 29, 373 (1962).

REACTIMETER WITH A PULSED MEASUREMENT CHANNEL

V. A. Lititskii, A. G. Kostromin,   UDC 621.039.514
V. V. Bondarenko, and F. B. Bryndin

When using the method of measuring deep subcriticality [1, 2], the intensity of the external neutron sources frequently is found to be inadequate for providing a chamber current (usually KNK-56), exceeding the leakage current of the chamber or the sensitivity of the input amplifier. It is obvious that this circumstance considerably restricts the range of the reactivity to be measured.

In order to measure small subcriticalities, a pulsed measurement channel was used, based on a high-efficiency counter and a linear intensity meter, assembled in a circuit with a dosing key [3]. This channel allowed subcriticality measurements to be carried out, corresponding to count rates of 100–10,000 pulses/sec.

In developing the procedure for operating with the pulsed measurement channel, particular attention was paid to its frequency characteristics, as it determines the range of frequencies where the condition of inversion of the transfer functions of the reactimeter and the reactor are satisfied, and which is essential for the correct measurement of the reactivity [4]. In the measurement channel being considered (Fig. 1), the input signal is a random sequence of pulses, corresponding to the number of recorded neutrons in unit time (we shall neglect the counting errors of the recording circuit), and the output signal is a voltage proportional to the count rate. In addition to this, the reaction of the pulse shaper to each recorded neutron is a rectangular voltage pulse (dosing pulse) with a constant amplitude a_0 and a width τ_0, the sequence of which is converted by the integrating circuit of the intensity meter into a corresponding analog signal, which arrives at the reactimeter input through a matching device.

Using the theory of random pulsed processes [5], it can be shown that the spectral density of a random sequence of rectangular voltage pulses at the output of the pulse-shaper, the number of which during time T is distributed by a Poisson law, is equal to

$$S(\omega) = \bar{n}(a_0\tau_0)^2 \left(\sin \frac{\tau_0}{2}\omega \Big/ \frac{\tau_0}{2}\omega \right)^2,$$ (1)

when $\bar{n}$ is the average number of pulsed recorded per second.

The spectral density of the voltage fluctuations at the output of the intensity meter can be obtained from the relation

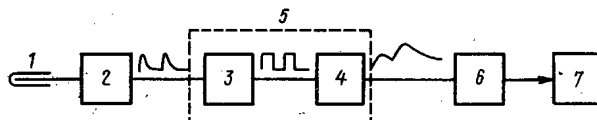$$S_u(\omega) = |K(\omega)|^2 S(\omega),$$ (2)

Fig. 1. Structural diagram of a pulsed measurement channel: 1) SNM-18 counter; 2) amplifier-discriminator; 3) pulse shaper; 4) integrating circuit; 5) intensity meter; 6) matching device; 7) reactimeter.

where $|K(\omega)|^2$ is the square of the modulus of the transfer function of the intensity meter, which is easily determined if the Fourier transform of the equation

$$\tau \frac{dU_{out}(t)}{dt} + U_{out}(t) = U_{in}(t),$$

is used, which describes the dependence of the output voltage $U_{out}(t)$ on the input voltage $U_{in}(t)$ in the intensity meter [3].

After transformation

$$|K(\omega)|^2 = \varepsilon^2/(\varepsilon^2 + \omega^2), \tag{3}$$

where $\varepsilon = 1/\tau$ (here τ is the time constant of the intensity meter integrating circuit).

As the input pulsed process is assumed to be Poisson, the spectral density of the output signal, determined by formulas (1)-(3), is proportional to the square of the modulus of the transfer function $|Z(\omega)|^2$ of the whole measurement channel, i.e.,

$$S_u(\omega) = \frac{\bar{n}\,[a_0\,(\tau_0/\tau)]^2}{\varepsilon^2 + \omega^2} \left(\sin \frac{\tau_0}{2}\omega \Big/ \frac{\tau_0}{2}\omega\right)^2 \sim |Z(\omega)|^2. \tag{4}$$

It can be seen from formula (4) that in the general case, the transfer function of the pulsed measurement channel depends on both the parameters of the dosing pulses (a_0, τ_0), and also on the time constant of the integrating circuit τ. However, usually $\omega\tau_0 \ll 1$ and, as it is not difficult to verify, in this case formula (4) is converted to the form

$$|R(\omega)|^2 \sim const/(\varepsilon^2 + \omega^2). \tag{5}$$

It can be seen from this expression that for frequencies $\omega \ll \varepsilon$, the square of the modulus of the transfer function $|R(\omega)|^2$ is independent of the frequency, i.e., in this region of frequencies the pulsed measurement channel does not carry an error as a result of the reactivity measurement.

For comparison we shall give the expression for the square of the modulus of the transfer function for the current measuring channel with a BF$_3$-filled ionization chamber, obtained in [6]:

$$|\Phi(\omega)|^2 \sim const/(\xi^2 + \omega^2), \tag{6}$$

where ξ is a quantity, the reciprocal time of collection of ions in the chamber. Formulas (5) and (6) have an identical dependence on the frequency, and in this sense the pulsed measurement channel does not differ from the current channel. However, if for the current measurement channel the frequency of the "kink" of the square of the modulus of the transfer function is determined by the ion collection time, then in the pulsed channel it is determined by the time constant of the integrating RC chain of the intensity meter.

We note that when the measurement of small intensities is achieved by an increase of the dosing pulse duration, the spectrum determined by the shape of the dosing pulses is displaced into the low-frequency region of the frequency curve of the measurement channel. The relative magnitude of the contribution of this spectrum $\delta(\omega, \tau_0) = [\,|Z(\omega)|^2 - |R(\omega)|^2]/|Z(\omega)|^2$ or

$$\delta(\omega, \tau_0) = 1 - \left(\tau_0\omega/2 \sin \frac{\tau_0}{2}\omega\right)^2.$$

By means of this formula, the range of frequencies being analyzed can be chosen where, with a choice of the value of τ_0, the contribution of the undesirable spectrum will be insignificant.

765
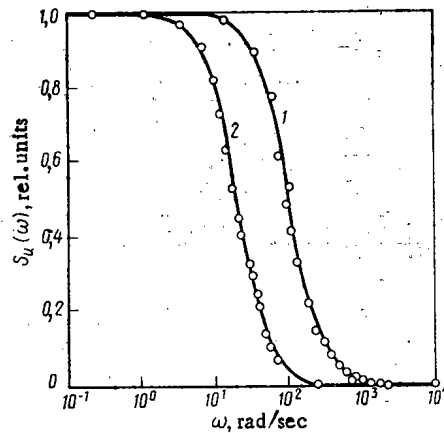
Fig. 2. Spectral density of the voltage fluctuations at the output of the pulsed measurement channel: ——) calculation; O) experiment.

Figure 2 shows the measured spectral density of the voltage fluctuations at the output of the pulsed measurement channel with time constants of the intensity meter of 0.01 (1) and 0.05 sec (2). It can be seen from Fig. 2 that the spectral densities obtained in the experiment are described well by formula (5). The width of the dosing pulse amounted to $1.5 \cdot 10^{-6}$ sec, and the amplitude was 6 V; the Pu—Be neutron source and the SNM-18 counter was installed in a graphite prism.

In conclusion, we give the results of measurements carried out by means of the reactimeter with a pulsed channel on a uranium—water subcritical test-rig. In these measurements, the "shooting" source method [1] was used. The use of the measurement channel described ensures a subcriticality measurement of up to $(10-14)\beta_{eff}$ — the effective fraction of delayed neutrons, which corresponds to a count rate of ~ 200 pulses/sec, with an injected neutron source intensity of 10^6 neutrons/sec, whereas the current of the KNK-56 chamber under these same conditions amounted to only $\sim 1.5 \cdot 10^{-12}$A, which is comparable with the leakage current for this chamber.

It should be noted that measurements at a lower neutron flux intensity are accompanied by an increase of the time constant of the integrating unit of the intensity meter which, in its turn, limits the range of the subcriticality measurement because of the deterioration of the speed of response of the measurement channel.

The authors thank Yu. A. Prokhorov for constant attention to this present task, and also R. É. Bagdasarov, V. I. Kozlov, and Yu. V. Volkov for assistance rendered during carrying out of the experiments and during the discussion of their results.

LITERATURE CITED

1. V. V. Bondarenko et al., At. Energ., 41, No. 4, 238 (1976).
2. V. V. Bondarenko et al., At. Energ., 45, No. 5, 375 (1978).
3. A. A. Bragin and R. F. Fedorin, Analog Conversion of Pulsed Fluxes [in Russian], Atomizdat, Moscow (1969).
4. N. A. Smirnov, in: Theory and Means of Automation [in Russian], Nauka, Moscow (1968), p. 305.
5. S. M. Rytov, Introduction to Statistical Radiophysics [in Russian], Nauka, Moscow (1966).
6. R. Osborn and J. Nieto, Nucl. Sci. Eng., No. 4, 515 (1966).

ESTIMATE OF THE RISK FROM THE COMBINED ACTION
OF RADIATION AND CHEMICAL AGENTS

V. N. Lystsov and V. A. Kinzhinkov   UDC 577.3.539.12.04

Control of the habitable environment is becoming an urgent practical problem of our time. In order to solve it, it is necessary in the first place to know to what consequences for the human population, the effect of one or other factor of the environment leads, even with a quite low level of exposure.

The appearance of the radiation factor, e.g., leads to an increase of the risk of stochastic harmful effects (malignant new formations and hereditary illnesses) which, for defined tolerances can be estimated quantitatively [1]. These estimates allow standards of radiation safety to be set up both for the population as a whole, and also for people subjected to occupational irradiation [2]. It is much more complicated to estimate the combined effect of radiation and chemical agents, when the risk of harmful effects may be found to be significantly higher than the sum of the risks for each of these factors individually. Moreover, the problem arises of a quantitative expression of the risk in some units which can be summed [3].

We shall introduce the concept of the risk R and the damage G, following the methodology developed in the report of the Scientific Committee of the United Nations, on the Effects of Atomic Radiation (SCEAR) [4]. Suppose that P_i is the probability of damage to the individual from the i-th illness. Then,

$$R = \sum_i P_i. \tag{1}$$

The damage for the population of N individuals is

$$G = NR. \tag{2}$$

A careful analysis of the total injury for the health of populations caused by different factors, shows that the mortality is determined just by the majority fraction of the injury and, moreover, the level of morbidity is related with the level of mortality in a regular way. The problem now consists in relating the level of exposure* X_j for the j-th factor of the environment with R. In the case of radiation, the most appropriate exposure parameter X_j is the absorbed dose D. It is assumed [4] that the probability of injurious effects in the region of small doses is directly proportional to the dose:

$$P_i = \alpha_i D. \tag{3}$$

Then for the damage G, we obtain

$$G = ND \sum_i \alpha_i = S \sum_i \alpha_i, \tag{4}$$

where S = ND is the collective dose. In the more general case when determining S, the dose distribution over the population and the change of the collective dose intensity $\dot{S}(t)$ with time [4] should be taken into account. However, the magnitude of the collective dose expectation S* is independent of time:

$$S^* = \int_0^\infty \dot{S}(t)\, dt. \tag{5}$$

Now, the damage from an event a (leading, e.g., to the discharge of radionuclides), can be defined as

$$G_a = S_a^* \sum_i \alpha_i. \tag{6}$$

---

*The term "exposure" is employed here in the broad sence of the word and refers to any physical value which adequately defines the level of any factor in the environment.

Often, in place of $S*$ it is more convenient to work with the quantity "dose expectation"† which is obtained by integrating over time, the average dose intensity per head of population [4]:

$$D* = \int_0^\infty \overline{D(t)}\, dt. \tag{7}$$

The first difficulty which is encountered when transferring this methodology to the case of chemical contaminations in the surrounding medium, consists in the correct choice of the parameter X_j, describing the exposure. Data about the concentration $C(t)$ of a specified chemical agent in any of the reservoirs of the medium or even in the human body (or its individual organs) frequently proves to be inadequate. Recently, even more data has been accumulated in favor of the fact that for certain compounds (in particular, alkylating agents) the cumulative concentration over time t in the critical organ can serve as the acceptable parameter:

$$X(t) = \int_0^t C(t)\, dt. \tag{8}$$

Assuming that the probability of the corresponding stochastic injurious effects depends linearly on X, the whole system of estimates can be used which have been developed in the field of radiation safety. Obviously, the analog of the dose expectation $D*$ will be the exposure expectation $X*$, which we define as

$$X* = \int_0^\infty C(t)\, dt. \tag{9}$$

The calculation of the exposure expectation can serve as the basis for the acceptance of specific solutions. For example, if a dangerous discharge has occurred and the agent has just started to enter the same reservoir of the medium which leads to man, the calculation of $X*$ shows that special measures are necessary to prevent this entry. The calculation of $X*$ is particularly necessary in those cases when transfer through a chain occurs with a large delay and the actual injurious effect of the agent appears, maybe, only in subsequent generations.

An attempt may be made to equate the effect of chemical contamination to a specified equivalent dose of radiation [5, 6]. For example, the concentration of ethylmethane sulfonate of 0.7 mg/kg causes the same frequency of mutations in a culture of rodent cells as 1 rem of radiation [5]. However, it is by no means obvious that this same concentration of chemical agent will lead to the same increase of risk, defined by Eq. (1), as 1 rem of total irradiation. Therefore, we shall construct a methodological estimate, related first of all with the magnitude of the average risk of death for the individual R. We shall consider an increment of risk equal to 10^{-6} as standard. We shall call the exposure $\varkappa_j$ for the j-th agent of the environment causing this standard increment of risk, the standard risk exposure (or, abbreviated, "reks"). Then, independently of the initial dimensionality of the quantity X_j, the exposure for any agent of the medium can be determined in dimensionless units (which we shall also call "reks"). The dimensionless exposure E_j will be equal to

$$E_j = X_j/\varkappa_j. \tag{10}$$

Being dimensionless, the values of E_j for different agents of the external medium (chemical or radiation) can be added directly. The risk for the individual in a population subjected to the effect M of different agents will be equal to

$$R = 10^{-6} \sum_{j=1}^M E_j. \tag{11}$$

The sensitivity of the population to the effect of the j-th agent obviously is given by the value of $\varkappa_j$. For example, for ionizing radiation, if the latest estimates of the risk of death for stochastic effects are used [1], it can be obtained that $\varkappa = 7$ mrad. The value of $\varkappa$ is averaged for the whole population and takes account of all i possible effects leading to the death of an individual. If, for each effect individually, the sensitivity is defined by the quantity $\varkappa_i$, then the total sensitivity to a given agent can be found from the relation

$$\frac{1}{\varkappa} = \sum_i \frac{1}{\varkappa_i}. \tag{12}$$

---

†In Soviet literature, there is no generally accepted equivalent for the conversion of the English term "dose commitment." The term "expected dose," which is used sometimes, clearly is ambiguous. Therefore, by analogy with the mathematical expectation, it is proposed to denote "dose commitment" as dose expectation. In this case, the probable nature of this quantity is emphasized, and also its difference from the actual absorbed dose.

The relations considered are valid in the case of linearity of the risk-exposure relation. However, even in the case of nonlinear relations, different sections of the risk-exposure curves can be approximated by straight lines and their relations can be used.

The proposed methodology also allows the introduction of uniformity into the quantitative description of the phenomena of synergism and the mutual suppression of certain agents simultaneously affecting the population. For example, if on the average there are first and second agents, the combined effect of which is non-additive, the following expression can be written for the effective dimensionless exposure E:

$$E = \omega(X_1, X_2)[X_1/\varkappa_1 + X_2/\varkappa_2]. \tag{13}$$

The numerical value of the coefficient ω is greater than unity in the case of synergism and less than unity in the case of mutual depression.

Obviously, the quantity E should serve as the basic normalization and can be used for comparing all types of practical worker, where there exists a risk of death of the individual. In this case, data about $\varkappa$ are essential for the most different agents. They can be obtained partially on the basis of analysis of the published data; however, special purposeful investigations are required to a considerable degree for this, in the first place experiments on animals, and also natural hygienic investigations, including a study of the environment and the health of staff and population.

It can be verified that the most complete information necessary for quantitative estimates and forecasts, are in the field of radiation hygiene [7]. The dose—effect relation for chemical carcinogens has been studied very inadequately [6]. Data which might be used for quantitative estimates of the effect in the case of combined action are still few. Numerous gaps in the available data indicate the direction of the immediate investigations which will be necessary for a correct estimate of the effect of the environment on man in the actual conditions of the combined effect of many agents.

LITERATURE CITED

1. Radiation Protection [Russian translation], Atomizdat, Moscow (Publication 26 ICRP) (1978).
2. Standards of Radiation Safety [in Russian], Atomizdat, Moscow (NRB-76) (1978).
3. V. Lyscov, "Comparative evaluation of risks from physical and chemical mutagens and carcinogens in the environment," in: Seventh International Biophysics Congress, September 3-9, 1978, Kyoto.
4. NKDAR Report United Nations 1977 [in Russian], New York (1978).
5. Science, 187, 503 (1975).
6. V. A. Knizhnikov, Gig. Sanit., No. 3, 96 (1975).
7. E. I. Vorob'ev et al., At. Energ., 43, No. 5, 374 (1977).

ESTIMATE OF DOPPLER BROADENING OF RESONANCES

V. V. Kolesov and A. A. Luk'yanov

UDC 539.5.173.162.3

The effect of the thermal motion of the nuclei of a medium on the form of the energy dependence of neutron cross sections in the resonance region must be taken into account in the analysis of neutron spectroscopy data and in estimates of nuclear temperature effects in reactors. The problem consists in the transformation of the cross section $\sigma(E')$, determined theoretically in the center of mass system as a function of the energy of the relative motion of the neutron and the nucleus E', to the laboratory system where the neutron energy is E:

$$\sigma(E) = \int \sigma(E') F(E-E')\, dE'. \tag{1}$$

The distribution function $F(E - E')$ characterizes the statistical spread of the energy E' resulting from the thermal motion of the nuclei of the medium. Usually the gas model approximation is used, where

$$F(E-E')\, dE' = (1/\sqrt{\pi}\Delta) \exp[-(E-E')^2/\Delta^2]\, dE'. \tag{2}$$

Here $\Delta = 2\sqrt{kTE/(A+1)}$ is the so-called Doppler width and kT is the average energy of thermal motion of the atoms [1, 2]. The energy structure of cross sections at resonances is determined by the superposition of the known functions [1]:

$$\Psi(x,\zeta) = \frac{\zeta}{\sqrt{\pi}} \int_{-\infty}^{\infty} \frac{\exp[-(x-y)^2\zeta^2]}{1+y^2}\, dy; \tag{3}$$

$$\chi(x,\zeta) = \frac{\zeta}{\sqrt{\pi}} \int_{-\infty}^{\infty} \frac{\exp[-(x-y)^2\zeta^2]}{1+y^2}\, y\, dy,$$

where $x = (E - E_\lambda)2/\Gamma_\lambda$, $\zeta = \Gamma_\lambda/2\Delta$, and Γ is the resonance width. These functions have been well studied, detailed tables of them exist, and descriptions of algorithms and numerical calculation programs are available [1-4]. The functions Ψ and χ are widely used in the analysis of neutron cross sections in the region of resolved levels, and also in the study of resonance effects in nuclear reactors [2]. However, the necessity of turning to numerical calculations even for qualitative estimates of the Doppler broadening of resonances frequently leads to considerable complications. Thus, in existing programs for seeking resonance parameters from experimental data, up to 90% of the machine time is consumed in calculating the functions Ψ and χ. The integral representation of these functions makes the construction of the solutions of the transport equation for resonance neutrons difficult even in the simplest problems.

For rough estimates of effects related to the Doppler broadening of resonances it is convenient to have rational approximations of the functions Ψ and χ obtained by using a distribution function of the Lorentz form [5] in (1):

$$\widetilde{F}(E-E')\, dE' = (\widetilde{\Delta}/2\pi)\, dE'/[(E-E')^2+\widetilde{\Delta}^2/4], \tag{4}$$

where $\widetilde{\Delta}$ is the characteristic width of the distribution at half-height. By averaging (1) we obtain approximate expressions for the Doppler functions:

$$\widetilde{\Psi}(x,\zeta) = (1+\delta)/[x^2+(1+\delta)^2]; \tag{5}$$

$$\widetilde{\chi}(x,\zeta) = x/[x^2+(1+\delta)^2],$$

where $\delta = \widetilde{\Delta}/\Gamma$ [5]. Relations between $\widetilde{\Delta}$ and Δ are established by comparing specific integral combinations of the Doppler functions. Thus, from the equality of the integrals of the squares of these functions it follows that

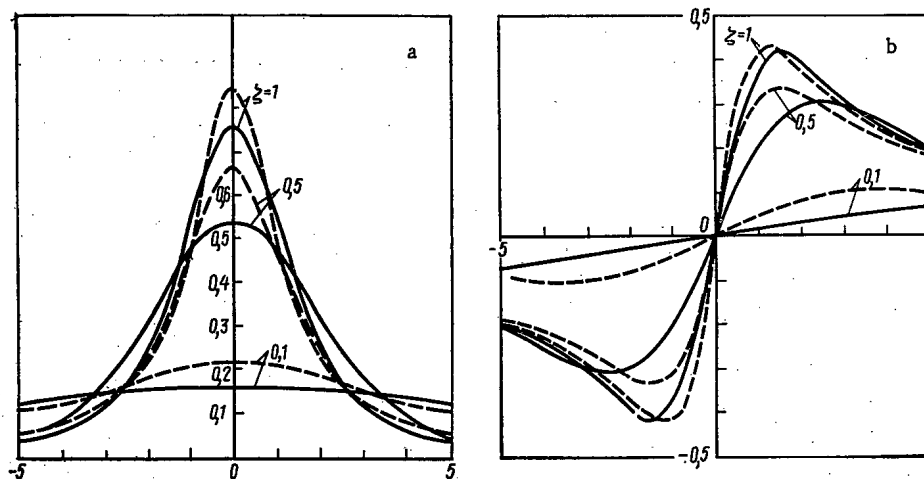$$(1+\delta)^{-1} = \Psi(0, \zeta\sqrt{2}). \tag{6}$$

Fig. 1. Exact (———) and approximate (---) functions for calculating
Doppler broadening of a resonance for various values of ζ; a) the functions
Ψ and $\tilde{\Psi}$; b) the functions χ and $\tilde{\chi}$.

The results of a numerical solution of this transcendental equation can be represented by the approximate
relation

$$\delta^{-1} = \zeta \; [2.5 + 2\zeta + \zeta^{(0.1+\zeta)/(0.12+\zeta)}]. \tag{7}$$

Figure 1 shows that the general qualitative agreement of the exact and approximate functions improves with
increasing ζ.

Various integral characteristics of cross sections in the resonance region are of practical interest. These
include transmissions averaged over the resonances as a function of sample thickness $\langle \exp[-n\sigma] \rangle$, average
cross sections measured with filtered beams $\langle \sigma_a \exp[-n\sigma] \rangle$, and effective resonance integrals. Thus, the
temperature dependence of the effective integral of an isolated resonance is characterized by the self-shielding
factor

$$K = \frac{1}{\pi} \int_{-\infty}^{\infty} \frac{\Psi \, dx}{1 + \alpha \, (\Psi \cos 2\varphi - \chi \sin 2\varphi)}, \tag{8}$$

where φ is the phase of the potential scattering, $\alpha = \sigma^0 / \sigma_p$ is the ratio of the cross section at the resonance
maximum to the potential cross section of the medium per nucleus of the resonance absorber [2]. When using
approximation (5) this integral is calculated as

$$\tilde{K} \approx 1 / \sqrt{\left(1 + \frac{\alpha}{1+\delta} \cos^2 \varphi\right)\left(1 - \frac{\alpha}{1+\delta} \sin^2 \varphi\right)}. \tag{9}$$

A comparison of the results of numerical calculations of the integrals (8) given in [4] with our results (9) yields
the approximate relation:

$$\delta^{-1} = \zeta \{2.5 + 2\zeta + [(1 + \alpha \cos 2\varphi) \; \zeta]^{(0.1+\zeta)/(0.12+\zeta)}\}, \tag{10}$$

which when used in Eq. (9) reproduces the values of the integrals with an error of less than $\sim 3\%$ over the whole
range of the parameters.

The result of averaging a resonance cross section with the distribution function (4) is equivalent to the
ordinary Breit–Wigner formula, where taking account of Doppler broadening appears only in the redefinition
of the total width ($\Gamma \rightarrow \Gamma + \Delta$). This enables one to obtain simple analytic expressions for the estimation and
parametrization of the temperature dependences of various integral characteristics of cross sections used in
reactor physics applications. The fundamental criterion of the accuracy of the approximation must be a com-
parison with the data of integral experiments, since calculations with the integral Doppler functions are gener-
ally approximate per se.

LITERATURE CITED

1. H. A. Bethe, Rev. Mod. Phys., 9, 69 (1937).
2. A. A. Luk'yanov, Slowing Down and Absorption of Resonance Neutrons [in Russian], Atomizdat, Moscow
(1974).

3.   V. N. Faddeeva and N. M. Terent'ev, Tables of Values of the Probability Integral of Complex Argument [in Russian], Gostekhteorizdat, Moscow (1954).
4.   L. P. Abagyan et al., Bulletin of the Nuclear Data Information Center. Propagation of Resonance Neutrons in Homogeneous Media. Theory and Special Functions [in Russian], Atomizdat, Moscow (1968).
5.   A. A. Luk'yanov, Structure of Neutron Cross Sections [in Russian], Atomizdat, Moscow (1978).

NEUTRON RESONANCES OF ^{247}Cm IN THE ENERGY RANGE

0.5-20 MeV

T. S. Belanova, A. G. Kolesov,
A. V. Klinov, S. N. Nikol'skii,
V. A. Poruchikov, V. N. Nefedov,
V. S. Artamonov, R. N. Ivanov,
and S. M. Kalebin

The neutron resonance parameters of ^{247}Cm were calculated on the SM-2 reactor from the transmission of a sample of curium, which was measured by the time-of-flight method. The neutron pulse was shaped by a mechanical selector with three rotors, suspended in a magnetic field [1]. The best resolution on the flight base of 91.7 m amounted to 120 nsec/m.

The sample for investigation was made from powder, calcined at a temperature of 900–1100°C, of the stable oxide of curium (Cm$_2$O$_3$) with a known oxygen content. Included in the impurities were ^{243}Am and ^{240}Pu; the latter is built-up in the sample as a result of the decay of ^{244}Cm. The maximum ^{247}Cm content at the time of measurement amounted to $0.64 \cdot 10^{-4}$ atom/b. The content of inert impurities, with the exception of oxygen, did not exceed 3%. The transmission was measured in the neutron energy range of 0.5-20 MeV with a statistical error on the resonance limbs of 1-2%. The neutron background did not exceed 2% of the effect.

The neutron resonance parameters were calculated by the shape method according to the Bright–Wigner single-level formula [1]. As the neutron resonance parameters of ^{244}Cm, ^{245}Cm, ^{246}Cm, ^{248}Cm, ^{243}Am, and ^{240}Pu are well known [2-6], the ^{247}Cm resonances could be identified in the measured transmission and their parameters were calculated (see Table 1). In [3, 5, 6], the ^{247}Cm resonances with energies of 1.247, 3.19, and 18.1 eV were erroneously ascribed to ^{245}Cm. The neutron resonance with an energy of 2.919 eV was not previously detected.

Only 5 neutron resonances of ^{247}Cm were identified with large values of $2g\Gamma_n$, because the ^{247}Cm content in the sample was low (1.7 mg) and the resonances of this isotope were identified on the background of the large number of resonances of ^{244}Cm, ^{245}Cm, ^{246}Cm, ^{248}Cm, ^{243}Am, and ^{240}Pu located in the energy region being investigated.

TABLE 1

E_0, eV	Γ, MeV	$2g\Gamma_n$, MeV
$1,247\pm0,005$	74 ± 4	$0,56\pm0,09$
$2,919\pm0,010$	70 ± 30	$0,10\pm0,04$
$3,189\pm0,010$	103 ± 6	$1,0\pm0,1$
$9,55\pm0,03$	166 ± 60	$0,91\pm0,33$
$18,1\pm0,1$	210 ± 170	$3,7\pm1,5$

LITERATURE CITED

1.   T. S. Belanova et al., Preprint, Scientific-Research Institute of Nuclear Radiation P-6 (272) [in Russian], Dimitrovgrad (1976).
2.   Neutron Cross Sections, BNL-325, Third Edition, Vol. 1 (1973).
3.   T. S. Belanova et al., At. Energ., 42, No. 1, 52 (1977).

4.   R. W. Benjamin et al., Nucl. Sci. Eng., <u>55</u>, No. 4, 440 (1974).

5.   T. S. Belanova et al., Preprint, Scientific-Research Institute of Nuclear Radiation P-13 (307) [in Russian], Dimitrovgrad (1977).

6.   T. S. Belanova et al., Proceedings of the Conference on "Neutron Physics," TsNIIatominform, Moscow, Pt. 3, 224 (1976).

CONFERENCES, MEETINGS, SEMINARS

SOVIET – BRITISH SEMINAR ON FAST REACTORS

R. P. Baklushin

At the Seminar on "Experience in the Design, Experimental Development, and Operation of the Basic Plant for Fast Sodium Reactors," the British specialists presented 17 reports on the construction of units and plant for the newly designed commercial CFR reactor and on the various material-behavior problems. The Soviet specialists participating in the Seminar, visited nuclear centers at Risley, Harwell, and Dounraey, and also the PFR, operating at a power of 20 MW (thermal) and with a nominal capacity of 600 MW. The nominal thermal capacity was achieved in February 1977, but the electrical output was below the design output as a consequence of one of the intermediate steam superheaters and certain of the regenerative water preheaters (mixing type) being switched off, and also because the vacuum in the condenser was below the calculated value. The reactor, in addition to the generation of electric power, is used for testing fuel elements, plant, and components of the CFR reactor. In the last 2 years, the PFR frequently has operated at only 66% of its power because of these investigations. There were no cases of failure of the regular fuel elements and the burnup was 5%. There were 6 experimental cassettes with fuel elements in the core, and after 6 months there were two cases of fuel element failure among them. In January 1979, after this failure, the power was reduced to 66%. The burnup of the experimental fuel elements then in the reactor, amounted to 9%, but in general it reached 22%. In the week before the arrival of the delegation, a leak appeared in the evaporator of the second steam generator, which was the reason for further reduction of power. Although the leaks in the steam-superheaters of stainless steel attracted the most attention of the specialists, and after which cracking occurred in consequence of alkaline corrosion, these leaks amounted in all to two or three out of 15. Others were observed in the evaporators at the site of the tube weld with the tube plate because of corrosion pitting in the zone of the welded seam from the water side.

Great attention was paid to the reprocessing of PFR fuel (plutonium dioxide). The British specialists consider that they have solved this problem. In the summer of 1979 at Dounraey, it is proposed to start up a facility which has been designed for the reprocessing of all the fuel unloaded from the PFR. On this same area, it is planned in the future to manufacture fuel element assemblies from the reprocessed fuel, and thus to close the fuel cycle.

The decision to construct a nuclear power station with a CFR has not been taken and the area has not been assigned. The reasons for this were named as the reserves of petroleum discovered in the North Sea and the opposition of the protectors of the environment. It is expected that the construction of the nuclear power station will be started in 1984. The following problems were discussed in more detail.

In the core of the CFR, three types of control and safety rods are distributed: 19 control rods (these are the burnup compensators) and 9 scram rods – main and auxiliary. The design of the control and scram rods is conventional. Their actuators are located above the core on rotatable plugs. The main interest is the auxiliary group of scram rods. It is not connected mechanically with the rotatable plugs, but can provide protection of the reactor during fuel recharging. The rods are retained above the core by the action of a stream of sodium, fed into the guiding sleeve from below by special electromagnetic pumps. The rods are divided into three groups, with three in each group, and fed with an individual pump. When the pump is switched off, the rods fall downwards under the action of their own mass with a velocity of 0.4 m/sec. On falling into the core, the three rods inject a reactivity of -1.12% $\Delta k/k$. The geometry of the sleeve and the rod is such that in the case of erroneous switch-on of the pump, the latter remains in the lower position. In the upper portion, in which it is retained by hydraulic forces, it is returned by a special pickup mechanism. After switching on the pumps, the pickups are disengaged from the rods and raised upwards.

For the scram system, a special electromagnetic pump was developed and tested; it has a winding of copper strands surrounded by a magnesite insulation and a winding of stainless steel. The pump can be operated when immersed in sodium at 600°C. It was designed so that its central part with the electrical winding could be withdrawn from its channel, in the event of the occurrence of a failure. The diameter of the central part of the pump of different stub-size varies from 32 to 300 mm, and the flow-rate correspondingly from 0.4 to 50 liter/sec.

The fuel recharging system of the CFR has significant differences from the PFR fuel recharging system. Fuel element assemblies are withdrawn from the core by three mechanisms of the "direct" type (without pantographs). They are lined-up with the fuel element assemblies by three rotatable plugs. The change of design is explained by the tendency to increase the reliability and the service life of the mechanisms, and also not to withdraw them from the sodium after recharging. Two of the recharging mechanisms have been designed for the fuel element assemblies (in order to speed up the process, they operate together), and the third is for recharging the sleeves with the control and safety rods which, in order to eliminate errors, have other gripping devices. The heat capacity of the recharging container, filled with sodium, has been chosen so that the temperature of the fuel element cladding in the most stressed fuel element assembly is not raised above 650°C. In the case of delay, the container is cooled additionally by blowing with argon.

The pump of the CFR primary circuit is two-stage, and it has been calculated on a flow-rate of 10,500 m^3/h with a pressure head of 928 kN/m^2, and an operating temperature range of 200-370°C, but may be 500°C for a short time. The extraction part of the pump has a length of more than 15 m. The drum rests on two bearings: the lower is hydrostatic, fed with sodium from the pressure head of the pump; the upper is an oil bearing, radially axial. The drum sealing, as it has been suggested, will be mechanical, lubricated with oil and friction pairs, based on flat rings. Each pump is provided with a cut-off valve, for which there are no requirements for fast closure or 100% leak-tightness. The arrangement of the valve, together with the pump, allows the diameter of the reactor vessel to be reduced significantly. The power supply of the pump is fed from a separate motor-generator and variation of the speed of rotation is effected by varying the frequency of the ac supply. The range of control is 20-100%. In the case of deenergizing of the facility, auxiliary motors are provided, fed from accumulator banks and they ensure a 10% sodium flow rate.

It is proposed to develop the design of the pump and of the individual components on test-rigs. In particular, a transparent 1/4-scale model has been provided for, test-rigs for developing the upper and lower bearings, sealing, cut-off valve, etc. The problem of full-scale tests of the pumps in sodium, however, has not been resolved. Many British specialists assume that it will be sufficient to conduct these tests on water, as was done for the PFR.

The intermediate heat-exchanger of CFR has 4280 tubes with an outside diameter of 22.2 mm and an effective length of 7.1 m, arranged in concentric circles and fixed into two flat tubular plates. The sodium in the primary circuit flows in the tubes, and the sodium of the secondary circuit flows in the intertube space. It has been assumed that this ensures smaller hydraulic losses in the primary circuit and a more reliable operation in transition temperature conditions. The tubular plates are supported by the jackets and the tubes are made flexible, which makes the structure insensitive to the flow and temperature distribution between individual tubes. A gap is also provided, which is necessary for stopping the sodium supply of the primary circuit through the intermediate heat-exchanger, when the loop of the secondary circuit is switched off.

The CFR steam generator has partial recirculation (the moisture content of the steam at the outlet from the evaporator is 10%). The concept of the recessed tube bundle with U-shaped tubes has been retained. The most important changes with respect to the PFR concern the choice of structural material. In the evaporators and superheaters Kh9M1 steel is used (stainless steel in the superheaters finally was rejected). The temperature of the live steam consequently is assumed to be 490°C. The British specialists assume that leaks in the PFR steam generators are due, to a considerable degree, to the design of the sealing subassembly of the tubes in the tube plates, which has been made too inflexible and has residual stresses which promote corrosion cracking. In the CFR steam generators, the tubes are secured with thermal couplings. A secondary sodium steam generator was rejected in CFR. It will be effected with live steam.

Work is proceeding in Great Britain on instruments for facilities with sodium coolant. In particular, an ultrasonic instrument for the inspection of components above the surface of the sodium was demonstrated on a water test-rig. At the end of 1979, it is proposed to test the instrument in the PFR. Several new sodium test-rigs have been built. The HTSL test-rig, introduced in 1978, makes it possible to simulate thermal shocks with a rate of up to 25 degC/sec (from 600 to 400°C over 8 sec). The volume of sodium is 21 m^3 and it is calculated on a temperature of up to 700°C and a flow rate of up to 320 m^3/h. The SCTR test-rig, with a sodium volume of 40 m^3, has 7 working vessel-receptacles with a diameter of 0.6-1.1 m and with a length of 3.3-26 m. It is designed for testing various subsassemblies and mechanisms in static sodium. It is also proposed to investigate on it the weldability of fuel element assemblies in sodium, the wear of tubes, etc. On the "Super NOAH" test-rig, interstitial flows (400 g/sec) are being simulated in tube bundles with ideal geometry, for studying leakage of water into the sodium in steam generators. Temperature processes at the site of the leak are being investigated, secondary leaks have been simulated and also the burning of tubes with defects with a diameter of up to 20 mm.

Considerable attention in Great Britain is being paid to the behavior of structural materials under realistic conditions. In the reports devoted to the behavior of stainless steel 316 under conditions of high temperature and stress, the results are described of investigations of the process of formation and development of cracks. In other reports, the results were given of investigations of the corrosion of Kh2M and Kh9M steel for steam generators.

The meeting of the British and Soviet specialists confirmed that there are many problems presenting mutual scientific—technical interest.

CONFERENCE ON HYDROGEN POWER GENERATION

Yu. I. Koryakin

On May 17-19, 1979, a conference was held in Baku, of the Bureau of the Commission on Hydrogen Power Generation of the Academy of Sciences of the SSSR, together with the Scientific Council on the Production and Utilization of Hydrogen of the Academy of Sciences of the Azerbaidzhan SSR. About 100 people attended from the institutes of the Republic and organizations of other cities. The purpose of the Conference was formulated by M. A. Topchibashov, Academician of the Academy of Sciences of the AzSSR, who mentioned the active participation of the scientists of the Republic in solving the important and many-sided hydrogen problem.

The position and significance of the hydrogen problem in the development of power generation in the long-term was highlighted in a report by Academician M. A. Styrikovich. Hydrogen and its derivatives are emerging first and foremost as an intermediate energy-carrier in industry, municipal-everyday heat supply, and the direct combustion of fuel. For these purposes, at the present time in the world about two-thirds of the fuel being extracted is burned up. Despite the mass production of hydrogen being a matter for the more distant future, it is essential to solve the hydrogen problem even now. In the situation expected in the long-term, the question is not about the orientation in this or other energy source or energy-carrier, but about their optimum combination, including the user factor.

The main attention in the report of M. A. Styrikovich was paid to the fuel-power situation in the world and its special features in the Soviet Union. It was noted that the practically inexhaustibility of the already widely used atomic energy and, in the future, possibly thermonuclear energy, will ensure the feasibility of the further growth of energy consumption. The increase of consumption, complicated by the "demographic explosion" of the last decades, will be limited by the negative secondary effects of power development, including in the first place the disturbance of the ecological equilibrium, created by excessive load on the environment.

The speaker defined certain determining factors in the forecasts of power development — the population increase, reserves and resources of the various types of energy, the importance of nuclear power forecasting especially in the long-term, and also the tonality of the forecasts being compiled, as in recent years dark predictions concerning the power future have been frequent abroad. There is no basis for this, although the gradual slowing down of the power increase can be expected with a high probability. Under these conditions, the forecasting in quite a large time depth, up to the end of the 21st century will acquire considerable importance. The duration of the development of power technology, computed as tens of years (e.g., nuclear power), and the great technological and invested inertia of the power generation branches and of the infrastructure will now require such endeavors, M. A. Styrikovich noted that Soviet and foreign investigations invariably will have an effect on the dominating role of nuclear power generation, despite the several complex and increasing negative factors accompanying its development. They are mainly due to the external fuel cycle.

The essence of the hydrogen problem, combining a different power generation technology including nuclear, was recounted by V. A. Legasov, Corresponding Member of the Academy of Sciences of the SSSR. He indicated the fundamental position on which is based the complex of work on hydrogen power generation in the Soviet Union. Hydrogen cannot be and must not be considered as a source of primary energy, but only as a factor of energy economy, and its optimum utilization. No alternative to hydrogen can be seen as yet in the solution of this problem (taking account not only of molecular hydrogen, but also its different forms — atomic, liquid, and chemically combined). The possession of the technology for the production of hydrogen will require a long time, and a delay in its utilization will strongly affect the future requirement for power. Its methods of production are indifferent to the sources of power, but are sensitive to temperature. The participation of nuclear power in

776

production is possibly twofold: electrolysis and high-temperature thermochemistry. Plasma electrolysis is interesting, by which hydrogen can be obtained in a nonequilibrium oscillatory process of the reaction of CO_2 and H_2O at 500°C. The process of direct production is interesting, although it is difficult to achieve from the point of view of radiation safety, due to the radiation output. Here, the interaction of radiation with the molecule of water is used. The speaker gave estimates of the possible scale of hydrogen production by nuclear methods, the structures of the consumption of hydrocarbons obtained by these methods, in future hydrogen power generation.

In order to solve the hydrogen problem, considerable work will be necessary, for which a program has been compiled by the Academy of Sciences of the SSSR and the State Committee for Science and Technology, and contains scientific—technical problems of the production and utilization of hydrogen.

A following group of reports, made by scientists of the Academy of Sciences of the AzSSR, concerned the different sides of the activity of the institutes of the Republics in solving the problem. This activity, defined in the report by M. I. Rustamov, rests on the petrochemical production base of the Republic, and starts from its potentialities, specific properties and requirement. About 100 people are participating in the investigations, work is proceeding in the direction of hydrogen production in different cycles, from hydrogen-containing gases using biological methods, by the creation of thermal and solar energy sources, photochemical decomposition of water, the use of synthesizers, and by the membrane method of separation (pure hydrogen ~ 70%). The problem consists in the utilization of hydrogen-containing incidental and waste gases of the petroleum extraction and petrochemical industries.

The large number of windy and sunny days in the Republic (180–200 and 300 days per year) justify the work on wind and solar power facilities, a description of which was given in the report by M. Ya. Bekirov. A photoelectric hydrogen facility with a silicon solar battery and an electrolyzer with a power of 100 W and a hydrogen output of 3 liter/h, a wind-powered facility of 240 W with an output of 7 liter/h, etc. have been constructed. The photochemical and combined methods of decomposition of water were the theme of the report by N. Z. Muradov. Photocatalyzers (dyestuffs) allow up to 30% of the visible region of the solar light spectrum to be used. Combined methods are being investigated with the use of light, thermal, and electric power. Preference is being given to the iodine and iron—chlorine cycles. The former allows a photochemical process to be used for the decomposition of water, and the second is based on the use of hydrochloric acid, which is a waste product of industry. The content of hydrogen and hydrogen-containing gases of the waste products of the petrochemical processes was the theme of the report by E. I. Pryanikov. The wastes from catalytic thermal cracking are a multitonnage supply for the production of hydrogen. It is an important element in the intensification of the reprocessing of petroleum and complex utilization in petrochemistry (report of I. I. Sidoruk). The membrane technique of separating hydrogen and the technology of production of improved membranes, developed in Azerbaidzhan, was the topic of the report by R. S. Alimardanov. The report of V. R. Rustamov was devoted to the radiolysis of water vapor in the presence of solid catalytic compounds — zeolytes. A report on the work of the Second Universal Conference on Hydrogen Power Generation (Zurich, 1978) was given by S. P. Malyshenko.

The consideration of the reports, discussion, and decision taken reflected the urgency and importance of the problem as a whole, as well as the work being carried out in the Azerbaidzhan SSR.

SECOND CONFERENCE OF THE CONSULTATIVE GROUP
ON NUCLEAR DATA FOR THE ISOTOPES OF THE ACTINIDE
ELEMENTS

V. M. Kulakov

From April 30 to May 5 1979 at Cadarache (France), two international conferences were held, convened by the IAEA. The first of these was a conference of two groups united by a program of coordinated investigations, and the second was a conference on nuclear data for the actinides.

The two groups, within the framework of the program of coordinated investigations, were formed after the First Conference on Nuclear Data for the Actinides (Federal Republic of Germany, November 1975) and they monitor the state of nuclear data. One of the groups is occupied with the status of nuclear data and the

comparison of estimates of the cross sections in reactions with neutrons, and the second is occupied with the status of the measured and estimated values of nuclear data concerning decay. The last meeting of these groups took place in Mid-1978 in Vienna. As a result, recommended estimated values of nuclear data were worked out and distributed both for reactions with neutrons and for the decay of isotopes of the actinide elements. At the meeting of the first group (on neutron data), 15 specialists participated from 10 countries (Belgium, Great Britain, Israel, India, Italy, Soviet Union, France, Federal Republic of Germany, Switzerland, and Japan). The state of work was considered at the Meeting, on the estimation of cross sections, the degree of their overlap, methods of circulation and exchange of data, and also the methodology for comparing the different estimates. At the Meeting of the second group, 10 specialists participated from 7 countries (Belgium, Great Britain, Soviet Union, USA, France, Federal Republic of Germany, and Japan). Reports were presented on the measurement and estimation of nuclear data on decay during the time elapsed since the last Conference in Vienna. The estimation of nuclear data was discussed, their presentation on magnetic tapes, and also their circulation and exchange. As a result, tables were compiled of recommended values, in which data were included about the half-lives, relative probability of spontaneous fission, the absolute value of the intensity of selected α and γ transitions, and also the most intense $L - x$ emission.

At the second meeting of the Consultative Group on Nuclear Data for the Actinides, 36 specialists from 10 countries participated. The Conference was organized by the Nuclear Data Section of the IAEA and, just as the first Conference at Carlsruhe, called upon specialists occupied with estimates of nuclear data and the direct measurements of the constants, to assemble together with the nuclear data users. The work of the Conference proceeded in accordance with this program. In Section A reports were heard on the requirements for nuclear data for standard U and U−Pu thermal and fast reactors and for reactors with alternative fuel cycles. The speakers of Section B reported on the status of nuclear data (both decay and cross section), the estimation of these data and the mutual comparison of the estimates. In addition, several reports were presented on the measurement, estimation of data for specific isotopes, and the methodology of compiling the estimates.

On one of the days, the participants of the Conference divided into two working groups, the problem of which was to discuss in more detail the status of the computed data, to compare them with the requirements formulated in the reports, to work out general recommendations for future work within the framework of the program of coordinated research, and specifically on the measurement and estimation of data for individual isotopes. One of the working groups discussed neutron data and the second discussed decay data. Tables were then compiled reflecting the current state of accuracy of the nuclear data and comparing them with the accuracy required for calculations in the various branches of nuclear technology and also in geology, medicine, cosmo-chronology, etc. Isotopes were noted for which data needed for the calculations were totally or partially absent.

The last session was devoted to the reports of the representatives of the working groups, the acceptance of general recommendations of the Conference and the special recommendations of the working groups. Of the general recommendations, the following may be mentioned:

international activity on the measurement and assessment of nuclear data for the actinides has been approved;

it is proposed that IAEA organize the next meeting after 4 years, assuming this period to be the optimum for reviewing the current state of nuclear data and for carrying out the necessary assessments;

it is proposed that meetings of the groups on the Program of Coordinated Research should take place every year. It is recommended that the next meeting take place in June 1980 in Vienna, before or after the meeting of the International Commission on Nuclear Data;

the issue of the journal "Actinide Newsletter," prepared by S. Raman (USA, Oakridge), was supported, was accepted as useful, and it was suggested that it is issued annually.

The Conference showed that at the present time, work on the measurement, collection and assessment of nuclear data for the actinides has acquired a considerable spread in all the developed countries, and the main attention was paid to the broad international collaboration within the framework of the IAEA. This is demonstrated, on the one hand, by the requirements for nuclear data in solving problems of nuclear power generation and technology, and certain applied problems, and on the other hand, international cooperation will allow access to the entire collection of data, thereby saving considerable material resources of each individual government.

SOVIET — SWEDISH SEMINAR ON THE BURIAL OF RADIOACTIVE WASTE

L. P. Zavyal'skii

The Seminar took place in Sweden in March 1979. Its program included the attendance of the Institute of Glass at Veksho, Control of Geological Services at Upsalla, the Geological Testing Ground at Finshen, the bituminizing workshop at the "Forsmark" nuclear power station, and the organization for the Planning of Nuclear Safety in Stockholm.

In Sweden, before obtaining governmental approval on the operation of an installed nuclear power station, it is necessary to present and defend the plan for the final burial of either the radioactive waste from the fuel element regeneration, or from spent fuel elements. At present there are 6 operating nuclear power stations and 6 under construction in the country. The "Forsmark" nuclear power station has not delivered under load, as there is no decision on the startup, although one unit of 900 MW (electric) was installed in 1977, construction of the second unit has been completed, and the area for the third unit with a capacity of 1040 MW (electric) has been reserved. In order to work out a standard plan for the final burial of waste or spent fuel elements, an organization was set up in 1976 on the Planning of Nuclear Safety (KBS), under the aegis of the National Council for the Treatment of Radioactive Wastes. Swedish industrial firms, institutes, and universities are working under contract to it, and also foreign organizations and companies, including from the USA, France, and the Federal Republic of Germany. In 1978 the efforts of the Swedish and foreign specialists resulted in the development of a plan for the final burial of spent (nonregenerated) fuel and the vitrefied wastes from fuel regeneration. At present in Sweden, both these concepts are being studied as alternatives. The right of the ultimate decision on the choice of the method of burial rests with the Governmental Committee on Radioactive Waste.

The first plan, entitled "Treatment of spent nuclear fuel and the final burial of vitrefied waste of high-level activity," consists of five volumes under the following headings: General Situation; Geology: Storage Vaults; Safety Analysis; and Review of Foreign Work.

At the present time the KBS has an agreement with the French firm COGEMA for the regeneration of Swedish spent nuclear fuel in the 1980s. After regeneration of the fuel, it is proposed to store the wastes in the form of vitrefied blocks for 10 years in France, in chrome—nickel steel containers, after reduction of the release of heat to 1000 W per container, to transport to Sweden, where they will be stored for 30 years with air cooling until the heat release is less than 525 W per container, in a specially constructed intermediate storage vault at a depth of 30 m. The intermediate storage vault has been calculated on 9000 containers, which corresponds to a quantity of waste from the regeneration of spent fuel from 13 Swedish nuclear power stations during 30 years. The Design of the intermediate storage vault is similar to the design of the storage vault at Marcoule. After a total of 40 years of storage, the vitrefied blocks will be finally buried in lead—titanium capsules at a depth of 500 m, in tunnels, at the bottom of which at a distance from one another of 4 m will be sited boreholes with a depth of 5 m. After loading in the containers the boreholes and tunnels will be filled with a mixture of quartz sand and bentonite. According to laboratory investigations, the service life of the container with unlimited contact with water is estimated at 30,000 years. In the case of final burial at 500 m, the contact of the container with water is estimated at 0.2 liter/m^2 per year, and the service life is estimated at 60,000 years.

The requirements are given in the plan for the transportation systems and the intermediate and final storage vaults, and a long-term forecast is given of the radiation safety during storage in hard rock.

The second plan "Treatment and Final Burial of Nonregenerated Spent Nuclear Fuel" issued in two volumes is considered as an alternative to the first plan. It is proposed that the regenerated fuel assemblies after intermediate storage during 40 years, should be placed in final burial in hard rock. The assemblies will be encapsulated in copper containers (diameter, 770 mm; height, 4700 mm; and wall thickness, 200 mm), lined inside with lead. The total mass of the container is 20 tons, including 2 tons of fuel, 2.5 tons of lead, and 15.5 tons of copper. The total number of containers is 9000. The encapsulation of fuel elements in canisters of aluminum oxide, obtained by hot isostatic pressing at 1350°C and a pressure of 100 MPa, is also being studied. The length of the proposed canister is 3 m, diameter 0.5 m, and mass 2 tons. They will be manufactured in

the high-pressure laboratory of the firm ASEA in Robertsford. The canister will hold 144 BWR fuel elements or 174 PWR fuel elements, twisted in the shape of a flat spiral. It is proposed that final burial be conducted just as in the first plan, but the boreholes for the copper containers are stipulated to be cased with pressed bentonite blocks.

As in the first plan, the amount of spent fuel in the container is analyzed here, the starting data are given for the design and description of the storage vault, the properties of the canister materials and the buffer materials, and an analysis of safety is given.

At the presen time, the program of scientific-research and experimental-design work of KBS is drawn up for 10 years and includes field geophysical, geochemical, and hydrogeological investigations; a study of vitrefied wastes and spent fuel; safety analysis; work at an experimental station in the Strir pit (Dallarn) at a depth of 400 m, and also economic studies and design work.

The high scientific—technical study by Swedish specialists should be mentioned, of problems associated with the final burial of highly active waste. The basis of the plans rests on 120 reports on scientific-research work.

NATIONAL CONFERENCE IN THE USA ON CHARGED-PARTICLE ACCELERATORS

Yu. M. Ado and I. N. Semenyushkin

The National Conference on Charged-Particle Accelerators in the USA, held once or twice a year, attracted the attention of a considerable number of scientists and specialists associated with the development and improvement of accelerators, as well as with their use for physics and applied research. The last conference took place on March 12-14, 1979 in San Francisco. About 900 specialists, including about 170 from other countries, participated in its work. At the two plenary and 12 sectional sessions, more than 250 reports were presented on the broad problem of accelerator science and technology. The use of accelerators for applied purposes was assigned an important place in the work of the Conference.

One of the principal trends of work on functioning proton accelerators is to increase the intensity of the accelerated particle beams. A large number of reports was concerned with studies of the dynamics of particles in accelerators under conditions of the powerful effect of the inherent electromagnetic field of the beam. For example, in the CERN reports, the correction of the principal quadratic betatron resonances and structural resonance in an 800-MeV booster which was carried out successfully were discussed; also the resistance wall instability of betatron oscillations in a 28-GeV accelerator with an intensity of $1.2 \cdot 10^{13}$ protons per cycle, the strong instability of the "head—tail" type in a 400-GeV accelerator, and the beam instability caused by parasitic oscillation modes in accelerating resonators. The operation of this accelerator with an intensity of $2 \cdot 10^{13}$ protons per cycle has been assured by the suppression of these effects. It should be mentioned that the proton energy was successfully increased up to 500 GeV for a short time. It will be possible to operate it at an energy of 450 GeV. The reports of the specialists of Fermi National Accelerator Laboratory (FNAL) concerning the use of negative hydrogen ions for recharge injection into a booster created interest. The use of recharge injection has allowed the intensity of the main accelerator to be increased up to $3.9 \cdot 10^{13}$ protons per pulse (design for $5 \cdot 10^{13}$). In the Brookhaven National Laboratory (BNL) the acceleration of polarized protons is being studied in a 33-GeV accelerator. It is assumed to be possible to maintain 70% of the polarizations up to 23 GeV and 50% up to 26 GeV with an intensity of 10^{12} protons per pulse. The cost of the work is estimated at 2.9 million dollars.

Included in the designs of large accelerator facilities that are being built at the present time are the DOUBLER (FNAL) accelerator with an energy of 1000 GeV (with completion in 1982) and the ISABELLE (BNL) facility with colliding proton beams of 400×400 GeV and with an emittance of up to 10^{33} cm$^{-2} \cdot$ sec^{-1} (completion in 1986). At CERN it is planned to obtain by 1982, proton—antiproton colliding beams of 270×270 GeV and with an emittance of about 10^{30} cm$^{-2} \cdot$ sec^{-1} in a 400-GeV operating accelerator. The antiprotons will be stored up in a special annular storage ring, using stochastic cooling. The specialists of FNAL also presented reports about plans for proton—antiproton beams, but using electronic cooling. The designs of the DOUBLER and

780

ISABELLE facilities are based on the use of superconducting magnets. After prolonged model investigations at BNL and FNAL, working specimens of the magnets have been developed and at the present time a study of them is being conducted at FNAL with a beam of particles.

Great interest was created by the report of the operation of the PETRA facility (Federal Republic of Germany), with colliding electron—positron beams of 19×19 GeV and the plans for its development. Doubling of the hf power in 1981 will permit the particle energy to be increased up to 23 GeV, and conversion at the end of the 1980s to superconducting resonators should increase the energy to 30 GeV. The large facilities also include the PEP facility (USA, Stanford) for colliding electron—positron beams of 19×19 GeV. The first experiments with the beam are planned for October 1979.

The normal system for producing colliding e^+e^- beams with an energy of 100 GeV and higher becomes complicated and expensive. The cost of the design for colliding e^+e^- beams with an energy of ~ 80 GeV is estimated at ~ 1 million Swiss francs. An alternative conventional scheme for this energy might be linear colliding beam systems, a study of which is being conducted at certain USA centers and in other countries.

Reports were presented at the Conference on the various aspects of the generation of intense pulsed beams and of a study of the process of collective particle acceleration.

The study of the behavior of a nuclear substance in extreme conditions, the study of multibaryon interaction, and also the prospects of using ion beams for medical—biological and applied purposes all stimulated the interest which is appearing in many large-scale physics centers of the world for the production of beams of heavy ions with high energy. Today, in five centers (Dubna, Berkeley, Saclay, Darmstadt, and Tokyo) there are, or are planned, heavy-ion accelerators with an energy in excess of 1 GeV/nucleon. The characteristics of an ion accelerator at this energy is determined mainly by the multicharged ion sources, the efficiency of the ion acceleration system with a low energy, etc. This was reflected in the reports presented at the Conference on this topic. Progress has been achieved by the French specialists working on an electron-beam source of multicharged ions of the Dontz type. With a current density of $\sim 10^5$ A/cm^2 and an ionization time of 6-10 msec at the source outlet $5 \cdot 10^9$ ions of N^{7+} and $3 \cdot 10^9$ ions of Ar^{18+} and Ar^{17+} are obtained. It is proposed that by the end of 1979, the source will be functioning on the Saturn-II accelerator. A heavy-ion accelerator complex, the design of which is being developed by JINR and the I. V. Kurchatov Institute of Atomic Energy, is intended for the production of a record ion energy of up to 4.5 GeV/nucleon. As the ion source in the first stage, the cryogenic electron-beam source, which is already functioning in the synchrophasotron will be used. In the next few years, it is planned to bring to completion the NUMATRON project (Japan). The accelerator complex is designed for the production of ion beams up to uranium, with an energy of 1.27 GeV/nucleon and an intensity of 10^9 ions/sec. The ions will be accelerated successively in three linear Wideroe accelerators, in two Al'varez linear accelerators with gradual increase of the charge of the ions, due to stripping on special targets, and two synchrotrons. In order to produce the high intensity of the accelerated particles, it is proposed to carry out multireversible injection in the first synchrotron during buildup of the beam.

Part of the reports was devoted to the high-powered 35-MeV deuteron accelerator, with a continuous beam current of 100 mA, being developed at Los Alamos. It is proposed to use this accelerator as a neutron generator (10^{15} neutrons/cm$^2 \cdot$ sec) for testing the structural materials of a thermonuclear reactor. Special attention during the development of the accelerator system is being paid to reducing the beam losses to values which are characteristic for operating linear accelerators. For the initial part of the accelerator, it is proposed to use a structure with spatially uniform focusing. It is proposed to develop a high-powered linear accelerator under project PYGMY (proton energy 650 MeV, average current 100 μA). The initial part of the accelerator is designed on the use of variable-phase focusing. Small-sized lenses in permanent magnets of rare-earth alloys will be used for the drift tubes. The accelerating structure of the end part of the accelerator will provide a high rate of acceleration — 6 MeV/m. Great interest was created by a report presented by specialists of the Institute of Theoretical and Experimental Physics (Soviet Union) concerning the accelerating structure of a linear accelerator with spatially uniform and quadrupolar focusing. The completion of these projects will be an important step in the development of accelerator technology.

A large number of reports was devoted to the generation and utilization of synchrotron radiation (SR) in electron cyclic accelerator-storage devices. Interest in the use of synchrotron radiation in biology, crystallography, microscopy, etc. is increasing. By 1979 in the USA, about 260 proposals for experiments were contributed from ~ 100 establishments in the USA and other countries. Abroad, beams of synchrotron radiation have been produced in 13 accelerator facilities and before 1981 their number will increase to 30.

One of the most important fields in science and technology, where accelerators can find extensive application and may determine the direction of future development, is that of nuclear power generation, using nuclear fission and thermonuclear fusion. Great attention was paid to these problems at the Conference. According to the calculations of the BNL specialists, the use of high-powered proton linear accelerators with an energy of ~ 1 GeV for turning out nuclear fuel (^{239}Pu and ^{233}U) will prove to be suitable for the provision of reactor fuel. Certain laboratories in the USA (Sandia, Berkeley, Livermore) presented reports on high-powered electron accelerators and heavy-ion accelerators designed for thermonuclear fusion.

Medical—biological research is occupying an ever-increasing position in the use of accelerators. At the Berkeley and Los Alamos laboratories, the Fermi Laboratory and others, particle beams already are being used for therapeutic purposes. The Committee for Radiooncological Research has formulated a program for the future development of medical—biological research and the application for therapy of different particles (neutrons, protons, heavy-ions, and π-mesons), including the construction of special accelerators for these purposes.

BRIEF COMMUNICATIONS

TENTH SPRING SYMPOSIUM ON HIGH ENERGY PHYSICS

A. B. Kaidalov

The Tenth Spring Symposium on High Energy Physics, organized annually by physicists of the Karl Marx University, Leipzig, was held in March 1979 at Bermsgrun (German Democratic Republic). About 30 physicists, the majority of whom were from the University of Leipzig and the Institute of High Energy Physics, Zeiten, participated in its work. Physicists from other countries were invited to the Symposium to lecture on the most urgent problems of the physics of elementary particles. Professor Renard (France) read a course of lectures on the various phenomena arising during e^+e^- annihilation. It is well known that in this field extremely important results have been obtained in recent years — the discovery of new particles Ψ, Ψ', χ, γ, and γ', having unusual properties and consisting of quarks of new types (c, b), the discovery of the new heavy τ-lepton, and indications have been obtained of the existence of quark and gluon jets, etc. In the lectures the possibilities for the experimental observation of the intermediate Z^0-boson were discussed in detail; the Z^0-boson is predicted in the gauge theory of the weak and electromagnetic Weinberg—Salem interaction in the colliding e^+e^- beams with an energy of about 100 GeV in the center of mass system, currently being planned. The reports of the German physicists (K. Hansen, G. Wetzig, and S. Ritter) were devoted to the study of the different aspects of formation of hadrons in e^+e^- interactions.

Great attention is being paid at the present time to the verification of the Salem—Weinberg model by the investigation of neutral currents. It is well known that recently effects of nonconservation of p-parity in neutral currents have been observed. The possibilities of further investigation of the properties of weak interactions in scattering processes of leptons by nucleons and deuterons were discussed in the reports of G. Motz and T. Raiman.

A. B. Kaidalov (Soviet Union) delivered lectures on the application of the dispersion rules of sums in the physics of elementary particles. By means of this method, an indication can be obtained of the possibility of existence of exothermic baryon resonances with large isospins.

Considerable attention at the Symposium was paid to the theoretical investigation of the interaction of quarks and gluons on the basis of quantum chromodynamics. Quantum chromodynamics is an asymptotically free theory, and therefore at a small distance (large imparted momenta), the theory perturbations can be used. Part of the reports was devoted to the consequences of quantum chromodynamics for processes with large imparted momenta (G. Perlit, R. Kirschner, A. Schiller, and I. Kripfhantz). Problems were considered, associated with violation of scaling in deep inelastic processes, with the existence of processes of the formation of several jets in e^+e^- annihilation processes and the formation of hadrons with large transverse mementa during collisions of hadrons, and with the calculation of the Drell—Yan process. The general method of calculating quark and gluon jets was also discussed within the scope of the quantum field theory.

Problems associated with the possible experiments on the hadron accelerators being planned, with an energy of about 500 GeV in the center of mass system, were discussed in the report by G. Ranft. Both conventional investigations of the total interaction cross sections, two-particle processes and reactions of multiple particle formation, and also processes with large imparted momenta and reactions of the formation of new particles were considered.

The Symposium was well-organized and was conducted successfully.

FIFTH MEETING OF THE COMBINED SOVIET – CANADIAN WORKING GROUP ON COLLABORATION IN THE FIELD OF POWER GENERATION

M. B. Agranovich

The Conference, held within the framework of the long-term program of economic, industrial, and scientific-technical collaboration between the Soviet Union and Canada, took place on May 11-18, 1979 in Moscow.

The delegation of Soviet engineers was led by the Deputy Minister of Power and Electrification of the Soviet Union N. A. Lopatin, and the Canadian delegation was led by the General Director of the Division of Foreign Projects of the Ministry of Industry and Commerce of Canada, F. Petri.

In the course of the meeting of the Working Group, reports of the sides were heard on the state and prospects for the development of power generation in the Soviet Union and Canada, and the role of nuclear power stations in the power generation of both countries. An exchange of opinions took place on the subjects and form of future cooperation, which were of mutual interest. The Working Group discussed the proposals of the Soviet and Canadian specialists for the conduct of future work and affirmed the program of collaboration in 1979-1981 in the fields of planning, construction, and operation of hydrotechnical plants in severe climatic conditions, forecasting the state of the plane and reliability of nuclear power stations with channel type reactors, the use of cheap electric power for the production of hydrogen as a fuel and a chemical raw material, and other problems of electric power generation.

In the minutes, signed by the delegations, it was noted that the joint activity of the specialists of both countries will allow a significant contribution to be made to solving the problems of the more efficient production and consumption of electric power, and thereby will assist the economy of the power resources.

FIRST MEETING OF THE JOINT SOVIET – FRENCH WORKING GROUP ON COLLABORATION IN THE FIELD OF ELECTRIC POWER GENERATION

M. B. Agranovich

The Meeting took place on May 24-31, 1979, in Moscow. In accordance with the subjects defined by the agreement between the governments of the Soviet Union and France of October 17, 1975, the possibilities were considered for collaboration in 1979-1980 in the following directions: planning, construction, and operation of hydrotechnical plants, State Regional Electric Power Stations and nuclear power stations with fast reactors. Understanding was reached concerning the exchange of information on the operation of nuclear power stations, the use of nuclear power stations for the supply of heat, and problems associated with earthquakes. At the suggestion of the Soviet delegation, new topics were included in the program of collaboration: "Theoretical developments and experimental research in the field of solar power facilities" and "Hydrogen power generation."

In the course of the Meeting of the Working Group, the reports of the sides were heard concerning the state and prospects of development of power generation in the Soviet Union and France.

A meeting took place between the leader of the French delegation of the Director of the Board of Gas, Electricity, and Coal of the Minister of Industry of France, I. Kupin and the Minister of Power and Electrification of the Soviet Union P. S. Neporozhnii. The sides emphasized that the creation of the Working Group is an important stage in the development of cooperation between the Soviet Union and France and will contribute to the more efficient development of power generation in both countries.

FIRST MOSCOW KURCHATOV LECTURE

I. A. Reformatskii

The First Moscow Kurchatov Lecture was conducted on May 13, 1979, at the Moscow Palace of Culture "Moskvorech." The organizers of the lectures — the Moscow City and Krasnogvardeisk Regional Organization of the company "Znanie," Moscow Engineering Physics Institute, I. V. Kurchatov Institute of Atomic Energy — invited scholars of the senior classes, teachers of the Vocational and Technical School and students in order to talk to them about the eminent Soviet scientist, organizer of the Soviet Nuclear industry, Academician I. V. Kurchatov, and about the development of modern physics and the scientific trends along which specialists are trained in the Moscow Engineering Physics Institute.

The opening lecturer, Prorector A. G. Zaluzhnyi, presented the assembled colleagues of the Moscow Engineering Physics Institute, who had worked with Igor Vasil'evich, and also two scientific workers of the Kurchatov Institute of Atomic Energy, who had arrived in order to take part in the lectures.

"The Moscow Engineering Physics Institute is the creation of Academician I. V. Kurchatov," said the Prorector of the MEPI in the address on the work of V. V. Khromov — "And now we are striving to train specialists, capable of creatively developing the ideas and trends put forward by Kurchatov."

The talk by Hero of Socialist Labor, State Prize Laureate V. S. Emel'yanov, who had occasion to work with I. V. Kurchatov for almost 15 years was interesting and lively. He sketched a bright image of the scientist and organizer, having been able in extremely short periods and under conditions of the difficult war years, to create friendly and energetic staff who, already in December 1946 had achieved the startup of the first nuclear reactor in Europe and Asia, and in 1949 tested the atomic weapon.

The address of State Prize Laureate, Honored Scientist of the RSFSR I. V. Savel'ev, was devoted to the style of work of I. V. Kurchatov for the education of scientific workers of the higher grades.

"I was indebted to I. V. Kurchatov in many respects in my Doctorate dissertation," he said — "Kurchatov not only showed that I had sufficient material for the dissertation, but also assisted in its rapid formulation and consolidation."

Yu. V. Sivintsev and I. A. Reformatskii devoted addressed to the work of I. V. Kurchatov with young scientific workers, gave recollections of how Igor Vasil'evich valued the opinion of his colleagues irrespective of rank, supporting their initiative and independence in scientific work.

An exhibition was mounted in the foyer of the Palace of Culture, devoted to the life of I. V. Kurchatov. In many photographs, Igor Vasil'evich was portrayed with friends and comrades, scientists, and statesmen. The works of I. V. Kurchatov were displayed on the stands, recollections of him and archive material about the establishment of Soviet nuclear physics.

The voice of I. V. Kurchatov resounded at the lectures, addressing the Twenty-First Congress of the Communist Party of the Soviet Union in 1959, and speaking about the plans and aims of Soviet physicists, and the documentary film "The Atomic Flame" was shown, devoted to the life and activities of the eminent Soviet scientist.

A welcoming telegram was received at the First Moscow Kurchatov Lectures from the President of the Academy of Sciences of the SSSR, Academician A. P. Aleksandrov.

NEW BOOKS

Kh. Wong

BASIC FORMULAS AND DATA ON HEAT EXCHANGE FOR ENGINEERS *

Reviewed by P. L. Kirillov

The book is a short handbook on the calculation of heat transfer in different heat-exchange devices. With the deficiency of reference literature, the issue of this publication undoubtedly is useful.

The book consists of 7 chapters, tables, and appendices. In the first chapter, which is the introduction, general data about heat transfer are explained. The second chapter is devoted to thermal conductivity. Here, the author introduces a new concept of the heat-transfer parameter — a quantity which is the reciprocal of the thermal resistance. Tables of heat-transfer parameters are given for important cases. In the third chapter, where convective heat exchange is considered, a large number of formulas are contained relating to free motion, flow in channels and superficial flow around objects. In the fourth chapter, the basic laws and methods of calculating thermal radiation are given. The fifth chapter contains brief data on boiling and condensation processes. Unfortunately, little attention is paid to the calculation of crisis. In the sixth chapter, which considers methods of calculating heat exchangers, there are data about heat-exchange intensification. The seventh chapter is devoted to heat transfer in engineering structures.

The recommended formulas in the majority of cases are reduced to thematic tables with clear designations, which considerably facilitates finding the formulas. A list of symbols and definitions of technical terms is appended to every chapter. The book is provided with an alphabetical index. Numerical data are given in the SI system.

The advantage of the handbook consists in the extensive coverage of many divisions of heat transfer. However, its drawbacks also are partly connected with this. The handbook is brief in content, and therefore it is difficult to criticize the publication for what is not in it. All the formulas and data are taken from foreign publications. The author, obviously, is not sufficiently familiar with the latest publications of Soviet journals and monographs. In every case these data have not been reflected in the handbook, and therefore in certain cases the author has included obsolete data. A preface to the handbook should have been given by the translators and editors, and a note or small addition should have been made at the necessary places. This concerns especially the sections associated with nuclear power generating facilities. There are no data in the handbook about the calculation of heat transfer and crisis in bundles of rods, i.e., those types of channels which are most widely used in nuclear power-generating facilities. At the same time, the calculation of certain exothermic channel configurations could have been omitted. Also, tables of Bessel functions and error functions could have been omitted without detriment. Unfortunately, during translation, terms and symbols accepted by the Soviet Union at the present time have not been preserved everywhere. For example, μ/s on p. 53 is called the rate of diffusion and on p. 54 (quite correctly) it is called the kinematic coefficient of viscosity.

In certain cases different symbols are not so harmless as may be indicated and could lead to misunderstandings. For example, t_S (p. 48) denotes the surface temperature, although in Soviet literature it is taken to denote the saturation temperature. This is all the more disappointing, as on p. 50 the surface temperature is denoted further by t_{cT}. In Table 6.4 Q denotes the power (or output) and Q_m denotes the mass flow rate. Therefore, when using the handbook additional increased attention must be paid to the symbols in general, and to one and the same quantity in its different sections in particular.

On the whole, the publication can be welcomed. The handbook is useful to engineers who are involved with heat-transfer calculations.

I. I. Malashinina and I. I. Sidorova

TRAINING EQUIPMENT FOR NUCLEAR POWER
STATION OPERATORS *

Reviewed by S. G. Muradyan

The development of nuclear power generation is a multiplicity of problems, one of which is the manning
of nuclear power stations which have been brought on stream, with highly qualified operative and operating
personnel. The increase of the unit capacities of the power units of nuclear power stations, the assurance of
their safe and accident-free operation imposes rigid demands on the level of their training. The training
of a large number of specialists with a high level of professional knowledge, skills and experience is possible
in scientific-training centers, equipped with the most up-to-date technical means of teaching, in particular
training equipment.

In recent years, publications on the training of staff for nuclear power stations are being encountered
even more frequently. Therefore, the book under review pays particular attention to the generalized accumu-
lation of experience in the development of training equipment for nuclear power station operators. The authors
have attempted to comprehensively highlight the problems arising in the development of training equipment,
and in the majority of cases they have successfully formulated the problems and have suggested specific
routes and methods for their solution. In this respect, the material of the third, fourth, and seventh chapters
is the most valuable. The instruction on the training equipment includes not only adequate reproductions of
the processes taking place in power unit systems, but also a multiplicity of problems from the fields of en-
gineering psychology, programmed training procedures and assessments of the extent of training of staff.
These problems are highlighted in general form in the book and specific work programs are given for their
solution.

But, just as the authors correctly remark, the introduction into educational training centers of training
equipment still does not resolve the training of staff. In addition to the training equipment at these centers,
there should be the means for theoretical and practical training (dialogic systems of training and control,
educational television systems, technological system simulators and nuclear power station plant mock-ups),
and also modern educational-methodological information of a general and specialized nature.

Up-to-date technical facilities will provide high efficiency of training and thanks to the application of
programmed training methods, the time in training staff has been shortened significantly. However, despite
the intensification of the training process, costs in training have a tendency to increase. There are larger
costs also on the setting-up of teaching-training centers. Taking account of the high cost of training nuclear
power station staff, the suggestion of the authors concerning the devising of unified requirements for the
characteristics and qualifications of operative staff is well-timed. In this connection, we consider it advan-
tageous to devise unified requirements for both the organization of the teaching process, and also for the
special features of technical training means and models of the technological nuclear power station power-unit
systems.

---

*Atomizdat, Moscow (1979), 152 pp., 1 ruble, 50 kopecks.

G. M. Fradkin (Editor)

RADIOISOTOPE SOURCES OF ELECTRIC POWER*

      Reviewed by A. A. Efremov

     The book is devoted to the scientific-technical basis and engineering problems of the creation of radio-isotope sources of electric power.

     Radioisotopic power generation is at the junction of several fields of science and technology, and the information given is many-sided. It highlights the problems of nuclear physics and technology, the conversion of radioactive decay energy into electric power, thermotechnology, and, finally, purely electrical problems.

     The book comprises three parts. The first is devoted to the basic physics concepts of radioactive decay, methods of production of radioisotopes, calculation and measurement of their heat release, and radiation shielding. Nonthermal and thermal methods of energy conversion are considered. The main attention is paid to the thermoelectric method, as the most developed. An approach to the thermophysical calculation of the isotope source as a whole is explained. The information in the second part of the book, concerning engineering problems, refers to thermoelectric systems. In this section, a selection of design solutions are considered, and also the designing and testing of thermoelectric converters, thermal insulation of the cladding, and other structural components. The following are described: radiation safety during manufacture, transportation and operation, reliability of radioisotope thermoelectric power sources, and also devices for matching the electrical parameters of the source with the consumer of the electric power. Power sources of millimicrowatt capacity are assigned to a subsection.

     Finally, in the last part of the book, designs are described and data are given about the operation of thermoelectric power sources using Ce, Sr, Cs, Co, and Pm. Numerical relations, structural and technological features of thermoemitting radioisotope sources of heat are given and also data on nuclear batteries.

     The book touches upon many aspects of the construction and operation of radioisotope power sources. In many sections, quite comprehensive numerical and reference data are contained, which are based on recent achievements in this field. In this respect, it will be undoubtedly of interest and will be useful to readers who are interested for the first time in these problems, and also specialists working in this field.

     Nevertheless, the book is not devoid of deficiencies. In particular, not all the information in the book is discussed at the same level. Thus, the chapter associated with the design of radioisotope thermoelectric power sources, which is mainly descriptive contains no reference information, which is so essential for designing. There is insufficiently specific data in the section on the thermophysical calculation of a radioisotope thermoelectric power source. There is no section related with the general classification of isotopic sources of electric power according to different types of criteria, which could be usefully located in the first introductory chapter or in the introduction. It is fair to mention, however, that a partial classification is given in the book, e.g., on conversion systems. In its content, the chapters on thermoemission sources of heat and nuclear batteries is somewhat out of place in the third part of the book, and they could have been included in the first part of the book.

     Finally, the most important deficiency is associated with the calculation of thermal batteries. It is regrettable that this concerns the problem which is most completely highlighted. The authors of the book have explained the state of the problem at the level of calculation of thermoelements with variable properties, i.e., thermogenerators with a given temperature of the junctions, and have not given the results of the calculation of thermoelectric generators with a specified temperature of the medium, of thermogenerators operating under space conditions, and also with the constant supply of heat. The omission is even more vexing, as the source, where these problems are discussed, is given in the bibliography of the book being reviewed, but not in connection with the problem being considered and not in the same section, and with a totally different approach. As a result, the procedure of the calculation given by the authors suffers obvious defects: there is no proper optimization of the electrical and thermal conditions of thermal batteries, the adequacy of the conditions of

_____

maximum efficiency and maximum power are stated erroneously, and convective or radiative heat exchange with the surrounding medium is not taken into account (only the case of conductive heat exchange is considered).

On the whole, and despite deficiencies, the issue of this book should be recognized as useful. This especially concerns its part where the practical problems of constructing isotopic sources of electric power are skillfully highlighted. Probably, it may be hoped that in the event of a reissue of the book, the authors will take account of these comments.

789

from
CONSULTANTS BUREAU

A NEW JOURNAL

Programming and Computer Software

A cover-to-cover translation of *Programmirovanie*

Editor: N. N. Govorun

This new journal provides authoritative and up-to-date reports on current progress in programming and the use of computers. By publishing papers ranging from theoretical research to practical results, this bimonthly will be essential to a wide circle of specialists. It features results of vital research in the following directions:

- logical problems of programming; applied theory of algorithms; and control of computational processes
- program organization; programming methods connected with the idiosyncrasies of input languages, hardware, and problem classes; and parallel programming
- operating systems; programming systems; programmer aids; software systems; data-control systems; IO systems; and subroutine libraries.

Subscription: Volume 6, 1980 (6 issues) $115.00

Random Titles from this Journal

PROGRAMMING THEORY
Structure of an Information System—N. A. Krinitskii, V. N. Krinitskii, and D. A. Stepanchenko
The Active Set of Program Pages and Its Behavior—V. P. Kutepov
Estimate of the Efficiency of Replacement Algorithms—Yu. A. Stoyan
PROGRAMMING METHODS
Method and Algorithm for Checking Group Items in the Machine Processing of Economic Information—G. L. Livshin
Parallelization of the Fast Fourier Transform Algorithm in Encephalogram Spectrum Analysis—V. S. Medovyi and V. D. Trush
COMPUTER SOFTWARE AND SYSTEM PROGRAMMING
Increasing the Efficiency of Object Programs by Changing the Initial Grammar of the Programming Language—S. Ya. Vilenkin and S. M. Movshovich
A Metalanguage, a Translation Scheme, and Syntactic Analysis in a System for Constructing Highly Effective Translators—M. I. Belyakov and L. G. Natanson
Tabular Information Output System—V. D. Prachenko, V. P. Semik, N. D. Tyutvina, and K. A. Chizhov
Questions in the Creation of Software for Terminal Devices—V. A. Kitov

NEW RUSSIAN JOURNALS

IN ENGLISH TRANSLATION

BIOLOGY BULLETIN
Izvestiya Akademii Nauk SSSR, Seriya Biologicheskaya

The biological proceedings of the Academy of Sciences of the USSR, this prestigious new bimonthly presents the work of the leading academicians on every aspect of the life sciences—from micro- and molecular biology to zoology, physiology, and space medicine.
Volume 7, 1980 (6 issues). $195.00

SOVIET JOURNAL OF MARINE BIOLOGY
Biologiya Morya

Devoted solely to research on marine organisms and their activity, practical considerations for their preservation, and reproduction of the biological resources of the seas and oceans.
Volume 6, 1980 (6 issues) $115.00

WATER RESOURCES
Vodnye Resursy

Evaluates the water resources of specific geographical areas throughout the world and reviews regularities of water resources formation as well as scientific principles of their optimal use.
Volume 7, 1980 (6 issues). $215.00

HUMAN PHYSIOLOGY
Fiziologiya Cheloveka

A new, innovative journal concerned *exclusively* with theoretical and applied aspects of the expanding field of human physiology.
Volume 6, 1980 (6 issues). $195.00

SOVIET JOURNAL OF BIOORGANIC CHEMISTRY
Bioorganicheskaya Khimiya

Features articles on isolation and purification of naturally occurring, biologically active compounds; the establishment of their structure, methods of synthesis, and determination of the relation between structure and biological function.
Volume 6, 1980 (12 issues). $245.00

SOVIET JOURNAL OF COORDINATION CHEMISTRY
Koordinatsionnaya Khimiya

Describes the achievements of modern theoretical and applied coordination chemistry. Topics include the synthesis and properties of new coordination compounds; reactions involving intraspheral substitution and transformation of ligands; complexes with polyfunctional and macro-molecular ligands; complexing in solutions; and kinetics and mechanisms of reactions involving the participation of coordination compounds.
Volume 6, 1980 (12 issues). $255.00

THE SOVIET JOURNAL OF GLASS PHYSICS AND CHEMISTRY
Fizika i Khimiya Stekla

Devoted to current theoretical and applied research on three interlinked problems in glass technology; the nature of the chemical bonds in a vitrifying melt and in glass; the structure-statistical principle; and the macroscopic properties of glass.
Volume 6, 1980 (6 issues) $145.00

LITHUANIAN MATHEMATICAL JOURNAL
Litovskii Matematicheskii Sbornik

An international medium for the rapid publication of the latest developments in mathematics, this quarterly keeps western scientists abreast of both practical and theoretical configurations. Among the many areas reported on in depth are the generalized Green's function, the Monte Carlo method, the "innovation theorem," and the Martingale problem.
Volume 20, 1980 (4 issues). $175.00

PROGRAMMING AND COMPUTER SOFTWARE
Programmirovanie

Reports on current progress in programming and the use of computers. Topics covered include logical problems of programming; applied theory of algorithms; control of computational processes; program organization; programming methods connected with the idiosyncracies of input languages, hardware, and problem classes; parallel programming; operating systems; programming systems; programmer aids; software systems; data-control systems; IO systems; and subroutine libraries.
Volume 6, 1980 (6 issues). $115.00

SOVIET MICROELECTRONICS
Mikroelektronika

Reports on the latest advances in solutions of fundamental problems of microelectronics. Discusses new physical principles, materials, and methods for creating components, especially in large systems.
Volume 9, 1980 (6 issues). $160.00

Send for Your Free Examination Copy